State of the Art in Large-Scale Soil Moisture Monitoring

Tyson E. Ochsner*
Dep. of Plant and Soil Sciences
Oklahoma State Univ.
368 Agricultural Hall
Stillwater, OK 74078

Michael H. Cosh
USDA-ARS
Hydrology and Remote Sensing Lab.
Beltsville, MD 20705

Richard H. Cuenca
Dep. of Biological and Ecological Engineering
Oregon State Univ.
Corvallis, OR 97331

Wouter A. Dorigo
Dep. of Geodesy and Geoinformation
Vienna Univ. of Technology
1040 Vienna, Austria

Clara S. Draper
Global Modeling and Assimilation Office
NASA Goddard Space Flight Center
Greenbelt, MD 20771
and
GESTAR
Universities Space Research Association
Columbia, MD 21044

Yutaka Hagimoto
Dep. of Biological and Ecological Engineering
Oregon State Univ.
Corvallis, OR 97331

Yann H. Kerr
Centre d'Etudes Spatiales de la Biosphere
31401 Toulouse, France

Kristine M. Larson
Dep. of Aerospace Engineering Sciences
Univ. of Colorado
Boulder, CO 80309

Eni G. Njoku
Jet Propulsion Laboratory
California Institute of Technology
Pasadena, CA 91109

Eric E. Small
Dep. of Geological Sciences
Univ. of Colorado
Boulder, CO 80309

Marek Zreda
Dep. of Hydrology and Water Resources
Univ. of Arizona
Tucson, AZ 85721

Soil moisture is an essential climate variable influencing land–atmosphere interactions, an essential hydrologic variable impacting rainfall–runoff processes, an essential ecological variable regulating net ecosystem exchange, and an essential agricultural variable constraining food security. Large-scale soil moisture monitoring has advanced in recent years, creating opportunities to transform scientific understanding of soil moisture and related processes. These advances are being driven by researchers from a broad range of disciplines, but this complicates collaboration and communication; and, for some applications, the science required to utilize large-scale soil moisture data is poorly developed. In this review, we describe the state of the art in large-scale soil moisture monitoring and identify some critical needs for research to optimize the use of increasingly available soil moisture data. We review representative examples of (i) emerging in situ and proximal sensing techniques, (ii) dedicated soil moisture remote sensing missions, (iii) soil moisture monitoring networks, and (iv) applications of large-scale soil moisture measurements. Significant near-term progress seems possible in the use of large-scale soil moisture data for drought monitoring. Assimilation of soil moisture data for meteorological or hydrologic forecasting also shows promise, but significant challenges related to spatial variability and model structures remain. Little progress has been made in the use of large-scale soil moisture observations within the context of ecological or agricultural modeling. Opportunities abound to advance the science and practice of large-scale soil moisture monitoring for the sake of improved Earth system monitoring, modeling, and forecasting.

Abbreviations: AirMOSS, Airborne Microwave Observatory of Subcanopy and Subsurface; AMSR-E, Advanced Microwave Scanning Radiometer for the Earth Observing System; ASCAT, Advanced Scatterometer; AWDN, Automated Weather Data Network; COSMOS, COsmic-ray Soil Moisture Observing System; DTS, distributed temperature sensing; ERS, European Remote Sensing; ESA, European Space Agency; ET, evapotranspiration; GPS, global positioning system; IR, interferometric reflectometry; ISMN, International Soil Moisture Network; NWP, numerical weather prediction; RFI, radio frequency interference; RZSM, root zone soil moisture; SCAN, Soil Climate Analysis Network; SMAP, Soil Moisture Active Passive; SMI, Soil Moisture Index; SMOS, Soil Moisture Ocean Salinity; SNR, signal to noise ratio; SWD, soil water deficit; TDR, time domain reflectometry.

The science and practice of large-scale soil moisture monitoring has entered a stage of unprecedented growth, with the potential to transform scientific understanding of the patterns and dynamics of soil moisture and soil-moisture-related processes. Large-scale soil moisture monitoring may lead to improved understanding of soil moisture controls on water, energy, and C fluxes between the land and atmosphere, resulting in improved meteorological forecasts and climate projections. Soil moisture measurements are also key in assessing flooding and monitoring drought. Knowledge gained from large-scale soil moisture observations can help mitigate these natural hazards, yielding potentially great economic and societal benefits. We use *large-scale* to refer to spatial support scales of $>1^2$ m^2 for a sensor or spatial extents of $>100^2$ km^2 for a sensor network

Soil Sci. Soc. Am. J.
doi:10.2136/sssaj2013.03.0093
Received 8 Mar. 2013.
*Corresponding author (tyson.ochsner@okstate.edu).

(Crow et al., 2012; Western and Blöschl, 1999). In this review, areas are often enumerated in the XX^2 format to indicate the length of one side of a square of the given area, e.g., 10,000 km^2 = 100^2 km^2. New developments continue within the realm of in situ sensors that monitor soil moisture at the point scale, i.e., $<1^2$ m^2 support. These point-scale sensors have been reviewed recently (Dobriyal et al., 2012; Robinson et al., 2008) and are not considered here except within the context of large-scale networks. Rather, this review aims to broadly describe the state of the art in large-scale soil moisture monitoring. Airborne and satellite remote sensing approaches for soil moisture are considered large-scale monitoring techniques in this review.

To provide context, it is helpful to begin with a brief historical overview of soil moisture monitoring in general. The first major technological advance in modern soil moisture monitoring can be traced to the development of the neutron probe after World War II (Evett, 2001). The measurement of soil moisture based on neutron thermalization first appeared in the peer-reviewed literature in a study by Iowa State College (now University) soil physicists, Gardner and Kirkham (1952). This technology was soon commercialized under a contract between the U.S. Army Corps of Engineers and Nuclear-Chicago Corporation, and by 1960, hundreds of neutron probes were in use around the world (Evett, 2001). The neutron probe remained the de facto standard for indirect soil moisture measurement until a soil physicist and two geophysicists working for the Government of Canada made a key breakthrough in using dielectric properties to measure soil water (Topp et al., 1980). Despite initial skepticism from the soil science and remote sensing communities (Topp, 2006), the time domain reflectometry (TDR) approach of Topp et al. (1980) eventually became a dominant technology for soil moisture monitoring and created for the first time the possibility of automated, multiplexed, unattended, in situ monitoring (Baker and Allmaras, 1990). By the 1990s, the TDR technology had proven the value of electromagnetic methods for monitoring soil moisture, and an avalanche of impedance or capacitance type probes followed (Robinson et al., 2008). These capacitance probes typically operate at frequencies much lower than the effective frequency of TDR. As a result, these probes are simpler and less expensive but also less accurate than TDR (Blonquist et al., 2005). Much effort has also been devoted to the development of heat dissipation (Fredlund and Wong, 1989; Phene et al., 1971; Reece, 1996) and heat pulse sensors (Bristow et al., 1993; Campbell et al., 1991; Heitman et al., 2003; Ochsner et al., 2003; Song et al., 1999; Tarara and Ham, 1997) for soil moisture measurement, with reasonable success.

While Canadian researchers were beginning to develop the groundbreaking TDR method, scientists in the United States were pioneering remote sensing of soil moisture from tower, aircraft, and satellite platforms using microwave radiometers (Schmugge et al., 1974), scatterometers (Dickey et al., 1974), synthetic aperture radar (Chang et al., 1980), and combined radar–radiometer systems (Ulaby et al., 1983). Various other techniques were also introduced during the same time, including methods based on polarized visible light (Curran, 1978), thermal inertia (Pratt and Ellyett, 1979), and terrestrial γ radiation (Carroll, 1981). Satellite remote sensing approaches in particular have engendered much enthusiasm and interest with their promise of global data coverage, leading Vinnikov et al. (1999) to speculate that, in regard to long-term soil moisture monitoring, "The future obviously belongs to remote sensing of soil moisture from satellites." And, in fact, the intervening decades of research on remote sensing of soil moisture are now beginning to bear fruit in terms of operational satellites for large-scale soil moisture monitoring.

Not everyone has been content to wait for the arrival of operational soil moisture satellites; rather, some have envisioned and created large-scale in situ monitoring networks for soil moisture. The earliest organized networks were in the Soviet Union and used repeated gravimetric sampling (Robock et al., 2000). The Illinois Climate Network was the first large-scale network to use a nondestructive measurement device, the neutron probe (Hollinger and Isard, 1994), while the USDA-NRCS Soil Climate Analysis Network (SCAN) (Schaefer et al., 2007) and the Oklahoma Mesonet (McPherson et al., 2007) pioneered the use of automated, unattended sensors in large-scale soil moisture networks during the 1990s. Since then, numerous networks have emerged around the world and have come to play vital roles in the science and practice of large-scale soil moisture monitoring, not the least of which is their role in calibrating and validating satellite remote sensing techniques.

The past 10 yr have witnessed the emergence of potentially transformative new soil moisture technologies, which are beginning to fundamentally alter the possibilities for large-scale monitoring. These new methods include the COsmic-ray Soil Moisture Observing System (COSMOS), GPS-based techniques, and fiber optic distributed temperature sensing (DTS) approaches (Larson et al., 2008a; Sayde et al., 2010; Steele-Dunne et al., 2010; Zreda et al., 2008). Meanwhile, the number and scope of large-scale automated soil moisture monitoring networks has been steadily increasing, both in the United States and around the world; and in 2009, the European Space Agency (ESA) launched the Soil Moisture Ocean Salinity (SMOS) satellite, the first one designed specifically for soil moisture monitoring (Kerr et al., 2010).

Despite these developments, many challenges remain within the realm of large-scale soil moisture monitoring. The recent progress in this field has been enabled by contributions from many different disciplines, and future progress will probably be interdisciplinary as well, but staying informed about new developments can be challenging when the research is spread across a broad range of science disciplines from soil science to remote sensing to geodesy to meteorology. Contemporary soil physicists, whose predecessors were instrumental in birthing the modern era of soil moisture monitoring, have been largely focused on development and testing of point-scale measurement techniques and have perhaps not been adequately engaged in advancing the science of large-scale monitoring. Great advances have been made in satellite remote sensing approaches for estimating surface soil moisture, but the coarse horizontal resolution and the shallow sensing depth are significant limitations for many applications

(Wagner et al., 2007). Furthermore, the science and technology required to actually use large-scale soil moisture data is relatively underdeveloped. There has been a dearth of research investment in developing modeling and forecasting tools informed by soil moisture data from large-scale in situ networks. There has also been little research on the use of remotely sensed soil moisture products for applications beyond weather forecasting or streamflow prediction. This was understandable in previous decades when the widespread availability of such data was a distant prospect, but the circumstances have changed. Soil moisture data are now common and may be ubiquitous in the near future.

In light of these circumstances, we seek to meet the need for a cross-disciplinary state-of-the-art review for the sake of improving communication and collaboration. We further seek to engage and mobilize the expertise of the international soil science, and specifically soil physics, community in advancing the science and practice of large-scale soil moisture monitoring. We also seek to highlight the pressing need to accelerate the pace of progress in the area of using large-scale soil moisture observations for advanced Earth systems monitoring, modeling, and forecasting applications. Our objectives are (i) to succinctly review the state of the art in large-scale soil moisture monitoring and (ii) to identify some critical needs for research to optimize the use of the increasingly available soil moisture data.

This review does not aim to be comprehensive. Rather we have selected specific topics that are illustrative of the opportunities and challenges ahead. This review is organized into four primary sections: (i) emerging in situ and proximal sensing techniques, (ii) dedicated soil moisture remote sensing missions, (iii) soil moisture monitoring networks, and (iv) applications of large-scale soil moisture measurements. In this context, in situ techniques are those using sensors embedded in the soil and proximal techniques are those using sensors that are in close proximity to the soil but not embedded in it. Some observations regarding the primary challenges and opportunities for large-scale soil moisture monitoring are provided at the end of the review.

EMERGING IN SITU AND PROXIMAL SENSING TECHNIQUES

Soil Moisture Monitoring Using Cosmic-Ray Neutrons

Area-average soil moisture can be measured in the field using cosmic-ray neutron background radiation, whose intensity in the air above the land surface depends primarily on soil moisture. The cosmic-ray probe integrates soil moisture over an area hundreds of meters in diameter, something that would require an entire network of point measurement devices. Measurements can be made using stationary probes, which provide an hourly time series of soil moisture, or mobile probes, which provide snapshots in time over an area or along a line.

Cosmic-ray protons that impinge on the top of the atmosphere create secondary neutrons that in turn produce additional neutrons, thus forming a self-propagating nucleonic cascade (Simpson, 2000; Desilets and Zreda, 2001). As the secondary neutrons travel through the atmosphere and then through the top few meters of the biosphere, hydrosphere, and lithosphere, fast neutrons are created (Desilets et al., 2010). Because fast neutrons are strongly moderated by H present in the environment (Zreda et al., 2008, 2012), their measured intensities reflect variations in the soil moisture (Zreda et al., 2008) and other H present at and near the Earth's surface (Zreda et al., 2012; Franz et al., 2013).

The process of neutron moderation depends on three factors that together define the neutron stopping power of a material (Zreda et al., 2012): (i) the elemental scattering cross-section or probability of scattering; H has a high probability of scattering a neutron; (ii) the logarithmic decrement of energy per collision, which characterizes how efficient each collision is; H is by far the most efficient element; and (iii) the number of atoms of an element per unit mass of material, which is proportional to the concentration of the element and to the inverse of its mass number. Because of the low atomic mass of H and the abundance of water in soils, H, next to O and Si, makes up a significant fraction of all the atoms in many soils. The extraordinarily high stopping power of H makes the cosmic-ray soil moisture method work.

The fast neutrons that are produced in air and soil travel in all directions within and between the air and soil, and in this way an equilibrium concentration of neutrons is established. The equilibrium is shifted in response to changes in the H content of the media, which in practice means changes in the amount of water on or in the soil. Adding water to the soil results in more efficient moderation of neutrons by the soil, causing a decrease in the fast neutron intensity above the soil surface. Removing water from the soil has the opposite effect. Thus, by measuring the fast neutron intensity in the air, the moisture content of the soil can be inferred, for example using the equation of Desilets et al. (2010), which is plotted in Fig. 1:

$$\theta=\frac{a_0}{\left(N/N_0\right)-a_1}-a_2 \qquad [1]$$

where θ is the neutron-derived moisture content, N is the measured neutron intensity, N_0 is the neutron intensity in air above a dry soil (this is a calibration parameter obtained from independent in situ soil moisture data), and a_0, a_1, and a_2 are fitted constants that define the shape of the calibration function. Neutron transport modeling shows that the shape of the calibration function is similar for different chemical compositions of soil and different soil textures (Zreda et al., 2008; Desilets et al., 2010) and in the presence of H pools other than pore water, for example vegetation or water vapor (Franz et al., 2013; Rosolem et al., 2013). Therefore, the same function can be used under different field conditions once corrections are made for all pools of H (Franz et al., 2013).

The probe senses all H present within the distance that fast neutrons can travel in soils, water, air, and other materials near the land surface. That distance varies with the chemical composition and density of the material, from centimeters in water through decimeters in soils to hectometers in air. The support volume can be visualized as a hemisphere above the soil surface placed on top of a cylinder in the soil (Fig. 2). For soil moisture measurements, the diameter and height of the

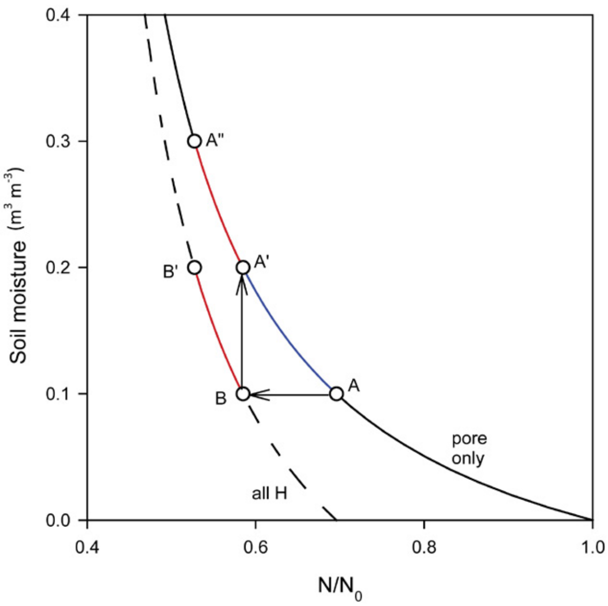

Fig. 1. Response function for cosmic-ray probe for soils with pore water only (solid black line) and those with pore water and other water, such as lattice and organic matter (dashed black line); N is the measured neutron intensity and N_0 is a calibration parameter representing the neutron intensity above dry soil. The presence of other water shifts the line horizontally from Point A to B and A′ to B′, and the new line is steeper than the original line for the same moisture range (B-B′ vs. A-A′). Section B-B′ can be placed on the original line by translating it up to fall on section A′-A″. Thus, accounting for additional (non-pore) water does not require a new response function but merely a translation along the original function by the amount equal to that non-pore-water component.

cylinder are important. The horizontal footprint, which is defined as the area around the probe from which 86% $(1 - e^{-2})$ of counted neutrons arise, is a circle with a diameter of 660 m at sea level (Zreda et al., 2008). It decreases slightly with increasing soil moisture content and with increasing atmospheric water vapor content, and it increases with decreasing air density (decreasing atmospheric pressure or increasing altitude) (Zreda et al., 2012). The horizontal footprint has been verified by field measurements (Zweck et al., 2011).

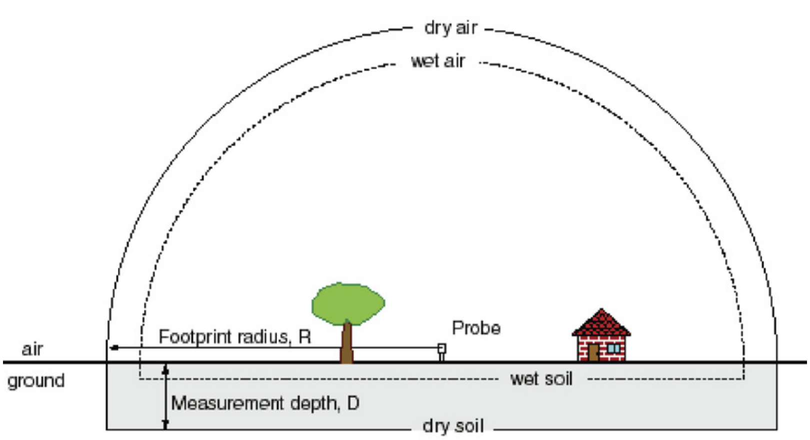

Fig. 2. Sensing volume of the cosmic-ray probe comprises a hemisphere in air (of radius R) and a cylinder in soil (of height D). All hydrogen within the sensing volume is reflected in the measured neutron intensity. The horizontal footprint, R, depends on air properties: mainly density and water vapor content. The vertical footprint depends on soil properties: mainly bulk density and total hydrogen content (pore water, lattice water, and organic matter water).

The effective depth of measurement, which is defined as the thickness of soil from which 86% $(1 - e^{-2})$ of counted neutrons arise, depends strongly on soil moisture (Zreda et al., 2008). It decreases nonlinearly from about 70 cm in soils with no water to about 12 cm in saturated soils and is independent of the air density. The effective depth of measurement decreases with increasing H in other reservoirs, such as lattice water, soil organic matter, or vegetation. The decrease in the vertical support volume is more significant at the dry end (on the order of 10 cm) than at the wet end (on the order of 1 cm). The vertical footprint has not been verified empirically.

Neutrons react with any H present near the Earth's surface. Therefore, the measured neutron intensity reflects the total reservoir of neutrons present within the sensing distance of the probe (Fig. 2), and hence the probe can be viewed as the total surface moisture probe. The greater the concentration of H, the greater is its impact on the neutron intensity. Large near-surface reservoirs of H, roughly in order of decreasing size, are (i) surface water (including snow), (ii) soils, (iii) lattice water and water in soil organic matter; (iv) vegetation, and (v) atmospheric water vapor. Because the neutron signal integrates all these factors, isolation of one of these components, for example soil moisture, requires that the others be (i) constant in time, (ii) if not constant, assessed independently, or (iii) negligibly small. In addition, the support volume (or the measurement volume) will be affected by these other sources of H.

Calibration requires simultaneous measurements of area-average soil moisture (θ) and neutron intensity (N), and solving Eq. [1] for the calibration parameter N_0. Area-average soil moisture representative of the cosmic-ray footprint is obtained by collecting numerous soil samples around the cosmic-ray probe and measuring the moisture content by the oven-drying method (Zreda et al., 2012); other methods, such as TDR, can be used as well. The measured neutron intensities must be corrected for atmospheric water vapor and pressure variations. Soil samples must be analyzed for their chemical composition to correct the calibration function for any additional water in mineral grains (lattice water) and in the organic matter present in the soil (Zreda et al., 2012). The presence of that extra water shifts the position of the calibration point to the left on the calibration function (Fig. 1), which results in a steeper curve and thus in reduced sensitivity of neutrons to changes in soil moisture. Other sources of water have a similar effect on the calibration function.

The measurement precision of soil moisture determination is due to neutron-counting statistics. The counts follow the Poisson distribution (Knoll, 2000) in which, for the total number of counts, N, the standard deviation is $N^{0.5}$. Thus, more counts produce better precision (i.e., a lower coefficient of variation), provided that the neutron intensity remains stationary during the counting time. High counting rates are expected under the following conditions: (i) high altitude and high latitude, because the incoming cosmic-ray intensity, which is the precursor to fast neutrons, increases with both (Desilets and Zreda, 2003; Desilets et al., 2006); (ii) dry soil, because of the inverse relation between soil moisture and neutron intensity (Fig. 1); (iii) dry atmosphere, because of the inverse relation between atmospheric moisture and neutron intensity (Rosolem et al., 2013); (iv) no vegetation; and (v) low lattice water and organic matter content of the soil. The opposite conditions will result in lower counting rates and poorer precision.

The accuracy of soil moisture determination depends on a few factors related to calibration and the presence of other pools of H within the cosmic-ray probe support volume. The calibration uncertainty is due to two factors: (i) the accuracy of the independent measure of area-average soil moisture, which is usually <0.01 m^3 m^{-3}; and (ii) the accuracy of the neutron count rate at the time of calibration, which is usually around 2%. (These calibration data sets can be viewed at cosmos.hwr.arizona.edu.) If these were the only contributing factors, the accuracy would be better than 0.01 m^3 m^{-3}. But there are a few complicating factors that may lead to an increase in the uncertainty. They include atmospheric water vapor, infiltration fronts, changing horizontal correlation scale of soil moisture, variable vegetation, and variations in the incoming cosmic-ray intensity. Corrections have been developed for these factors, but their contributions to the overall uncertainty of soil moisture determination have not been assessed rigorously. At a desert site near Tucson, AZ, Franz et al. (2012) found a root mean square error (RMSE) of 0.017 m^3 m^{-3} between the soil moisture estimates from a well-calibrated cosmic-ray probe and the depth-weighted soil moisture average from a network of point-scale sensors distributed across the probe footprint.

Cosmic-ray soil moisture probes are used as stationary or roving devices. Stationary probes are installed above the land surface to measure and transmit neutron intensity and ancillary data at user-prescribed time intervals (Zreda et al., 2012). These measurements are then used, together with cosmic-ray background intensity data, to compute soil moisture. A network of stationary probes, called COSMOS, has been installed in the United States, with the main aim to provide area-average soil moisture data for atmospheric applications (Zreda et al., 2012). Data are available with 1-h latency at http://cosmos.hwr.arizona.edu. Other networks or individual probes are being installed in Australia (the network named CosmOz), Germany (Rivera Villarreyes et al., 2011), and elsewhere around the globe.

A mobile version of the cosmic-ray soil moisture probe, called COSMOS Rover, is under development. Its main application is mapping soil moisture across large areas from a car or an aircraft; a backpack version is possible as well. The vehicle-mounted instrument is approximately 10 times larger than the stationary cosmic-ray probe to provide more counts (better statistics) in a short time as the vehicle progresses along the route. The measured neutron intensity is converted to soil moisture using the usual calibration equation (Desilets et al., 2010). Transects (Desilets et al., 2010) or maps (Zreda et al., 2011) of soil moisture can be produced within hours or days. Such maps may prove useful for many applications, including calibration and validation of satellite soil moisture missions like SMOS.

Soil Moisture Monitoring Using Global Positioning System Signals

While the cosmic-ray probe utilizes an existing natural "signal," the ambient fast neutron intensity, to infer soil moisture, new methods utilizing GPS receivers use existing anthropogenic signals. The GPS signals follow two types of paths between the satellites that transmit GPS signals and the antennas that receive them (Fig. 3). Some portions of GPS signals travel directly from satellites to antennas. These direct signals are optimal for navigation and geodetic purposes. Antennas also receive GPS signals that reflect off the land surface, referred to as *multipath* by the geodetic community (Georgiadou and Kleusberg, 1988). The GPS satellites transmit microwave L-band signals (1.57542 and 1.22760 GHz) that are optimal for sensing water in the environment (Entekhabi et al., 2010). For bare soil conditions, the reflection coefficients depend on the permittivity of the soil, surface roughness, and elevation angle of the reflections. Therefore, reflected GPS signals can be used to estimate soil moisture, as well as other environmental parameters. The GPS antennas and receivers can also be mounted on satellites (Lowe et al., 2002) or on planes (Katzberg et al., 2005). The data collected by these instruments are considered remote sensing observations. Alternatively, GPS reflections can also be measured using antennas mounted fairly close to the land surface (Larson et al., 2008a; Rodriguez-Alvarez et al., 2011a), yielding a proximal sensing technique. Ground-based GPS studies use the interference of the direct and reflected GPS signals, and thus the method is often called GPS interferometric reflectometry (GPS-IR).

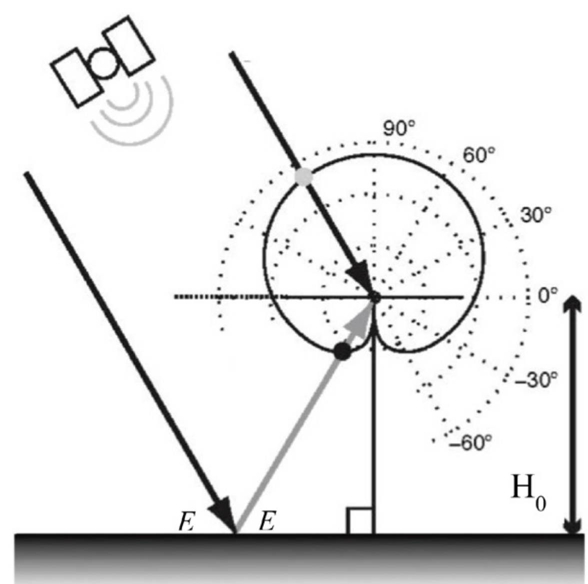

Fig. 3. Geometry of a multipath signal, for antenna height (H_0) and satellite elevation angle (E). Black arrows represent the direct signal transmitted from the satellite. The gray arrow is the reflected signal from the ground. The solid line represents the gain pattern of the antenna. Dashed circles indicate relative power levels of the gain pattern (Reprinted from Larson et al., 2008a with permission from Springer–Verlag.).

For GPS-IR systems, the sensing footprint depends on (i) the height of the antenna above the ground and (ii) the range of satellite elevation angles used in the analysis. As satellite elevation angle increases, the portion of the ground that yields specular (i.e., mirror-like) reflections both shrinks and moves closer to the antenna. For the case of a typical geodetic antenna height of 2 m, the center of the area sensed varies from 25 m at an elevation angle of 5° to 5 m at an elevation angle of 30°. Larger sampling areas can be achieved by raising the antenna to heights of ~100 m, above which observations are complicated by the GPS code lengths (Rodriguez-Alvarez et al., 2011a). Because GPS is a constellation of >30 satellites, different GPS satellites rise and set above a GPS soil moisture site throughout the day. These reflections are measured from different azimuths depending on the orbital characteristics of each satellite. For the best sites, more than 60 soil moisture estimates can be made per day, so the soil moisture data estimated from GPS reflections should be considered as daily in temporal frequency, once it is averaged across an area of ~1000 m^2 for antenna heights of 2 m (Larson et al., 2008b).

Two methods of GPS soil moisture sensing have been developed. The first is based on using GPS instruments designed for geodesists and surveyors. These GPS instruments traditionally measure the distance between the satellites and antenna to estimate position; however, these GPS instruments also measure signal power, or the signal to noise ratio (SNR). Embedded on the direct signal effect are interference fringes caused by the reflected signal being in or out of phase with respect to the direct signal. The SNR frequency is primarily driven by the height of the antenna above the ground. As the permittivity of the soil changes, the amplitude, phase, and frequency of the SNR interferogram varies (Larson et al., 2010; Zavorotny et al., 2010). Of the three parameters, the phase of the SNR interferogram is the most useful for estimating soil moisture.

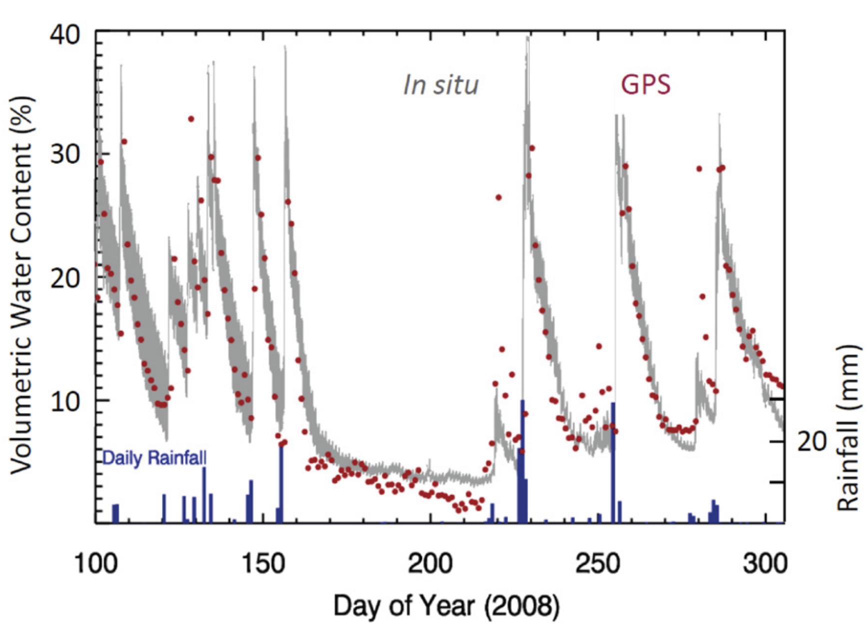

Fig. 4. Soil volumetric water content measured by water content reflectometers (WCR) at 2.5-cm depth (grey areas shows range from five probes), soil water content estimated by GPS–interferometric reflectometry (circles), and daily precipitation totals (bars) from a site near Marshall, CO (adapted from Larson et al., 2010).

Chew et al. (2013) demonstrated theoretically that phase varies linearly with surface soil moisture. For the soils described by Hallikainen et al. (1985), the slope of this relationship does not vary with soil type. For most conditions, phase provides a good estimate of average soil moisture in the top 5 cm. The exception is when very wet soil overlies dry soil, for example immediately following short-duration rainstorms when the wetting front has not propagated to ~5 cm (Larson et al., 2010). Estimates of soil moisture from phase have been compared with in situ soil moisture measurements (Fig. 4). At grass-dominated sites with relatively low vegetation water content (<0.5 kg m^{-2}), the SNR phase varies linearly with in situ soil moisture (r^2 > 0.76) (Larson et al., 2010), consistent with the theoretical analysis by Chew et al. (2013). The vegetation at these sites is typical of many rangeland areas in the western United States. A SNR interferogram is also affected by higher water content vegetation, for example that which exists in irrigated agricultural fields (Small et al., 2010). Methods are being developed to retrieve surface soil moisture from SNR interferograms under these conditions.

One advantage to using geodetic GPS equipment to measure soil moisture is that existing geodetic networks can provide much needed hydrologic information. The National Science Foundation's Plate Boundary Observatory network has >1100 stations with effectively identical GPS instrumentation. Many of the stations are located amid complex topography, which does not facilitate estimation of soil moisture via GPS-IR. However, soil moisture is being estimated at 59 stations with relatively simple topography. The data are updated daily and are available at http://xenon.colorado.edu/portal/.

A second GPS soil moisture sensing method is also under development (Rodriguez-Alvarez et al., 2009). Similar to the approach of Larson et al. (2008a), this system measures the interference pattern resulting from the combination of direct and reflected GPS signals. A dual-polarization antenna measures the power of the vertically and horizontally polarized signals separately, which is not possible using standard geodetic instrumentation. The satellite elevation angle at which the reflectivity of the vertically polarized signal approaches zero, i.e., the Brewster angle, varies with soil moisture (Rodriguez-Alvarez et al., 2011a). The existence of this Brewster angle yields a notch in the interference pattern. The position of the notch is then used to infer soil moisture.

Over a bare soil field, this technique yielded 10 soil moisture estimates during period of about 50 d; they show good agreement with those measured in situ at a depth of 5 cm (RMSE < 0.03 m^3 m^{-3}) (Rodriguez-Alvarez et al., 2009). A vegetation canopy introduces additional notches to the observed interference pattern. The position and amplitude of these notches can be used to infer both vegetation height and soil moisture. This approach yielded excellent estimates of corn (*Zea mays* L.) height throughout a growing season (RMSE = 6.3 cm) (Rodriguez-Alvarez et al., 2011b). Even beneath a 3-m-tall corn canopy, soil moisture estimates typically differed by <0.04 $m^3 m^{-3}$ from those measured with in situ probes at 5 cm. The main difference between these two techniques is that the approach of Larson et al. (2008a) uses commercially available geodetic instrumentation—which typically already exists and can be simultaneously used to measure position. The approach of Rodriguez-Alvarez et al. (2009) uses a system specifically designed for environmental sensing, but it is not yet commercially available.

Soil Moisture Monitoring Using Distributed Temperature Sensing

Much as the Larson et al. (2008a) GPS-IR method repurposes commercially available GPS receivers to monitor soil moisture, other researchers have sought to develop new soil moisture monitoring methods using commercially available DTS systems. In a DTS system, an optical instrument is used to observe temperature along a continuum of points within an attached optical fiber cable, typically by the principle of Raman scattering (Selker et al., 2006). The spatial location corresponding to each temperature measurement is determined based on the travel time of light in the fiber in a manner analogous to TDR. Weiss (2003) pioneered the use of DTS systems for soil moisture monitoring by successfully demonstrating the potential use of fiber optics to detect the presence of moisture in a landfill cover constructed from sandy loam soil. A 120-V generator supplied current to the stainless steel sheath of a buried optical fiber cable for ~626 s at a rate of 18.7 W m^{-1}, and the corresponding spatially variable temperature rise of the cable was observed at 40-s temporal resolution and 1-m spatial resolution. Analysis of the temperature rise data using the single-probe method (Carslaw and Jaeger, 1959) resulted in satisfactory estimates of the spatial variability of soil thermal conductivity along the cable, which in turn reflected the imposed spatial variability of soil moisture. The temperature uncertainty achieved was ~0.55°C, however, and Weiss (2003) concluded that without improvements in the SNR, the system would not be able to resolve small changes in soil moisture >0.06 $m^3 m^{-3}$ for the sandy loam soil used in that study.

The potential of using passive (unheated) DTS methods for soil moisture estimation was explored by Steele-Dunne et al. (2010). Optical fiber cable was installed in a tube on the soil surface and at depths of 8 and 10 cm. The soil texture was loamy sand, and the vegetation cover was sparse grass. With temperatures from the upper and lower cables as time-dependent boundary conditions, the temperature at the middle cable was modeled by numerical solution of the one-dimensional heat conduction equation. A numerical search routine was used to find the thermal diffusivity that produced the best agreement between the simulated and observed temperatures at the 8-cm depth. The results demonstrated that the passive DTS system could detect temporal changes in thermal diffusivity associated with rainfall events, but the accuracy of the diffusivity estimates was hindered by uncertainties about the exact cable depths and spacings. Furthermore, deriving soil moisture estimates was complicated by uncertainty and nonuniqueness in the diffusivity–soil moisture relationship.

Sayde et al. (2010) modified the active DTS approach of Weiss (2003) by interpreting the temperature rise data in terms of cumulative temperature increase, i.e., the integral of the temperature rise from the beginning of heating to some specified time limit. Based on a laboratory sand column experiment with 2-min, 20 W m^{-1} heat pulses, they developed an empirical calibration function that fit the observed cumulative temperature increase (0–120 s) vs. soil moisture data. Based on that function and the observed uncertainty in the cumulative temperature increase data, the uncertainty in the soil moisture estimates would increase approximately linearly from 0.001 $m^3 m^{-3}$ when the soil moisture is 0.05 $m^3 m^{-3}$ to 0.046 $m^3 m^{-3}$ when the soil moisture is 0.41 $m^3 m^{-3}$. Gil-Rodríguez et al. (2013) used the approach of Sayde et al. (2010) to satisfactorily monitor the dimensions and evolution of a wetted bulb during infiltration beneath a drip emitter in a laboratory column of sandy loam soil.

Striegl and Loheide (2012) used an active DTS approach to monitor the spatial and temporal dynamics of soil moisture along a 130-m transect associated with a wetland reconstruction project (Fig. 5). They used a 10-min, 3 W m^{-1} heat pulse, a lower heating rate than used in previous active DTS stud-

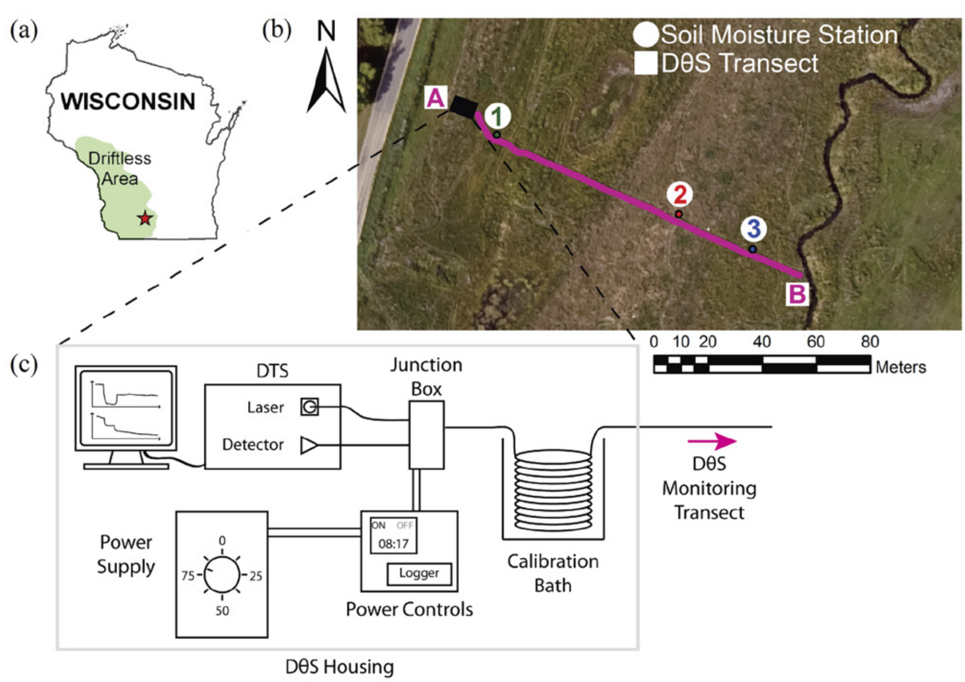

Fig. 5. (a) Location of study site used by Striegl and Loheide (2012), (b) aerial photo of active distributed temperature sensing (DTS/DθS) transect with three independent soil moisture (θ) monitoring stations, and (c) schematic diagram of active DTS system components (Reprinted from *Groundwater* with permission of the National Ground Water Association. Copyright 2012; Striegl and Loheide, 2012).

ies. They followed Sayde et al. (2010) in adopting a primarily empirical calibration approach, but rather than cumulative temperature increase, they related soil moisture to the average temperature rise observed from 380 to 580 s after the onset of heating. A calibration function was developed by relating the observed temperature rise data to independent soil moisture measurements at three points along the transect, and the resulting function had a RMSE of 0.016 $m^3\ m^{-3}$ for soil moisture <0.31 $m^3\ m^{-3}$ but a RMSE of 0.05 $m^3\ m^{-3}$ for wetter conditions. Their system successfully monitored the field-scale spatiotemporal dynamics of soil moisture at 2-m and 4-h resolution during a period of about 60 d consisting of marked wetting and drying cycles (Fig. 6).

The passive and active DTS methods for monitoring soil moisture offer the potential for unmatched spatial resolution (<1 m) in long-term soil moisture monitoring on field-scale (>100-m) transects. These methods may, in the near future, greatly impact our understanding of the fine-scale spatiotemporal structure of soil moisture and shed new light on the factors influencing that structure. Thus far, the active DTS methods have shown more promise than passive DTS, but more sophisticated data assimilation approaches for interpreting passive DTS data are in development. The active DTS method is still in its infancy, and many key issues remain to be addressed. None of the active DTS methods developed to date involve spatial variability in the soil moisture calibration function, so heterogeneity in soil texture and bulk density could give rise to appreciable uncertainties in field settings. Field installation of the optical fiber cables at the desired depths with good soil contact and minimal soil disturbance is also a significant challenge. Custom-designed cable plows (Steele-Dunne et al., 2010) and commercial vibratory plows (Striegl and Loheide, 2012) have been used with some success. The active DTS methods have demonstrated good precision for low to moderate soil moisture levels, but further improvements in measurement precision are needed for wet conditions. Obtaining good-quality temperature measurements using a DTS instrument in the field requires that thermally stable calibration baths be included in the system design. The instrument itself must also be in a thermally stable environment because sizeable errors can result from sudden changes in the instrument temperature (Striegl and Loheide, 2012). The measurement principles behind DTS were discussed in more detail by Selker et al. (2006), and practical aspects of DTS, including key limitations and uncertainties, were described by Tyler et al. (2009).

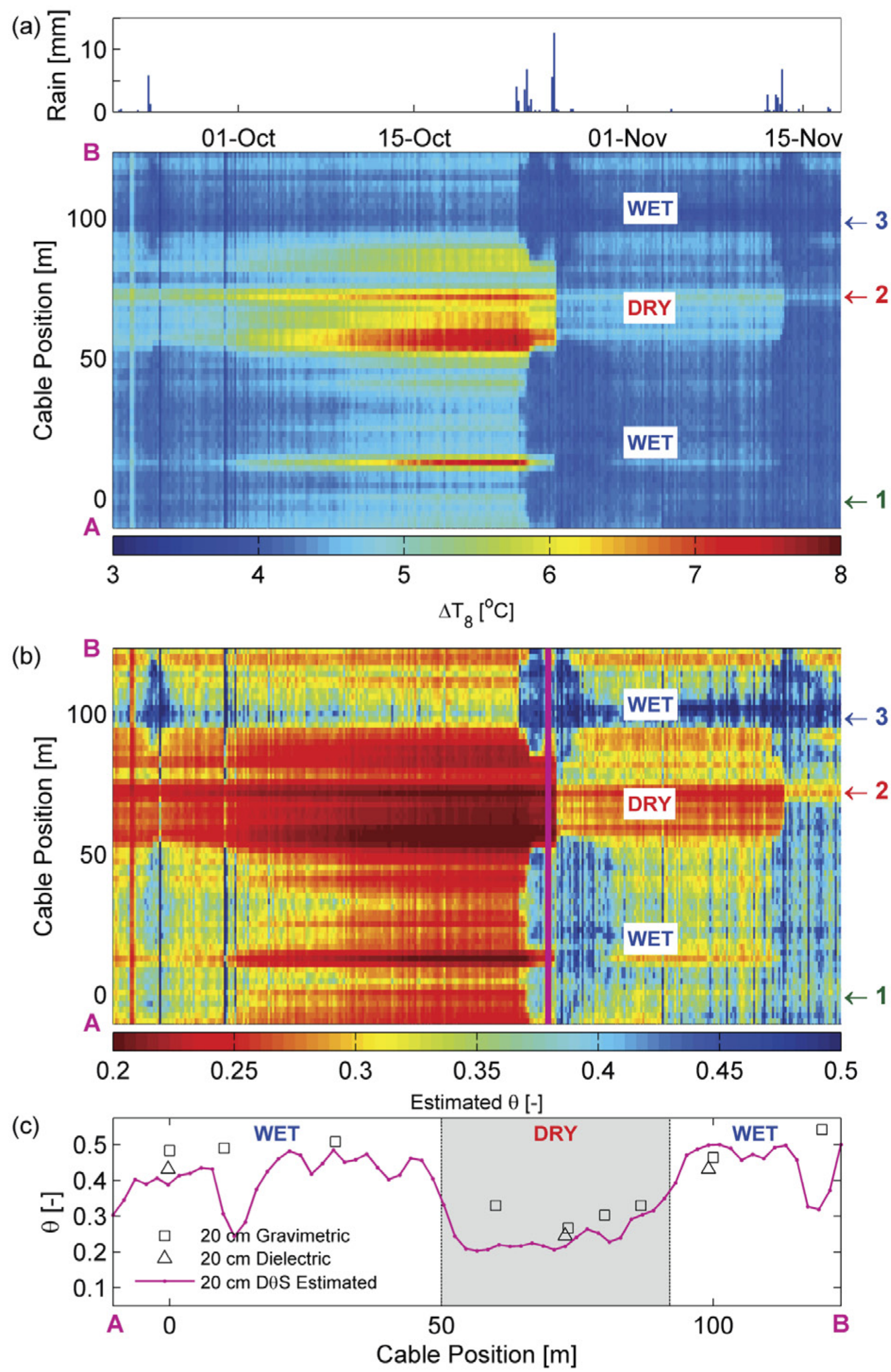

Fig. 6. (a) Time series (*x* axis) of 4-h rainfall totals and distributed temperature sensing (DTS/DθS) measured average temperature rise 8 min after heating began for each 2-m interval along a 130-m cable transect, (b) time series of estimated soil moisture values based on the active DTS data from each 2-m interval along the cable, and (c) a plot of active DTS soil moisture estimates and independent soil moisture estimates vs. cable position on 25 Oct. 2010 at 1600 h (Reprinted from *Groundwater* with permission of the National Ground Water Association. Copyright 2012; Striegl and Loheide, 2012)..

DEDICATED SOIL MOISTURE REMOTE SENSING MISSIONS

Remote sensing approaches for soil moisture monitoring have been investigated since the 1970s, although the first dedicated soil moisture mission, SMOS, was not launched until 2009. However, soil moisture estimates are also being retrieved from satellite instruments not specifically designed for sensing soil moisture, most notably from microwave sensors operating at suboptimal frequencies. The Advanced Microwave Scanning Radiometer for the Earth Observing System (AMSR-E) instrument was carried into orbit aboard the NASA Aqua satellite in 2002 and provided passive measurements at six dual-polarized frequencies until October 2011, when a problem with the rotation of the antenna ended the data stream (Njoku et al., 2003). Several different retrieval algorithms have been developed to retrieve soil moisture from the lowest two frequencies (6.9 and 10.6 GHz) observed by AMSR-E (e.g., Owe et al., 2001; Njoku et al., 2003). Soil moisture information is also being retrieved from active microwave sensors, specifically from ESA's Advanced Scatterometer (ASCAT), which was launched in 2006 aboard the MetOp-A meteorological satellite (and before that from ASCAT's predecessors, the European Remote Sensing [ERS] satellites) The ERS and ASCAT instruments are C-band radar scatterometers designed for measuring wind speed; however, soil moisture retrievals have also been developed (Wagner et al., 1999). An operationally supported, remotely sensed soil moisture product derived from the ASCAT instrument is currently available (Wagner et al., 2013). Wagner et al. (2007) provided an excellent review of then-existing satellite remote sensing approaches for soil moisture; here, we focus on two newer satellite approaches and one airborne approach.

Soil Moisture and Ocean Salinity Mission

The SMOS mission (Kerr et al., 2010), an Earth Explorer Opportunity mission, was launched on 2 Nov. 2009 and concluded its commissioning phase in May 2010. It was developed under the leadership of the ESA with the Centre National d'Etudes Spatiales (CNES) in France and the Centro para el Desarrollo Teccnologico Industrial in Spain.

Microwave radiometry at low frequencies is an established technique for estimating surface soil moisture with an adequate sensitivity. The choice of L-band as the spectral range in which to operate was determined from a large number of studies that demonstrated that L-band has high sensitivity to changes in moisture in the soil (Schmugge and Jackson, 1994) and salinity in the ocean (Lagerloef, 2001). Furthermore, observations at L-band are less susceptible to attenuation due to the atmosphere or vegetation than measurements at higher frequencies (Jackson and Schmugge, 1989, 1991). Also, L-band enables a larger penetration depth into the surface soil layer than is possible with shorter wavelengths (Escorihuela et al., 2010).

Even though the L-band radiometry concept was demonstrated early by a space experiment (SKYLAB) back in the 1970s, no dedicated space mission followed because achieving a ground resolution ≤50 to 60 km required a prohibitive antenna size (≥8 m). The so-called interferometry design, inspired from the very large baseline antenna concept (radio astronomy), made such a venture possible. Interferometry was first put forward in the 1980s (Le Vine, 1988) and validated with an airborne prototype (Le Vine et al., 1994, 1990). The idea consists of deploying an array of small receivers distributed along a structure that folds for launch, then unfolds in orbit. This approach enables reconstruction of a brightness temperature (T_B) field with a resolution corresponding to the spacing between the outermost receivers. The two-dimensional interferometer allows measuring T_B at several incidence angles with full polarization. Such an instrument instantaneously records a whole scene; as the satellite moves, a given point within the two-dimensional field of view is observed from different view angles. The series of independent measurements allows retrieving surface parameters with much improved accuracy.

The baseline SMOS payload is thus an L-band (1.413 GHz, 21 cm, located within the protected 1400–1427 MHz band) two-dimensional interferometric radiometer designed to provide accurate soil moisture data with moderate spatial resolution. The radiometer is Y-shaped, with three 4.5-m arms, as shown in Fig. 7. The SMOS is on a sun-synchronous (0600 h ascending) circular orbit and measures the T_B emitted from the Earth at L-band across a range of incidence angles (0–55°) across a swath of approximately 1000 km with a spatial resolution of 35 to 50 km (average is 43 km) and a maximum revisit time of 3 d for both ascending and

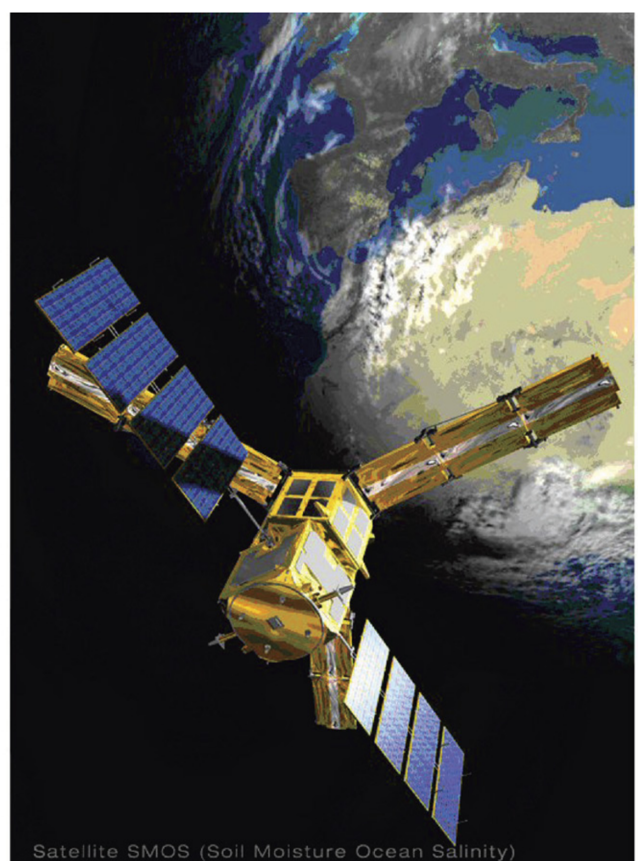

Fig. 7. Artist's view of the Soil Moisture and Ocean Salinity (SMOS) satellite (courtesy of Centre d'Etudes Spatiales de la BIOsphere, [CESBIO]).

descending passes (Kerr et al., 2001, 2010). A retrieval algorithm incorporating an L-band microwave emission forward model is applied to the T_B data to estimate soil moisture (Kerr et al., 2012).

The SMOS data quality was sufficient to allow the production—from an interferometer—of prototype global surface soil moisture maps within 1 yr after launch. It was the first time ever that such maps had been obtained. Initially, the accuracy was relatively poor and many retrievals were not satisfactory. The data were much impaired by radio frequency interference (RFI), leading to degraded measurements in several areas including parts of Europe and China (Oliva et al., 2012). Actions have since been taken by ESA and CNES to reduce the RFI. Specific RFI sources are now identified and their locations are provided to ESA personnel who interact directly with the appropriate national agencies. These efforts have resulted in >215 powerful and persistent RFI sources disappearing, including the U.S. Defense Early Warning System in northern Canada and many sources in Europe. Unfortunately, the remaining number of sources in some countries is large.

While RFI reduction and retrieval algorithm improvements were ongoing, efforts to validate the SMOS soil moisture retrievals began. In one of the first SMOS validation studies, locally calibrated relationships between surface soil moisture and microwave T_B allowed estimation of surface soil moisture from SMOS T_B data with RMSE values ranging from 0.03 to 0.12 $m^3\ m^{-3}$ when compared with the 5-cm soil moisture data from 11 stations of the SMOSMANIA in situ network in France (Albergel et al., 2011). A subsequent study using 16 stations in the SMOSMANIA network and a different SMOS soil moisture retrieval produced RMSE values ranging from 0.03 to 0.08 $m^3\ m^{-3}$ (Parrens et al., 2012). Across four in situ networks in the United States that are approximately the size of the SMOS footprint, Jackson et al. (2012) found RMSE values for SMOS ranging from 0.03 to 0.07 $m^3\ m^{-3}$. Collow et al. (2012) evaluated SMOS soil moisture retrievals against in situ soil moisture observations in Oklahoma and in the northern United States and found a consistent dry bias, with SMOS soil moisture values ranging from 0.00 to 0.12 $m^3\ m^{-3}$ lower than the in situ data from the 5-cm depth. In the northern United States, RFI from the Defense Early Warning System contributed to the bias. A dry bias for SMOS was also found by Al Bitar et al. (2012) using data from NRCS SCAN and snow telemetry (SNOTEL) in situ networks and by Albergel et al. (2012a) using data from in situ stations around the world. Understanding the causes of the apparent underestimation of surface soil moisture by SMOS in these studies is an important area of ongoing research.

One of the primary challenges in using SMOS soil moisture data is that the spatial support volume, roughly 40 km by 40 km by 5 cm, is not ideal for some applications. Significant horizontal spatial variability in soil moisture is likely to occur within a SMOS footprint. This sub-footprint-scale soil moisture variability can significantly influence catchment runoff responses (e.g., Zehe et al., 2005) and simulation of latent heat flux in a land surface model (e.g., Alavi et al., 2010; Li and Avissar, 1994). Some progress has been made toward deriving accurate soil moisture estimates with higher spatial resolution by using SMOS data together with other data sources. By combining SMOS data with data from the Moderate Resolution Imaging Spectroradiometer, surface soil moisture estimates with 4-km resolution (Merlin et al., 2010) and 1-km resolution (Merlin et al., 2012; Piles et al., 2011) have been developed. Further work is needed to refine and validate these higher resolution surface soil moisture estimates and to expand their spatial coverage beyond limited test areas.

The SMOS data are freely available from different sources, depending on the type (or level) of data required. Level 1 (T_B) and Level 2 (ocean salinity over oceans or soil moisture/vegetation opacity over land) data are available through the ESA (https://earth.esa.int/web/guest/missions/esa-operational-eo-missions/SMOS). Level 3 data consist of composited data for either 1 d (i.e., all the Level 2 data of 1 d in the same file), 3 d, 10 d, or a particular month and for the globe (either morning or afternoon passes) for soil moisture and vegetation opacity. Over oceans the sampling is either daily or monthly. Level 3 data are available from the Centre Aval De Traitement des Données SMOS through an ftp site (ftp://eftp.ifremer.fr/catds/cpdc; write to support@catds.fr to get access). The implementation of these Level 3 products may bring significant improvements, particularly in the vegetation opacity retrieval using temporal information (Jacquette et al., 2010). Figure 8 shows a typical monthly Level 3 soil moisture product. Note that the SMOS surface soil moisture maps are global in extent but contain gaps where no soil moisture retrieval is currently possible. These gaps are associated with RFI, steep topography, dense vegetation, snow cover, or frozen soils.

Soil Moisture Active Passive Mission

The NASA Soil Moisture Active Passive (SMAP) mission (Entekhabi et al., 2010) is scheduled to launch in October 2014. Like SMOS, the SMAP mission will utilize L-band measurements to determine surface soil moisture conditions, but SMAP will feature both active and passive L-band instruments, unlike SMOS, which relies on passive measurements alone. The SMAP measurement objective is to provide frequent, high-resolution global maps of near-surface soil moisture and freeze–thaw state. These measurements will play a role in improving estimates of water, energy, and C fluxes between the land and atmosphere. Observations of the timing of freeze–thaw transitions over boreal latitudes may help reduce major uncertainties in quantifying the global C balance. The SMAP soil moisture mission requirement is to provide estimates of soil moisture at 10 km spatial resolution in the top 5 cm of soil with an error of no >0.04 $m^3\ m^{-3}$ at 3-d average intervals across the global land area, excluding regions of snow and ice, frozen ground, mountainous topography, open water, urban areas, and vegetation with water content >5 kg m^{-2} (averaged across the spatial resolution scale). This level of performance will enable SMAP to meet the needs of hydrometeorology and hydroclimate applications.

The SMAP spacecraft (Fig. 9) will carry two L-band microwave instruments: a non-imaging synthetic aperture radar operating at 1.26 GHz and a digital radiometer operating at 1.41 GHz.

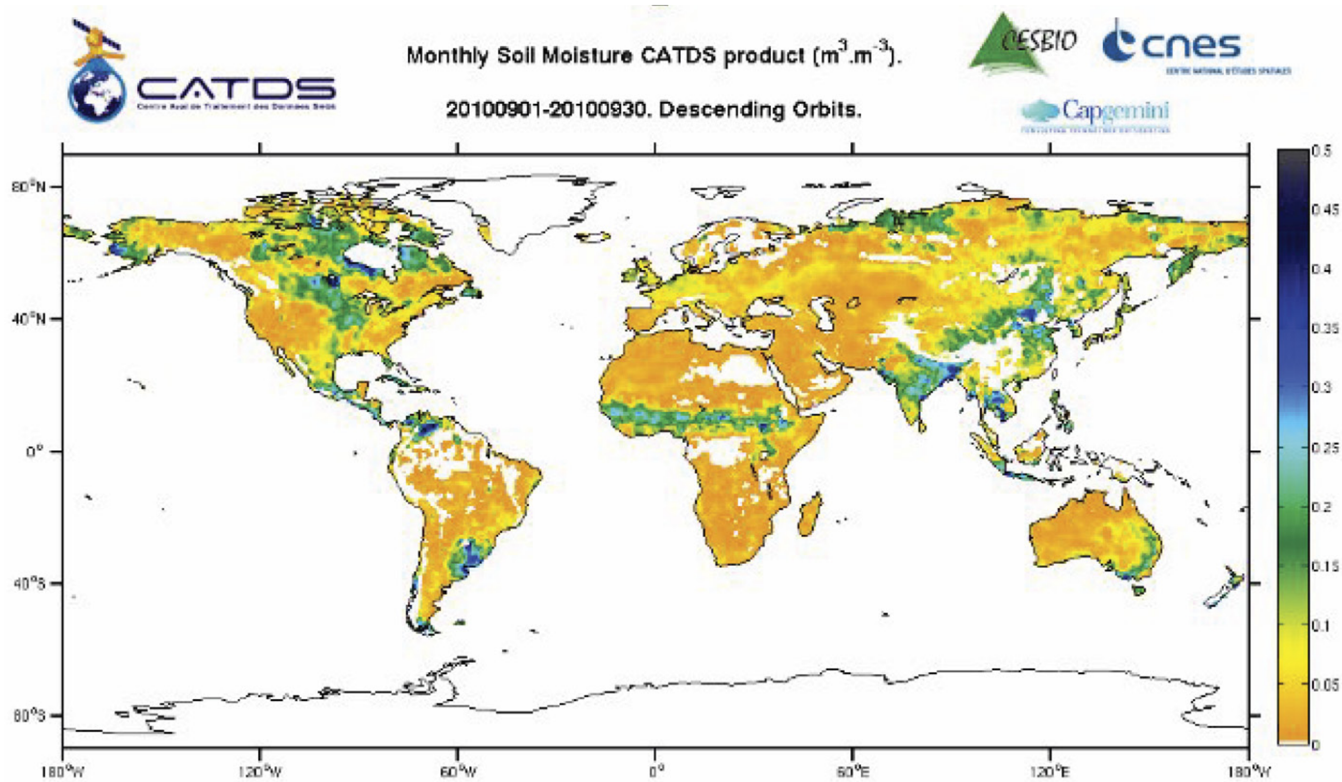

Fig. 8. Monthly soil moisture product (September 2010) (in m^3 m^{-3}). Note the wet patches in Argentina and the receding Intertropical Convergence Zone influence in the Sahel. Where topography is too steep, radio frequency interference too important, vegetation too dense (tropical rain forest), or soils are frozen or covered by snow, the retrievals are either not attempted or not represented (courtesy of CESBIO).

The instruments share a rotating 6-m offset-fed mesh reflector antenna that sweeps out a 1000-km-wide swath. The spacecraft will operate in a 685-km polar orbit with an 8-d repeating ground track. The instrument is designed to provide global maps of the soil moisture and freeze–thaw state with a maximum revisit time of 3 d using combined active (radar) and passive (radiometer) instruments. The radiometer incorporates RFI mitigation features to protect against RFI from human-made transmitters. The radiometer is designed to provide accurate soil moisture data at moderate spatial resolutions (40 km) by measuring microwave emission from the surface. The emission is relatively insensitive to surface roughness and vegetation. The radar measures backscatter from the surface with high spatial resolution (1–3 km in high-resolution mode) but is more influenced by roughness and vegetation than the radiometer. The combined radar and radiometer measurements are expected to provide soil moisture accuracy approaching radiometer-based retrievals but with intermediate spatial resolution approaching radar-based resolutions. Thus, the driving aspects of SMAP's measurement requirements include simultaneous measurement of L-band T_B and backscatter with a 3-d revisit and high spatial resolution (40 and 3 km, respectively). The combined SMAP soil moisture product will be output on a 9-km grid. Significant progress has been made toward developing a suitable soil moisture retrieval algorithm for merging the SMAP radiometer and radar data (Das et al., 2011).

The planned data products for SMAP are being developed by the SMAP project and Science Definition Team and include: Level 1B and 1C instrument data (calibrated and geolocated radar backscatter cross-sections and radiometer T_B); Level 2 geophysical retrievals of soil moisture; Level 3 daily composites of Level 2 surface soil moisture and freeze–thaw state data; and Level 4 value-added data products that are based on the assimilation of SMAP data into land surface models. The SMAP Level 1 radar data products will be archived and made available to the public by the Alaska Satellite Facility in Fairbanks, AK, while the Level 1 radiometer and all higher level products will be made available by the National Snow and Ice Data Center in Boulder, CO.

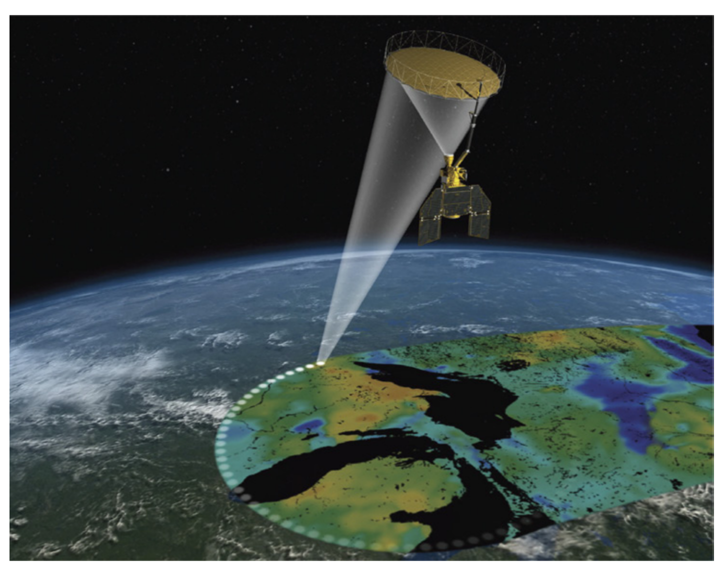

Fig. 9. Artist's view of the Soil Moisture Active Passive (SMAP) satellite.

The Level 4 products will support key SMAP applications and address more directly the driving science questions of the SMAP mission. The SMAP L-band microwave measurements will provide direct sensing of surface soil moisture in the top 5 cm of the soil column; however, several of the key applications targeted by SMAP require knowledge of root zone soil moisture (RZSM) in the top 1 m of the soil column, which is not directly measured by SMAP. The SMAP Level 4 data products are designed to fill this gap and provide model-based estimates of RZSM that are informed by and consistent with assimilated SMAP surface observations. The Level 4 algorithm will use an ensemble Kalman filter to merge SMAP data with soil moisture estimates from the NASA Catchment land surface model (Reichle et al., 2012). Error estimates for the Level 4 soil moisture product will be generated as a byproduct of the data assimilation system. A Level 4 carbon product will also be produced that utilizes daily soil moisture and temperature inputs with ancillary land cover classification and vegetation gross primary productivity inputs to compute the net ecosystem exchange (NEE) of CO_2 with the atmosphere over northern (>45° N) vegetated land areas. The SMAP Level 4 carbon product is intended to provide regional mapped measures of NEE and component C fluxes that are within the accuracy range of tower-based eddy covariance measurement approaches.

Airborne Microwave Observatory of Subcanopy and Subsurface Mission

Current estimates of NEE at regional and continental scales contain such important uncertainties that among the 11 or so models tested there could be differences of 100% or more, and it is not always clear whether the North American ecosystem is a net sink or source for C (Denning et al., 2005; Friedlingstein et al., 2006). Root zone soil moisture is widely accepted to have a first-order effect on NEE (e.g., Suyker et al.,2003), yet RZSM measurements are not often available with the spatial or temporal extent necessary for input into regional- or continental-scale NEE models. Unlike the L-band missions, SMOS and SMAP, which measure surface soil moisture, the Airborne Microwave Observatory of Subcanopy and Subsurface (AirMOSS) mission is designed to measure RZSM directly. The hypothesis of the NASA-funded AirMOSS project is that integrating spatially and temporally resolved observations of RZSM into ecosystem dynamics models can significantly reduce the uncertainty of NEE estimates and C balance estimates.

The AirMOSS plan is to provide measurements to estimate RZSM using an ultra-high-frequency (UHF, also referred to as P-band) airborne radar over representative sites of the nine major North American biomes (Fig. 10). These include boreal

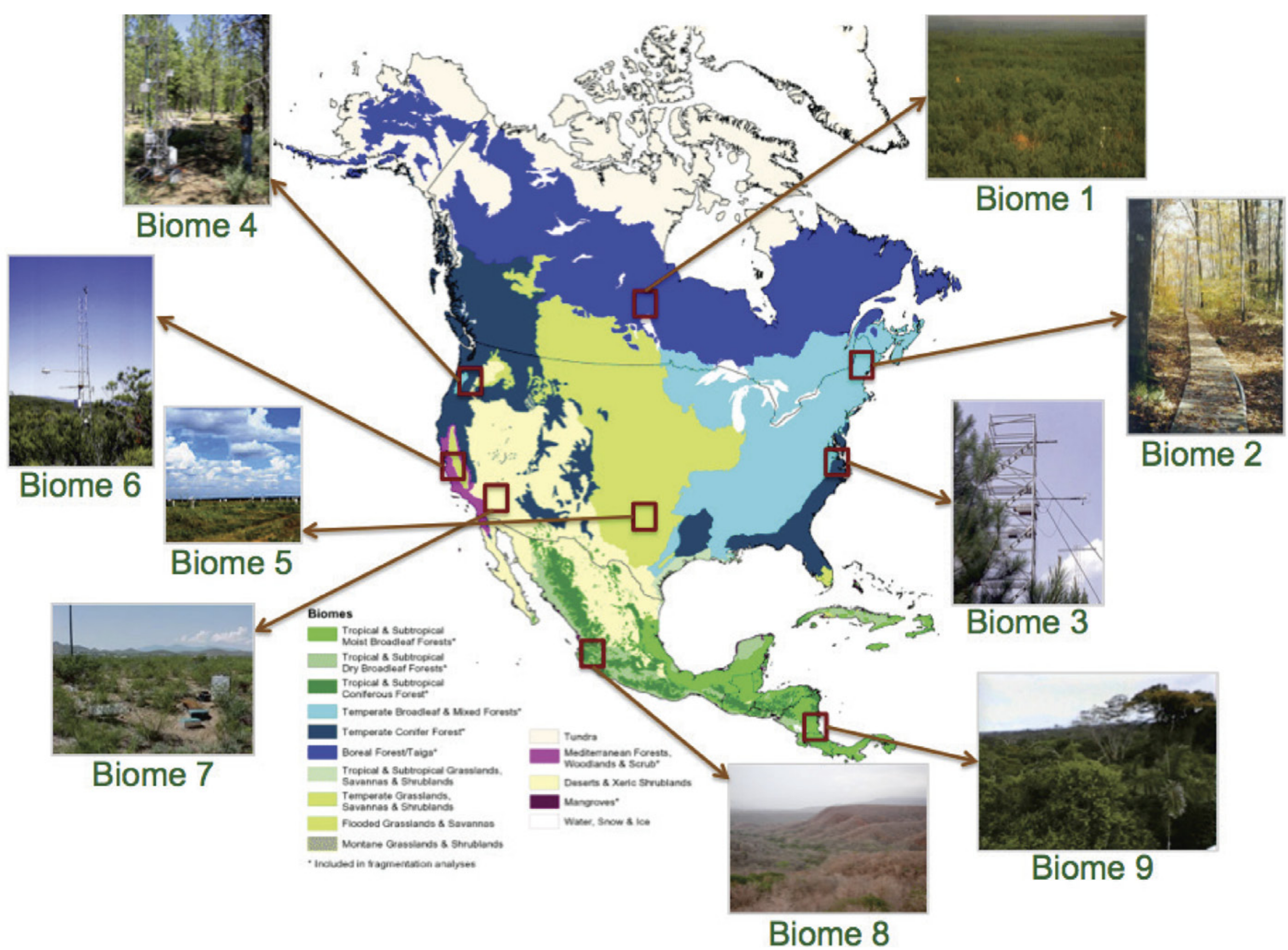

Fig. 10. Nine Airborne Microwave Observatory of Subcanopy and Subsurface (AirMOSS) flux sites covering the major distribution of vegetation types in North American biomes(courtesy of NASA/JPL-Caltech).

forest (Biome 1), temperate grassland and savanna shrublands (Biome 5), temperate broadleaf and mixed forest (Biome 2), temperate conifer forest east (Biome 3), temperate conifer forest west (Biome 4), Mediterranean woodlands and shrublands (Biome 6), arid and xeric shrublands (Biome 7), tropical and subtropical dry forest (Biome 8), and tropical and subtropical moist forest (Biome 9). These radar observations will be used to retrieve RZSM, which along with other ancillary data, such as topography, land cover, and various in situ flux and soil moisture observations, will provide the first comprehensive data set for understanding the processes that control regional C and water fluxes. The public access web site for the AirMOSS project is http://airmoss.jpl.nasa.gov/.

The airborne P-band radar system, flown on a NASA Gulfstream III aircraft, has a flight configuration over the experimental sites of typically 100 by 25 km made up of four flight lines (Fig. 11). This represents an intermediate footprint between the flux tower observations (on the order of 1 km) and regional- to continental-scale model simulations. Each AirMOSS flux site also has a hydrologic modeling domain of on the order of 100 by 100 km that will be populated with the corresponding ancillary data sets to allow flexibility in the flight line design. The hydrologic simulation domain is determined based on maximizing the overlap of full watersheds with the actual flight domain. These watersheds are to be simulated using the fully distributed, physically based finite element model Penn State Integrated Hydrologic Model (PIHM) (Qu and Duffy, 2007; Kumar et al., 2010). Carbon dioxide modeling will be performed using the Ecosystem Demography (ED2) model (Moorcroft et al., 2001). Each AirMOSS site has flux tower measurements for water vapor and CO_2 made using an eddy covariance system.

The P-band radar operates in the 420 to 440 MHz frequency range (70 cm), with a longer wavelength than typically used in the L-band missions such as SMOS or the upcoming U.S. SMAP mission. Previous studies using similar wavelengths have shown that RZSM can be computed with an absolute accuracy of >0.05 $m^3 m^{-3}$ and a relative accuracy of 0.01 to 0.02 $m^3 m^{-3}$ through a canopy of up to 120 Mg ha^{-1} and to soil depths of 50 to 100 cm, depending on the vegetation and soil water content (Moghaddam et al., 2000; Moghaddam, 2009). This P-band radar system has evolved from the existing Uninhabited Aerial Vehicle Synthetic Aperture Radar subsystems, including the radio frequency electronics subsystem, the digital electronics subsystem, the power subsystem, and the differential GPS subsystem. The radar backscatter coefficients are available at both 0.5 arc-s (approximately 15 m, close to the fundamental spatial resolution of the radar) and at 3 arc-s (approximately 100 m), and the retrieved RZSM maps will be at 3 arc-s resolution.

The AirMOSS flight operations began in fall of 2012, and all sites in North America except the tropical sites (Chamela, Mexico, and La Selva, Costa Rica) and the woody savanna site (Tonzi Ranch, CA) were flown. A three-band raw data image showing the spatial variation of soil moisture over the Metolius, OR, site, along with soil roughness and vegetation effects that have not yet been removed, is shown in Fig. 12.

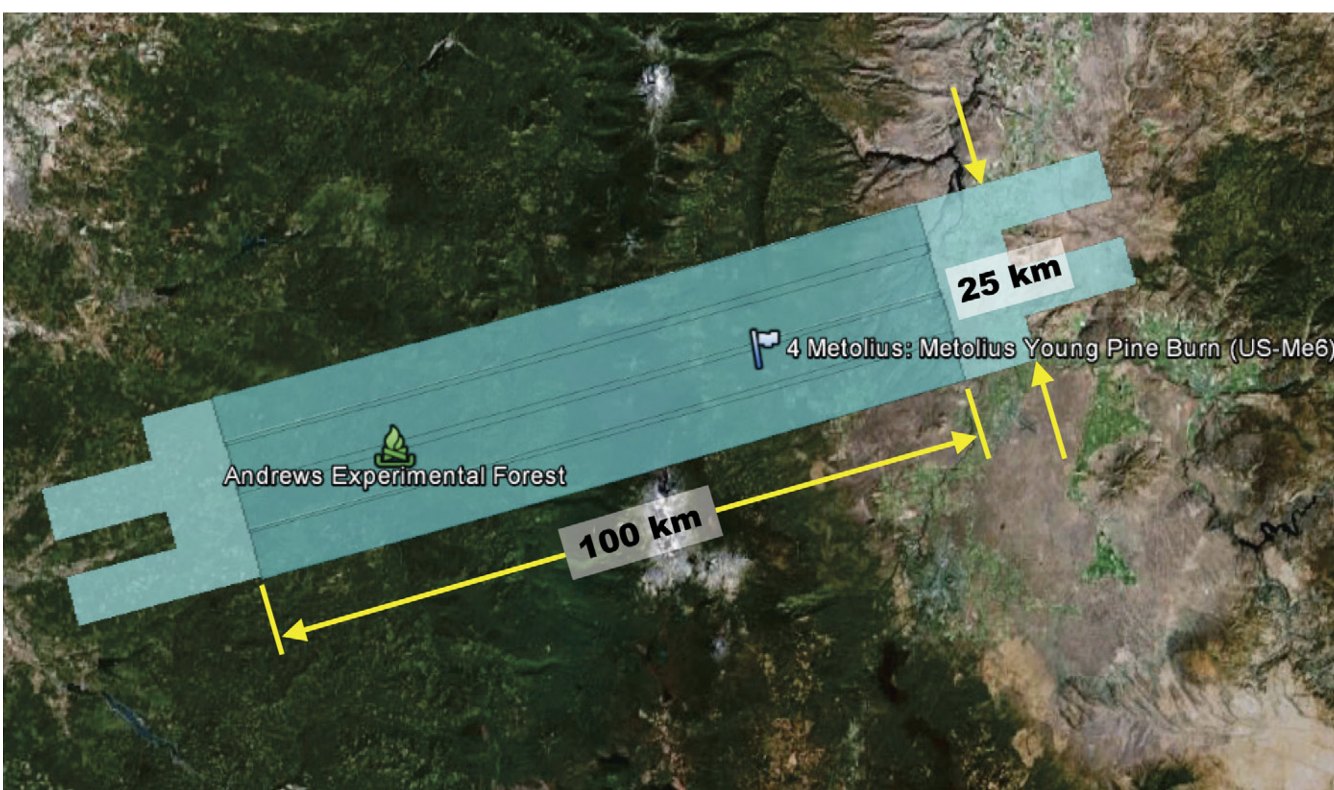

Fig. 11. Airborne Microwave Observatory of Subcanopy and Subsurface (AirMOSS) flight path made up of four flight lines, Metolius flux site, Cascade Mountains, Oregon.

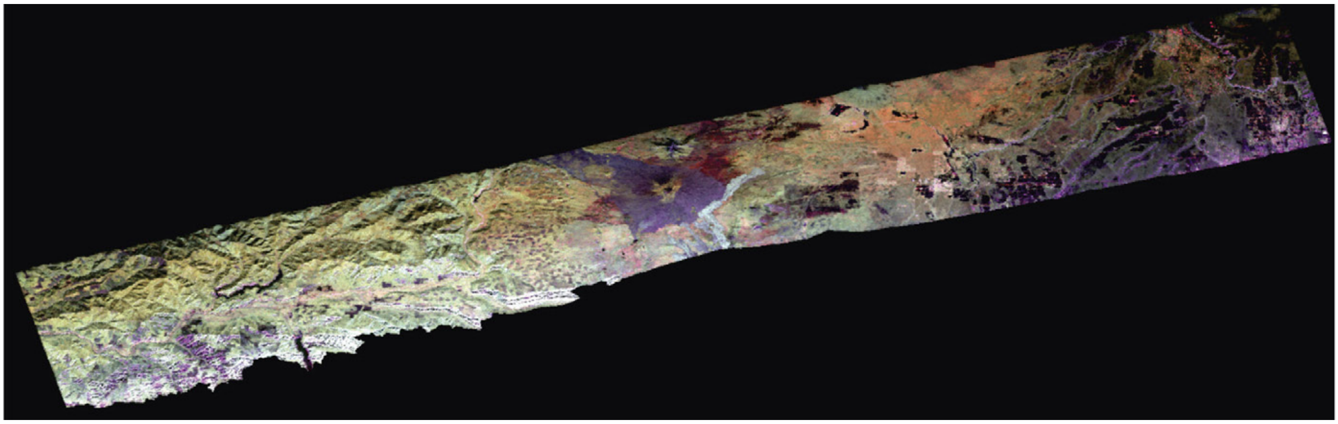

Fig. 12. Airborne Microwave Observatory of Subcanopy and Subsurface (AirMOSS) three-band (red = HH, green = HV, and blue = VV, where H is horizontal polarization and V is vertical polarization) radar image showing the spatial variation in backscattering cross section, corresponding to combined variations of soil moisture, soil roughness, and vegetation effects at the Metolius flux site, Cascade Mountains, Oregon. Effects of vegetation and surface roughness are removed in higher-order processing steps to produce maps of soil moisture profiles. The volcanic feature center of image is Black Butte cinder cone. (Image and description courtesy of Mahta Moghaddam, Univ. of Southern California. Image available from Alaska Satellite Facility AirMOSS image archives: https://www.asf.alaska.edu/program/sdc/data.)

LARGE-SCALE SOIL MOISTURE MONITORING NETWORKS

Soil moisture networks with spatial extents of $>100^2$ km^2 are well suited for monitoring the meteorological scale of soil moisture spatial variability as defined by Vinnikov et al. (1999) because atmospheric forcings often exhibit spatial autocorrelation lengths of 100s of kilometers. These large-scale networks are also appropriate for studies related to basin-scale hydrology and mesoscale meteorology. Numerous smaller networks exist worldwide with spatial extents $<100^2$ km^2, both within and outside the United States. For example, the USDA-ARS has developed several soil moisture networks to enhance their experimental watershed program. Locations include the Little Washita in Oklahoma, Walnut Gulch in Arizona, Reynolds Creek in Idaho, and Little River in Georgia (Jackson et al., 2010). The smaller scale networks are often well suited for watershed-scale hydrologic studies. A recent surge in the creation of these smaller scale networks has been driven by the need to validate soil moisture estimates from satellites such as SMOS and SMAP. A partial list of current and planned soil moisture networks with spatial extents $<100^2$ km^2 was provided by Crow et al. (2012).

Large-Scale Soil Moisture Networks in the United States

Large-scale soil moisture networks in the United States are currently operating in a variety of configurations at both national and state levels (Fig. 13; Table 1). In 1981, the Illinois Water Survey began a long-term program to monitor soil moisture in situ (Hollinger and Isard, 1994; Scott et al., 2010). This network was limited by its use of neutron probes, which required significant resources to operate and maintain. These neutron probes were used to measure soil moisture as frequently as twice a month.

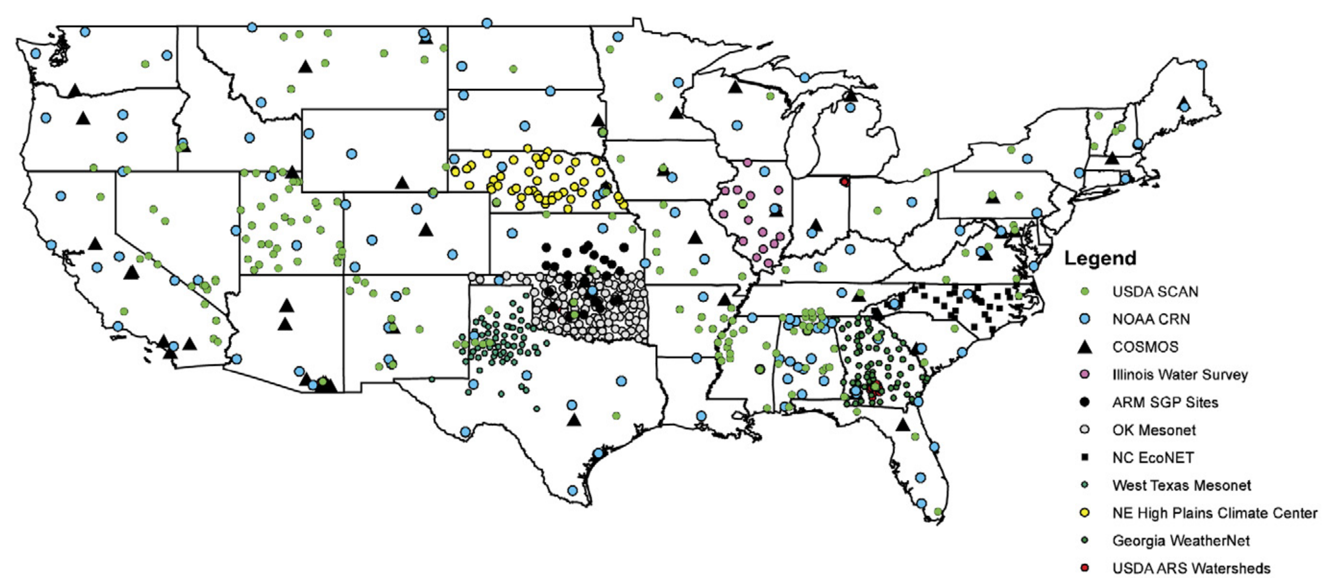

Fig. 13. In situ soil moisture monitoring sites across the continental United States, including those of the Soil Climate Analysis Network (SCAN), Climate Reference Network (CRN), Cosmic-Ray Soil Moisture Observing System (COSMOS), Atmospheric Radiation Measurement–Southern Great Plains (ARM-SGP) extended facility network, Oklahoma Mesonet, North Carolina Environment and Climate Observing Network (ECONet), and Northeastern High Plains Climate Center.

These stations were collocated with the Illinois Climate Network stations as the Water and Atmospheric Resources Monitoring Program and ultimately totaled 19 stations with measurements from the surface to a depth of 2 m. Beginning in 1998, these stations were converted to continuously monitor soil moisture using dielectric sensors (Hydra Probe, Stevens Water Monitoring Systems), providing regular statewide estimates of soil moisture.

The next network to develop was in Oklahoma, which has become a focal point for mesoscale weather and climate research. The Oklahoma Mesonet was launched in 1991 and became fully operational in 1994, now consisting of 120 stations, with at least one station in each county of Oklahoma (Brock et al., 1995; McPherson et al., 2007). Each station hosts a suite of meteorological measurements, including air temperature, wind speed and direction, air pressure, precipitation, and soil temperature. These stations monitor soil matric potential using heat dissipation sensors (CS-229, Campbell Scientific) at the 5-, 25-, and 60-cm depths, with archived data from the 75-cm depth available for some sites. These matric potentials can be converted to soil moisture estimates via site- and depth-specific water retention curves (Illston et al., 2008). Recent improvement in the accuracy of the water retention curve parameters has resulted in a field-validated, network-wide accuracy for the soil moisture data of ± 0.053 m^3 m^{-3} (Scott et al., 2013). Also distributed throughout Oklahoma is a network of stations belonging to the Southern Great Plains (SGP) site of the USDOE Atmospheric Radiation Measurement (ARM) Program (Schneider et al., 2003). This network uses the same type of sensor as the Oklahoma Mesonet. This network began in 1996 and spanned portions of Oklahoma and Kansas. There are a variety of facilities administered by the ARM-SGP site including a large central facility, as well as extended and boundary facilities, hosting meteorological, surface, and soil profile measurements.

While the Oklahoma Mesonet was being developed, the USDA NRCS began a pilot soil moisture–soil temperature project to monitor these parameters at the national scale. This project developed into the SCAN, which now numbers approximately 180 stations across the United States (Schaefer et al., 2007). This network has a standardized depth profile of Hydra Probe sensors at 5, 10, 20, 50, and 100 cm. A similar network to SCAN is the Climate Reference Network, operated by the NOAA National Climatic Data Center (Palecki and Groisman, 2011). This network commissioned 114 stations to provide a national-scale weather and climate monitoring network. Soil moisture sensors are being added to these stations based on the SCAN configuration (Hydra Probes at 5, 10, 20, 50, and 100 cm), but three profiles of sensors are installed at each site, providing data in triplicate for each depth. In addition to soil moisture, standard weather variables such as air temperature, solar radiation, precipitation, and wind speed are also collected.

A number of other statewide or large-scale networks have been developed since the mid-1990s. In 1998, the High Plains Regional Climate Center added soil moisture sensors to 14 Automated Weather Data Network (AWDN) stations in Nebraska. Since then, sensors have been added to other stations so that

Table 1. Partial list of large-scale (>100^2 km^2) in situ soil moisture monitoring networks ordered from largest to smallest in areal extent. The areas are enumerated by XX^2 to indicate the length of one side of a square of the given area; 100^2 km^2 = 10,000 km^2.

Network name	Country or state	Sites	Extent	Density†	Reference
		no.	km^2	km^2 $site^{-1}$	
Inside the United States					
Soil Climate Analysis Network	USA	180	3100^2	230^2	Schaefer et al. (2007)
Climate Reference Network	USA	114	3100^2	290^2	Palecki and Groisman (2011)
Cosmic Ray Soil Moisture Observing System	USA	67	3100^2	380^2	Zreda et al. (2012)
Plate Boundary Observatory Network	western USA	59	1800^2	240^2	Larson et al. (2008a)
Automated Weather Data Network	Nebraska	53	450^2	62^2	Hubbard et al. (2009)
Oklahoma Mesonet	Oklahoma	108	430^2	41^2	Illston et al. (2008)
Automated Environmental Monitoring Network	Georgia	81	390^2	44^2	Hoogenboom (1993)
Water & Atmospheric Resources Monitoring Program	Illinois	19	390^2	89^2	Scott et al. (2010)
Environment and Climate Observing Network	North Carolina	37	370^2	61^2	Pan et al. (2012)
West Texas Mesonet	Texas	53	300^2	41^2	Schroeder et al. (2005)
ARM-SGP extended facilities‡	Oklahoma/Kansas	13	150^2	42^2	Schneider et al. (2003)
Outside the United States					
Tibet-Obs	China	46	1600^2	230^2	Su et al. (2011)
Geological Survey of Finland (GTK)	Finland	23	580^2	121^2	Sutinen et al. (2008)
OzNet	Australia	38	290^2	47^2	Smith et al. (2012)
SMOSMANIA	France	21	200^2	44^2	Calvet et al. (2007)
Gourma mesoscale site	Mali	10	170^2	55^2	de Rosnay et al. (2009)
Automatic Stations for Soil Hydrology	Mongolia	12	140^2	40^2	Yang et al. (2009)
Central Tibetan Plateau SMTMN§	China	50	100^2	14^2	Zhao et al. (2013)
Umbria Region Hydrometeorological Network	Italy	15	100^2	26^2	www.cfumbria.it

† Density was calculated as the ratio of extent to number of sites.

‡ The Atmospheric Radiation Measurement–Southern Great Plains (ARM-SGP) extended facility network is being restructured. Values listed are projections for summer 2013.

§ Soil Moisture/Temperature Monitoring Network.

now there are 53 stations throughout the state monitoring soil moisture on an hourly basis. These stations monitor soil moisture using impedance sensors (Theta Probe ML2x, Delta-T Devices Ltd.) at depths of 10, 25, 50 , and 100 cm (Hubbard et al., 2009).

The North Carolina Environment and Climate Observing Network (ECONet) has been in operation since 1999, when 27 stations were instrumented with Decagon ECH_2O probes (Pan et al., 2012). In 2003, these stations were converted to Theta Probe sensors and the network was expanded to 37. Unlike most other networks, this network does not have a near-surface measurement depth because these data are collected only at the 20-cm depth. The West Texas Mesonet was initiated by Texas Tech University in 1999 and currently monitors soil moisture at 53 stations at depths of 5, 20, 60, and 75 cm using water content reflectometers (615, Campbell Scientific) (Schroeder et al., 2005). In addition, the network monitors wind information, atmospheric pressure, solar radiation, soil temperature, precipitation, and leaf wetness. The Georgia Automated Environmental Monitoring Network began in 1991 (Hoogenboom, 1993) and has since grown to include 81 stations. Soil moisture sensors have been added to these stations at a depth of 30 cm for the purpose of agricultural and meteorological monitoring. The newest large-scale soil moisture networks in the United States are the COSMOS and GPS-IR networks described above. Additional networks are on the horizon as well, including the National Ecological Observatory Network (NEON), which will operate study sites in 20 ecoclimatic domains throughout the United States in the coming years (Keller et al., 2008).

Large-Scale Soil Moisture Networks Outside the United States

In recent years, several large-scale soil moisture monitoring networks have been established outside of the United States, serving research purposes, supporting natural hazard forecasting, or being an integrative part of meteorological observing systems (e.g., Calvet et al., 2007). Table 1 gives an overview of known large-scale networks that are currently measuring soil moisture on an operational or quasi-operational basis. No active network outside the United States has a spatial extent as large as that of the U.S. national networks, but several have spatial extents and densities comparable to the state-level networks in the United States. Some networks, such as those in France and Mongolia, were installed for validating satellite soil moisture missions and thus have a setup that allows representation of soil moisture variations as accurately as possible at the spatial scale of a satellite footprint.

The networks described in Table 1 have each been designed to meet different research and operational objectives, and this has resulted in a large variety of measurement setups and techniques, available metadata, data access points, and distribution policies. The first action to offer a centralized access point for multiple, globally available in situ soil moisture data sets was the Global Soil Moisture Data Bank (GSMDB; Robock et al., 2000, 2005). The GSMDB collected data sets existing at that time but did not perform any harmonization of variables or data formats. The first international initiative addressing the latter has been FLUXNET (Baldocchi et al., 2001), a "network of networks" dedicated to monitoring land–atmosphere exchanges of C, energy, and water. Unfortunately, within FLUXNET soil moisture is not measured at all sites, while, more importantly, practical use of soil moisture data from FLUXNET is severely hampered by restricted accessibility and the large time gap between acquisition of the data and their availability to the science community.

In 2009, the International Soil Moisture Network (ISMN; http://ismn.geo.tuwien.ac.at/) was initiated to overcome the issues of timeliness in data delivery, accessibility, and heterogeneity of data (Dorigo et al., 2011a, 2011b). This international initiative is a result of the coordinated efforts of the Global Energy and Water Cycle Experiment in cooperation with the Group of Earth Observations and the Committee on Earth Observation Satellites to support calibration and validation of soil moisture products from remote sensing and land surface models and to advance studies on the behavior of soil moisture across space and time. The decisive financial incentive was given by ESA, who considered the establishment of the ISMN critical for optimizing the soil moisture products from the SMOS mission.

The ISMN collects and harmonizes ground-based soil moisture data sets from a large variety of individually operating networks and makes them available through a centralized data portal. Currently, the database contains almost 7000 soil moisture data sets from more than 1600 sites, distributed among 40 networks worldwide (Fig. 14). Not all the networks are still active. Also, the data sets contained in the former GSMDB were harmonized and transferred into the ISMN. Recently, several updates of the ISMN system were performed to keep up with the increasing data amount and traffic and to meet the requirements of advanced users. Many data sets from operational networks (e.g., SCAN, the U.S. Climate Reference Network, and ARM) are now assimilated and processed in the ISMN on a fully automated basis in near-real time. In addition, an enhanced quality control system is being implemented (Dorigo et al., 2013) while novel methods are being explored to obtain objective measures of reliability and spatial representativeness of the various sites (Gruber et al., 2013).

Challenges and Opportunities Related to Large-Scale Soil Moisture Networks

The steadily increasing number of soil moisture monitoring stations goes hand in hand with the growing awareness of the role of soil moisture in the climate system. Nevertheless, Fig. 14 and 15 show that the current stations are concentrated geographically and mainly represent a limited number of Köppen–Geiger climate classes in temperate regions. The number of permanent soil moisture stations is still very limited in the tropics (A category), dry areas (Bw classes), and in high-latitude areas (Dfc and E classes). Especially in the latter, the hydrologic cycle is not yet well understood, and these regions are expected to be particularly sensitive to climate change. Thus, international efforts should concentrate on expanding networks in these areas.

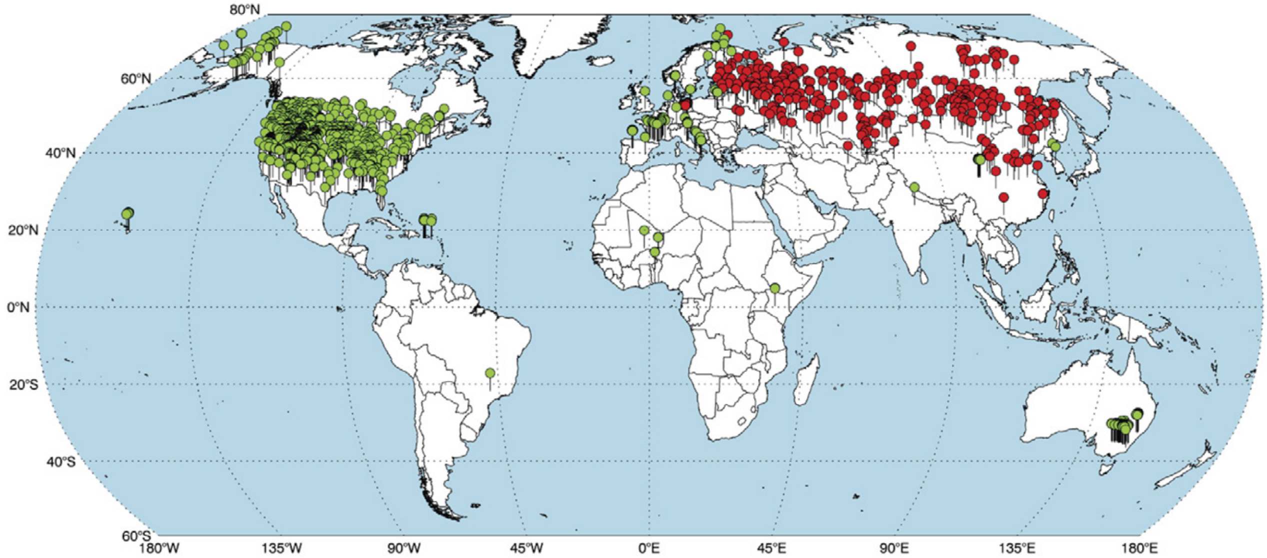

Fig. 14. Overview of soil moisture stations currently contained in the International Soil Moisture Network (ISMN). Green dots show the stations that are still measuring soil moisture, red dots the stations that were imported from the Global Soil Moisture Data Bank.

The major challenge, however, is not only to set up new networks but also to keep them operational in the future. Because many networks rely heavily on project funding, their continuation is typically only guaranteed for the lifetime of the project. Thus, internationally coordinated efforts should focus on developing mechanisms for continued financial and logistical support. One such mechanism is the integration of the ISMN into the Global Terrestrial Network for Hydrology as part of the Global Climate Observing System (2010). Alternatively, the integration of soil moisture monitoring sensors into existing operational meteorological stations may increase the probability for continued operation.

Another significant challenge for in situ networks is defining standards for the measurements themselves to enhance the consistency among sites. Best practices for sensor calibration, installation, and in situ validation, as well as data quality control procedures and data archiving and retrieval standards, need to be developed. The AWDN in Nebraska (Hubbard et al., 2009), the Oklahoma Mesonet (Illston et al., 2008), and the ISMN (Dorigo et al., 2013) have documented, automated quality control procedures in place that may prove useful for other networks. The Oklahoma Mesonet soil moisture network has also been subjected to in situ validation by soil sampling (Illston et al., 2008; Scott et al., 2013), allowing quantitative estimates of the accuracy of the soil moisture data. Calibration and validation are two separate

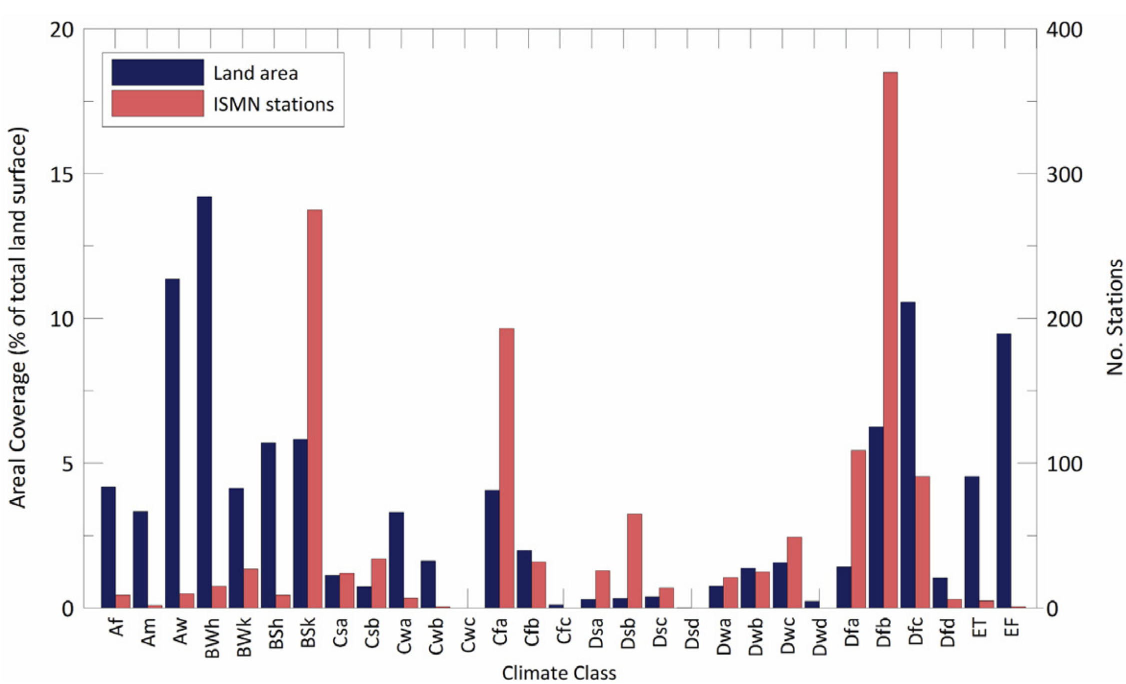

Fig. 15. Number of stations found within and area covered by the different Köppen-Geiger classes after Peel et al. (2007). For the class legend we refer to that publication. (Image credit: Mariette Vreugdenhil.)

and necessary steps in measurement. Calibration in this context means developing a relationship between the sensor output and the true soil moisture value. Validation in this context means collecting independent soil moisture data in situ after sensor installation to quantify the accuracy of the calibrated and installed sensor. Such in situ validation is needed for all networks.

APPLICATIONS OF LARGE-SCALE SOIL MOISTURE MEASUREMENTS

Drought Monitoring

Droughts are typically classified as meteorological, agricultural, or hydrologic (Mishra and Singh, 2010). Meteorological drought is indicated by a lack of precipitation over a specified region during a particular period of time. Agricultural drought occurs when declining soil moisture levels negatively impact agricultural production. Some have used the term ecological drought to designate similar conditions that reduce primary productivity in natural ecosystems (Le Houérou, 1996). These two drought concepts are closely related and should perhaps be represented by the composite term *agroecological drought*. A third common drought classification is hydrologic drought, which is a period of inadequate surface and subsurface water resources to support established water uses. Soil moisture is most directly related to agroecological drought, which is often preceded by meteorological drought and comes before hydrologic drought. This places soil moisture squarely in the center of the spectrum of drought classifications and drought indicators, but soil moisture measurements have been largely neglected in the science and practice of drought monitoring to date.

In earlier decades, this deficiency was unavoidable because sufficient soil moisture data were simply not available to enable their use in operational drought monitoring. That situation began to change dramatically in the 1990s with the rise of large-scale soil moisture monitoring networks in the United States (Hollinger and Isard, 1994; McPherson et al., 2007; Schaefer et al., 2007), a change now spreading around the world. Even more recently, global maps of surface soil moisture based on satellite remote sensing have become available, and these could be useful in drought monitoring. The primary impediment to the use of soil moisture measurements in operational drought monitoring is no longer a lack of data but rather a lack of scientific understanding regarding how soil moisture measurements quantitatively indicate agroecological drought. Strong and transparent conceptual models are needed to link soil moisture measurements with vegetation impacts in agricultural and ecological systems.

The first known attempt to use large-scale soil moisture measurements in drought monitoring was the Soil Moisture Index (SMI) introduced by Sridhar et al. (2008) based on data from the AWDN in Nebraska. Their results demonstrated that continuous soil moisture measurements at the 10-, 25-, 50-, and 100-cm depths from 37 stations in Nebraska formed the basis for a strong quantitative drought indicator. The SMI was subsequently revised by Hunt et al. (2009), who proposed the following relationship:

$$\mathrm{SMI} = -5 + 10\mathrm{F}_{\mathrm{AW}} \qquad [2]$$

where FAW is the fraction of available water, calculated as

$$\mathrm{FAW} = \frac{\theta - \theta_{\mathrm{wp}}}{\theta_{\mathrm{fc}} - \theta_{\mathrm{wp}}} \qquad [3]$$

where θ is the volumetric water content at a specified depth, θ_{fc} is the volumetric water content corresponding to field capacity, and θ_{wp} is the volumetric water content corresponding to the permanent wilting point. Hunt et al. (2009) calculated the SMI using data from sensors at the 10-, 25-, and 50-cm depths and then calculated the average SMI across depths.

The use of FAW as the basis for SMI is substantiated by current scientific understanding of plant water stress because water stress is more strongly related to the relative amount of plant-available water in the soil than to the absolute amount of soil moisture (Allen et al., 1998). Values of FAW are typically between 0 and 1; however, both higher and lower values are possible. The scaling relationship in Eq. [2] thus causes SMI values to typically fall in the range from −5 to 5. This scaling was chosen to make the range of SMI comparable to the range of other drought indicators (e.g., Drought Monitor; Svoboda et al., 2002). Although stress thresholds vary somewhat with plant species and weather conditions, generally FAW values <0.5 result in water stress (Allen et al., 1998). When FAW is 0.5, the SMI value is 0, the transition between stressed and unstressed conditions. Again using data from the Nebraska AWDN, Hunt et al. (2009) found that the modified SMI was effective for identifying drought onset as well as soil recharge from rainfall events following significant dry periods.

Recently, the SMI was applied using daily measurements of soil moisture in the 0- to 50-cm depth layer from a network of six monitoring stations in the Czech Republic (Mozny et al., 2012). That study supported the drought intensity scheme proposed by Sridhar et al. (2008) in which SMI values lower than −3 signify severe or extreme drought. Mozny et al. (2012) related the concept of *flash drought* to the SMI, specifying that a flash drought occurs when SMI values decrease by at least five units during a period of 3 wk. Thus, the SMI concept has shown good potential as a quantitative drought indicator based on soil moisture measurements, but some key uncertainties remain. The indicator is sensitive to the site- and depth-specific values chosen for θ_{fc} and θ_{wp}. These critical water contents can be estimated from the in situ soil moisture time series in some cases (Hunt et al., 2009), measured directly in the laboratory, calculated using pedotransfer function models (Schaap et al., 2001), or estimated from literature values (Sridhar et al., 2008), but best practices for determining these parameters in the SMI context need to be developed.

Recently, Torres et al. (2013) introduced a method for using long-term measurements of the soil water deficit (SWD) from a large-scale monitoring network to compute site-specific drought probabilities as a function of day of the year. Improved quantification of seasonal patterns in drought probability may allow crop cycles to be better matched with periods when drought is less likely to occur; therefore, yield losses due to drought may be reduced. The SWD for each soil layer (D) is defined as

$$D=\left(\theta_{fc}-\theta\right)\Delta z \qquad [4]$$

where Δz is the thickness of the soil layer; the SWD is calculated by summing D across the desired soil layers. Soil moisture data from eight stations of the Oklahoma Mesonet spanning 15 yr were used to calculate deficits for the 0- to 10-, 10- to 40-, and 40- to 80-cm layers. Drought was defined in this context as a period when the SWD is sufficient to cause plant water stress, i.e., SWD exceeds a predetermined threshold. The threshold was set for each site and layer as 0.5TAW, where TAW is the total available water calculated by substituting θ_{wp} for θ in Eq. [4]. Values of SWD calculated from 0 to 40 cm (SWD_{40}) were similar to 7-d cumulative atmospheric water deficits (AWD), calculated as reference evapotranspiration minus precipitation, during much of the spring and fall, but the soil and atmospheric deficits diverged in the winter and summer months (Fig. 16).

Historical drought probabilities estimated for each day of the year using the SWD data were consistent between depths and agreed with general knowledge about the climate of the region (Fig. 17), while probabilities estimated using AWD data (Purcell et al., 2003) were substantially lower and inconsistent with general knowledge about the region and with prior drought probability estimates in nearby states. Torres et al. (2013) proposed modifications to the AWD method, either lowering the AWD threshold used to define drought or extending the summation period from 7 to 15 d, both of which resulted in drought probability estimates more consistent with the estimates from the SWD method. They concluded that the new SWD method gave plausible and consistent results when applied to both the 0- to 40- and 0- to 80-cm soil layers and should be utilized when long-term soil moisture data are available.

The first known operational use of large-scale soil moisture measurements for drought monitoring involved not SMI or SWD, but a related measure, plant-available water (PAW). Plant-available water is defined as

$$PAW=\sum_{i=1}^{n}\left(\theta_i-\theta_{wpi}\right)\Delta z_i \qquad [5]$$

for soil layers i = 1, ..., n of thickness Δz_i. In 2012, the Oklahoma Mesonet (McPherson et al., 2007) introduced daily-updated PAW maps based on its network of >100 stations monitoring soil moisture at standard depths of 5, 25, and 60 cm. These maps are intended for use in drought monitoring and show PAW for the 0- to 10-cm (4-inch), 0- to 40-cm (16-inch), and 0- to 80-cm (32-inch) soil layers (www.mesonet.org/index.php/weather/category/soil_moisture_temperature). The depth units (e.g., millimeters or inches) of PAW make it compatible with familiar hydrologic measurements such as precipitation and evapotranspiration (ET). Figure 18 shows maps of departure from average PAW for the 0- to 40-cm (16-inch) soil layer across Oklahoma for the months of May 2012 and May 2013. The maps show that significantly drier than average PAW conditions prevailed across large areas of central and eastern Oklahoma in May 2012, but significantly wetter than average PAW conditions covered much of the state in May 2013. These soil moisture patterns bear little resemblance to U.S. Drought Monitor (Svoboda et al., 2002) maps from the same time periods (Fig. 18c and 18d), which suggests that drought conditions were substantially worse in May 2013 than May 2012 across the entire state. These maps illustrate that a drought indicator based on large-scale soil moisture monitoring can provide a dramatically different assessment of drought severity than the Drought Monitor, which blends information from meteorological indicators, streamflow percentiles, a soil moisture model, and expert opinion.

These recent developments in the use of soil moisture measurements for drought monitoring are encouraging; however, the research needs in this area are significant. As yet, little is known re-

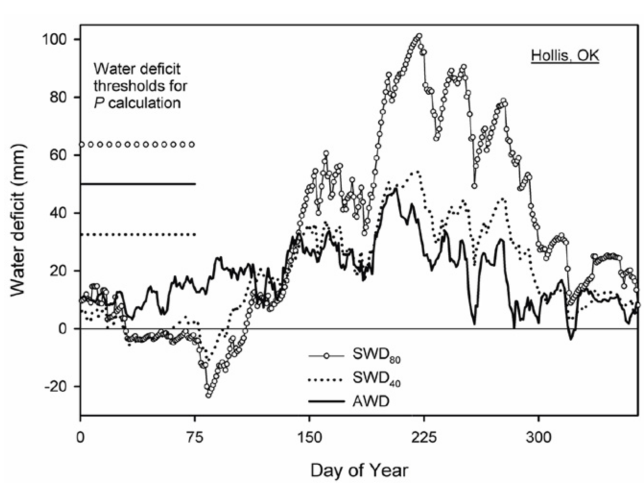

Fig. 16. Water deficit estimation by the atmospheric water deficit (AWD) method and soil water deficit methods for the 0- to 40- (SWD_{40}) and 0- to 80-cm depths (SWD_{80}), with corresponding water deficit thresholds used for calculating the probability (*P*) of drought. Averages of 15 yr for Hollis, OK (reproduced from Torres et al., 2013).

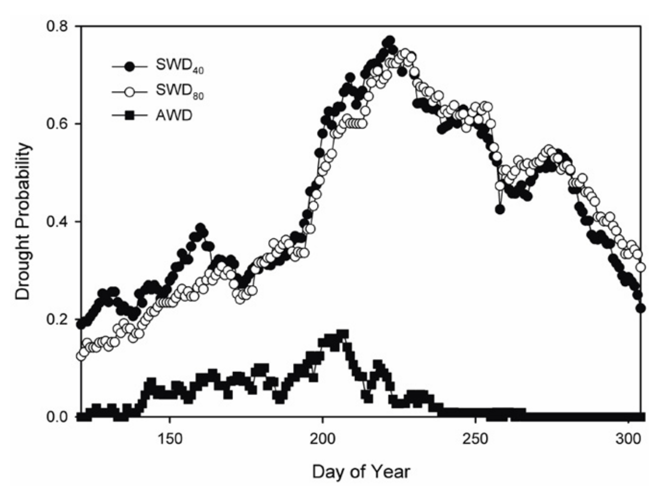

Fig. 17. Drought probabilities estimated by the atmospheric water deficit (AWD) method and soil water deficit (SWD) methods for the 0- to 40- (SWD_{40}) and 0- to 80-cm depths (SWD_{80}). Average for 15 yr and eight sites in Oklahoma for 1 May through 31 October (reproduced from Torres et al., 2013).

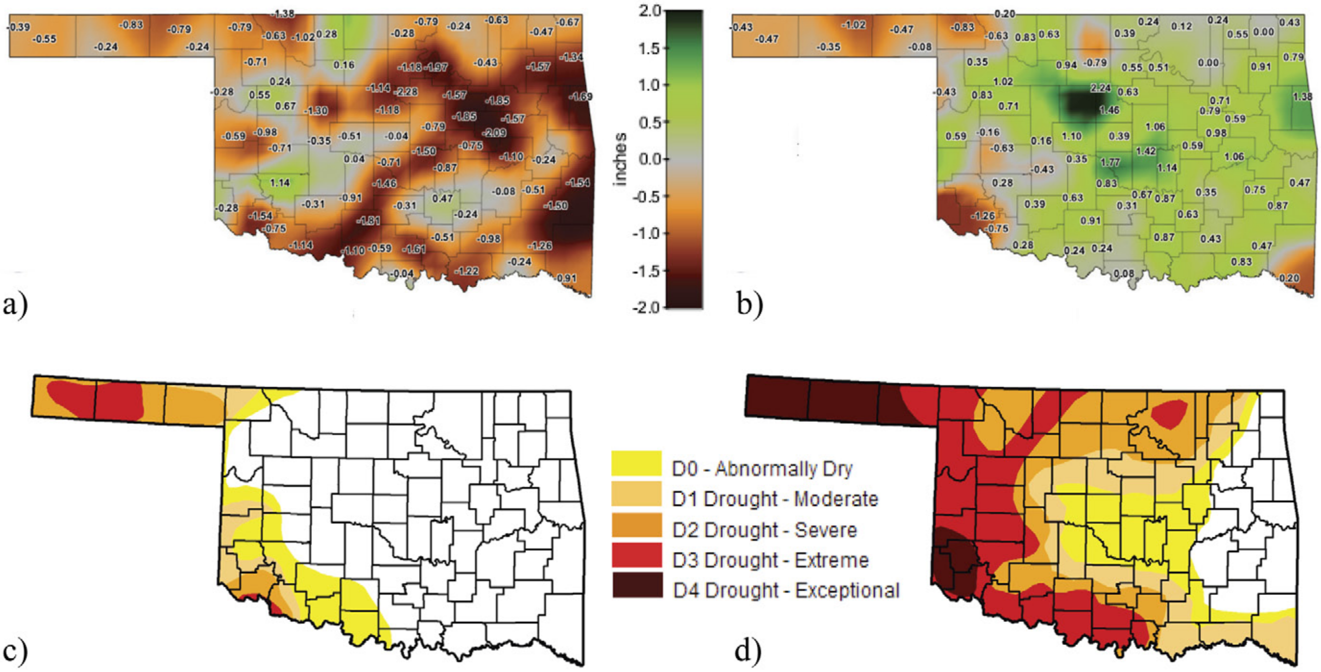

Fig. 18. Departure from average plant-available water (PAW) for the 0- to 40-cm (16-inch) soil layer across Oklahoma for (a) May 2012 and (b) May 2013, and U.S. Drought Monitor maps for Oklahoma for (c) 15 May 2012 and (d) 14 May 2013. The PAW maps were adapted from the Oklahoma Mesonet long-term averages maps (www.mesonet.org/index.php/weather/mesonet_averages_maps). The Drought Monitor maps were adapted from the U.S. Drought Monitor archives (droughtmonitor.unl.edu/archive.html).

garding how soil moisture-based drought indicators relate to other widely accepted drought indicators like the Standardized Precipitation Index (Guttman, 1999) or the Palmer Drought Severity Index (Palmer, 1965). Likewise, we do not know how soil moisture-based drought indicators are related to actual drought impacts in agricultural or ecological systems. Already SMI, SWD, and PAW have demonstrated potential as soil moisture-based drought indicators driven by in situ measurements. Other soil moisture-based indicators have been proposed on the basis of numerical modeling studies. These include the model-based Normalized Soil Moisture index (Peled et al., 2009) and the Soil Moisture Deficit Index (Narasimhan and Srinivasan, 2005), neither of which has been evaluated using actual soil moisture measurements.

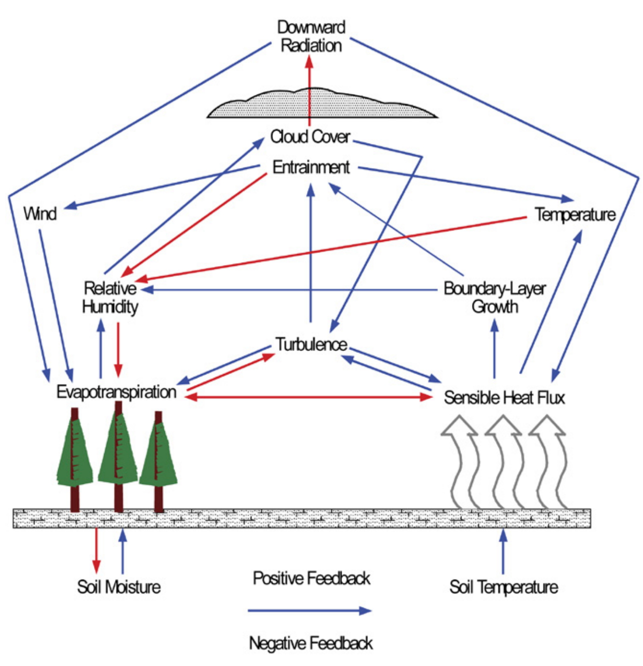

Fig. 19. Schematic of principle atmospheric boundary layer interactions with the land surface conditions (modified from Ek and Mahrt, 1994). Note that two consecutive negative feedbacks result in a positive feedback.

Furthermore, most in situ soil moisture measurements are made under grassland vegetation because of problems with establishing long-term meteorological stations in cropland or forest. There is a dearth of research on how to estimate soil moisture under contrasting land use–land cover combinations based on in situ observations under grassland vegetation. This deficiency complicates the interpretation of agroecological drought indicators based on in situ soil moisture measurements. Clearly, there should be a role for satellite remote sensing of soil moisture to assist in overcoming some of the deficiencies of drought monitoring by in situ soil moisture observations. Bolten et al. (2010) showed that AMSR-E surface soil moisture retrievals could add significant value to RZSM predictions in an operational drought modeling framework. Soil moisture data from AMSR-E have also shown potential as part of an integrated drought monitoring system for East Africa (Anderson et al., 2012); however, there are as yet no operational systems for drought monitoring that utilize satellite soil moisture measurements. We anticipate a surge in this type of research in the near future.

Meteorological Modeling and Forecasting

Drought provides a clear example of the interaction between the atmosphere and the land surface, an interaction strongly influenced by soil moisture conditions. A schematic of atmospheric boundary layer (ABL) interactions with the land surface is presented in Fig. 19. Daytime growth of the ABL is directly affected by soil and vegetation states and processes, and these processes play a role in partitioning the energy balance, which relates net radiation to soil heat flux, sensible heat flux, and latent heat flux, i.e., ET. Root zone soil moisture can influence the ABL by controlling land surface energy and moisture fluxes. For example, Basara and Crawford (2002) found that the soil water content in the root zone, particularly the 20- to 60-cm depth, during the summer was linearly correlated with daytime evaporative fraction and daily-maximum values of sensible heat flux and latent heat flux on days with strong radiative forcing and weak shear in the lower troposphere. Root zone soil moisture was also linearly related to key parameters in the ABL such as the daily maximum air temperature at 1.5 m.

Numerous large-scale hydrologic–atmospheric–remote sensing experiments have been conducted to better understand the soil moisture-moderated interactions of the soil–vegetation system with the diurnal ABL. Improved parameterization of general circulation models was one of the initial objectives of the experiments. Table 2 gives a concise overview of a few of these experiments, including HAPEX-MOBILHY, which was the first experiment conducted at this scale (André et al., 1986, 1988). Most of the experiments listed cover large geographic areas that play significant roles in the general circulation system of the planet.

The strong linkage of surface soil moisture and parameterization of soil hydraulic processes with the ABL response was demonstrated by Ek and Cuenca (1994) based on data from the HAPEX-MOBILHY. This study found that variations in soil hydraulic process parameterization could have a clear impact on the simulated surface energy budget and ABL development. This impact was accentuated for dry to moderate soil moisture conditions with bare soils. Ek continued to do considerable work in the area of simulation of the ABL and the influence of soil moisture conditions, often using data from regional experiments such as HAPEX-MOBILHY and the Cabauw data set from the Netherlands (Monna and van der Vliet, 1987). Data from HAPEX-MOBILHY were used to evaluate the evolution of the relative humidity profile in the ABL (Ek and Mahrt,1994). The relationships among canopy conductance, root density, soil moisture, and soil heat flux with simulation of the ABL using the Cabauw data set were investigated by Ek and Holtslag (2004). The ABL simulation evolved from the Oregon State University one-dimensional planetary boundary-layer model (OSU1DPBL) (Mahrt and Pan, 1984; Pan and Mahrt, 1987) to the Coupled Atmospheric Boundary Layer–Plant–Soil (CAPS) model. These models in turn are the basis for the Noah land-surface model (Chen and Dudhia, 2001; Ek et al., 2003), which plays a major role in the medium-range forecast model for numerical weather prediction (NWP) at the NOAA National Center for Environmental Prediction.

Given its influence on ABL development, RZSM can have a strong influence on weather forecasts. If not suitably constrained, the RZSM in an atmospheric model will drift from the true climate, resulting in erroneous boundary layer forecasts (Drusch and Viterbo, 2007). Since the mid 1990s, many NWP centers have been indirectly constraining their model soil moisture using methods that minimize the errors in measured screen-level (1.5–2.0-m) temperature and humidity (Best et al., 2007; Hess, 2001; Mahfouf, 1991; Mahfouf et al., 2009). While this approach reduces boundary layer forecast errors, it does not generate realistic soil moisture because the latter is often adjusted to compensate for model errors unrelated to soil moisture (Douville et al., 2000; Drusch and Viterbo, 2007; Hess, 2001). Ultimately, a model with inaccurate soil moisture cannot accurately describe the atmosphere across the full range of forecast lengths produced from NWP models.

Hence, the NWP community has been working toward improving model soil moisture by assimilating remotely sensed near-surface soil moisture. Near-surface soil moisture is more directly related to RZSM than screen-level variables, and assimilating near-surface soil moisture data (0–5 cm) has been shown to improve model RZSM (Calvet et al., 1998; Hoeben and Troch, 2000; Montaldo et al., 2001). Figure 20 compares several experiments constraining model RZSM by assimilating observations of near-surface soil moisture and screen-level temperature and relative humidity, highlighting the fundamental difference between these two approaches. These experiments were conducted with Météo-France's NWP land surface model using an extended Kalman filter and the AMSR-E Land Parameter Retrieval Model near-surface soil moisture data (Owe et al., 2001; for further details, see Draper et al., 2011).

In general, assimilating the screen-level observations improved the fit between the mean forecast and observed screen-level variables compared with the open loop; however, the assimilation had a slight negative impact on the fit between the mean forecast and observed near-surface soil moisture. In contrast, assimilating the AMSR-E soil moisture improved the fit between the mean forecast and observed near-surface soil moisture while degrading the fit between the modeled and observed screen-level variables. This result is consistent with previous studies showing that adjusting model soil moisture to improve screen-level forecasts does not necessarily improve soil moisture (Douville et al., 2000; Drusch and Viterbo, 2007; Seuffert et al., 2004), and

Table 2. Selected large-scale hydrologic–atmospheric–remote sensing experiments.

Experiment	Lead agency	Location	Climatic regime	Observation period†
HAPEX-MOBILHY	Météo, France	southwest France	temperate forest	summer, 1986
HAPEX-Sahel	Météo, France	Niger	tropical arid	summer, 1992
BOREAS	NASA	Canada	boreal forest	spring/fall 1994, 1996
IHOP	National Science Foundation (NSF)	Kansas, Oklahoma, Texas	continental	2002
HYMeX	Global Energy and Water Exchanges Project (GEWEX)	Europe	Mediterranean	2010–2020 (LOP) 2011–2015 (EOP)
CZO	NSF	6 sites	varies	2007–current
AirMOSS	NASA	7 sites	varies	2011–2015

† LOP, long-term observation period; EOP, enhanced observation period.

conversely, improving the model soil moisture does not necessarily improve atmospheric forecasts (Seuffert et al., 2004). Consequently, in the foreseeable future it is unlikely that remotely sensed near-surface soil moisture will be used in NWP in place of screen-level observations. Combining the assimilation of both observation types, however, can reduce errors in both model soil moisture and low-level atmospheric forecasts. For example, when both data types were assimilated together (Fig. 20), the fit between the model and both observation types was improved, although the mean soil moisture improvements were very small (see also Seuffert et al., 2004).

Currently, near-surface soil moisture observations are assimilated operationally at the UK Met Office (UKMO) and the European Centre for Medium Range Weather Forecasting (ECMWF). While the development of soil moisture assimilation in NWP is motivated by the eventual use of L-band observations (e.g., SMOS and SMAP), both centers are currently assimilating ASCAT Surface Degree of Saturation (SDS) data (Bartalis et al., 2007), an operationally supported remotely sensed soil moisture product with global coverage. At the UKMO, the screen-level observation based soil moisture analysis was amended in July 2010 to also constrain the near-surface soil moisture by nudging it with ASCAT SDS data (Dharssi et al., 2011). Compared with nudging with only screen-level observations, adding the ASCAT data very slightly improved near-surface soil moisture forecasts across selected sites in the United States while also improving screen-level temperature and relative humidity forecasts across the tropics and Australia (with neutral impact elsewhere). At the ECMWF, the NWP land surface analysis was updated in November 2010 to an extended Kalman filter based scheme, enabling the assimilation of remotely sensed data (de Rosnay et al., 2013; Drusch et al., 2009). To date the ASCAT data are not being used in their weather forecating model but are being assimilated together with screen-level observations in an offline land surface analysis system. Including the ASCAT data in this system has had a neutral impact on near-surface soil moisture and screen-level forecasts (Albergel et al., 2012b; de Rosnay et al., 2013).

The above examples highlight some challenges of land data assimilation specific to NWP applications. For example, the computation cost of the assimilation is a major limitation in NWP (de Rosnay et al., 2013; Drusch et al., 2009), hence the assimilation methods applied must be relatively simple. Further work is required to improve the land surface analysis schemes used in NWP, and in particular to propagate the surface soil moisture information into the root zone (not currently achieved by the schemes in place at the UKMO or ECMWF). Additionally, Dharssi et al. (2011) and de Rosnay et al. (2013) identified the observation bias correction strategy, i.e., the method by which satellite-derived surface soil moisture values are adjusted to be consistent with the

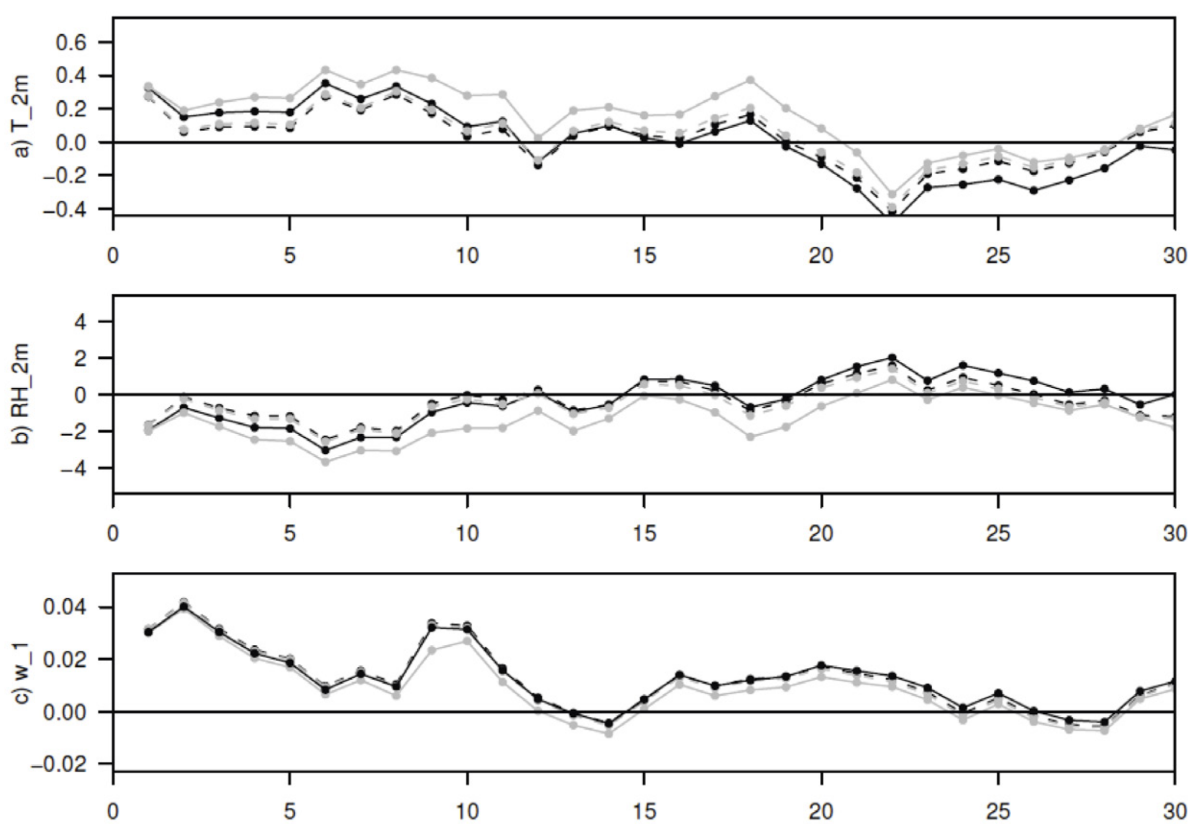

Fig. 20. Daily mean for each day in July 2006, averaged across Europe, of the observation minus 6-h forecast of (a) screen-level temperature (K), (b) screen-level relative humidity (%), and (c) near-surface soil moisture ($m^3 m^{-3}$), from no assimilation (black solid lines), and assimilation of screen-level temperature and relative humidity (black dashed lines), Advanced Microwave Scanning Radiometer for the Earth Observing System (AMSR-E) near-surface soil moisture (gray solid lines), and both (gray dashed lines) experiments. The assimilation was performed with an extended Kalman filter using Météo-France's Interactions between Soil, Biosphere, and Atmosphere (ISBA) land surface model(Reproduced from Draper et al., 2011).

model used for assimilation, as a likely cause of the limited impact of assimilating the ASCAT data. Bias correction of remotely sensed soil moisture is difficult in NWP because the long data records required to estimate statistics of the model climatology are not available from NWP models due to frequent model updates and the prohibitive cost of rerunning models.

The greatest challenge faced by soil moisture assimilation in NWP, however, is that improving the model soil moisture may not immediately improve atmospheric forecasts due to errors in the model physics. It is likely that the greatest contribution of using remotely sensed near-surface soil moisture observations in NWP will be in helping to identify and address these physics errors. Already, the availability of remotely sensed soil moisture and efforts to assimilate those data have stimulated improvements in modeling soil moisture processes. For example, in response to discrepancies between modeled and SMOS-observed T_B, the ECMWF recently improved their bare soil evaporation parameterization, resulting in improved model near-surface soil moisture and T_B (Albergel et al., 2012b). As soil moisture data are used more extensively in NWP models, this should also help to expose and eventually address other errors in the model surface flux processes.

Ecological Modeling and Forecasting

Ecological modeling is another area that could logically benefit from increased availability of large-scale soil moisture monitoring. Soil moisture is a key parameter in the control of plant growth, soil respiration, and the distribution of plant functional types in terrestrial ecosystems (Blyth et al., 2010; Ren et al., 2008; Pan et al., 1998; Neilson, 1995). Plant growth (i.e., assimilation of CO_2 through photosynthesis) is coupled with water loss through transpiration, which is regulated by soil water availability (Yang et al., 2011; Sellers et al., 1997; Field et al., 1995). Decomposition of soil organic C is also sensitive to soil moisture content via microbial activity and other processes (Ise and Moorcroft, 2006; Xu et al., 2004; Orchard and Cook, 1983). Furthermore, temporal and spatial availability of soil moisture content constrains the distribution and properties of plant functional types (Bremond et al., 2012; Seneviratne et al., 2010; Gerten et al., 2004; Breshears and Barnes, 1999).

A striking example of the interactions between vegetation and soil moisture conditions was provided by the Tiger Bush sites in the HAPEX-Sahel experiment. The Tiger Bush is made up of relatively long and narrow patches of vegetation approximately 40 m wide separated by nearly cemented patches of bare soil approximately 60 m wide, and these sites are characteristic of certain regions in the Sahel. One can note in the >3-m-deep profile in Fig. 21 (monitored by neutron probe) that there is limited variation in the soil moisture content and only in the upper 50 cm of the bare soil profile, while there are appreciable soil moisture changes even past 300 cm in the vegetated strip. The result is that nearly all of the high-intensity rainfall during the rainy season in this environment runs off the bare soil into the vegetated

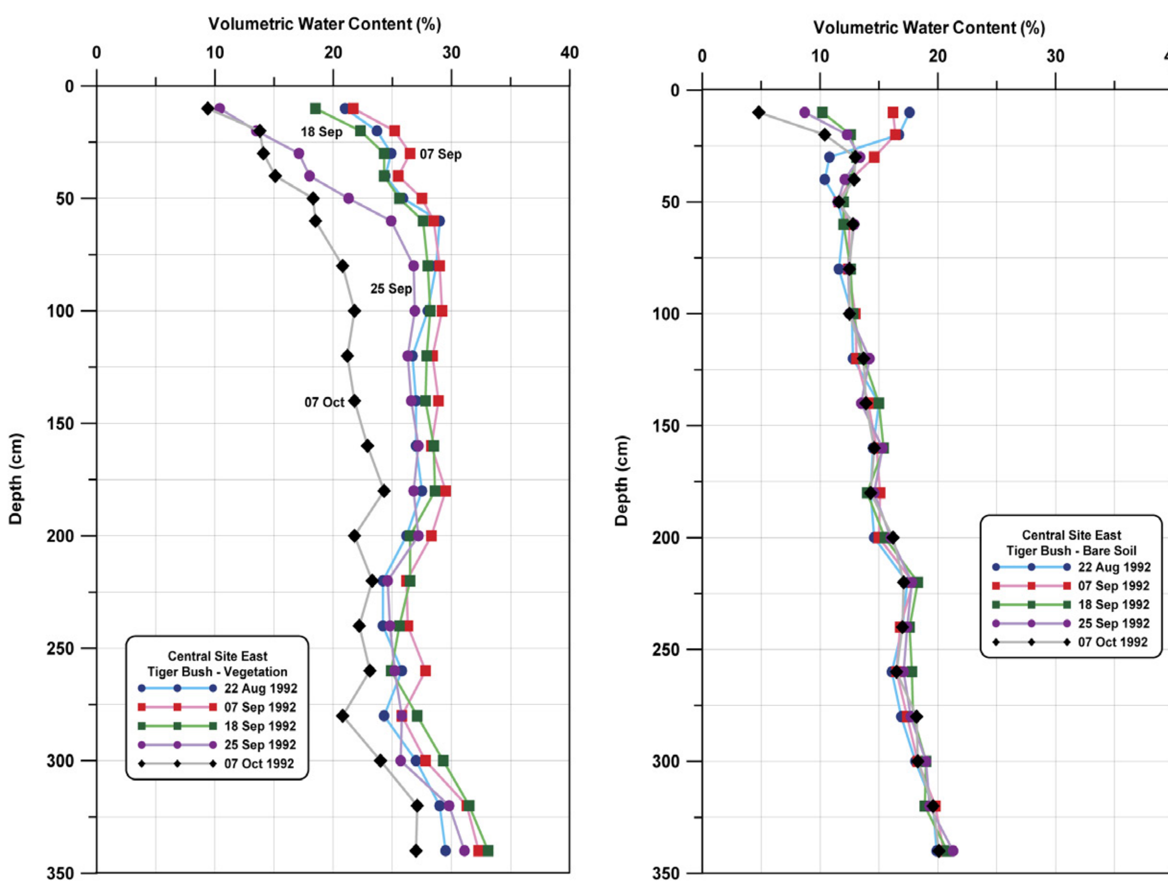

Fig. 21. Contrasting soil water depletion profiles from Central Site East–Tiger Bush, HAPEX-Sahel project (a) vegetated section and (b) bare soil section (modified from Cuenca et al., 1997).

strip, which thereby receives on the order of 200% of the precipitation. Verhoef (1995) noted this effect and that the result was a well-watered vegetation strip adjacent to a very dry bare soil strip in this environment. Verhoef (1995) was able to show that under the generally hot and dry conditions of the Sahel, advective conditions for sensible heat flux from the bare soil resulted such that the ET from the vegetated strip clearly exceeded the potential, or reference, ET rate (Verhoef et al., 1999; Verhoef and Allen, 2000). Carbon fluxes would obviously be affected by the heterogeneity in the Tiger Bush system as well.

To better understand and predict ecosystem dynamics such as these, different classes of ecological models have been developed for various scales and emphases. For example, biogeography models such as MAPSS (Neilson, 1995) and BIOME (Prentice et al., 1992; Haxeltine and Prentice, 1996) focus on the distribution of species and ecosystems in space. Biogeochemistry models such as CENTURY/DAYCENT (Parton et al., 1987, 1998), RothC (Jenkinson and Coleman, 1994), and DNDC (Li et al., 1992) place emphasis on the C and nutrient cycles within ecosystems. Biophysics models based on soil–vegetation–atmosphere transfer (SVAT) schemes (SiB: Sellers et al., 1986; BATS: Dickinson et al., 1986) have been developed to support regional and global climate modeling to provide accurate information for the fluxes of water, radiation, heat, and momentum between the atmosphere and the various land surfaces. Recently developed dynamic global vegetation models such as the Lund–Potsdam–Jena (LPJ) model (Sitch et al., 2003), IBIS (Foley et al., 1996), and MC1 (Bachelet et al., 2001) generally incorporate the above classes of models and schemes to simulate the dynamics of potential vegetation and its associated biogeochemical and hydrologic cycles.

These models estimate soil moisture content or its proxy using different schemes such as the bucket method (Robock et al., 1995; Manabe, 1969), the precipitation to potential evapotranspiration ratio method (Scheffer et al., 2005), and the water balance model (Law et al., 2002). Details of these and other schemes were discussed by Shao and Henderson-Sellers (1996) and Ren et al. (2008). These schemes often use simple algorithms to reduce computational demand and are less reliable than schemes used in hydrologic models (e.g., the Richards equation [Richards, 1931]). Also, especially in cases of large-scale ecological models, a more realistic parameterization of soil moisture content at subgrid-scale as related to topography is often desirable (Gordon et al., 2004). Optimization of the degree of the simplification and the spatial resolution is necessary due to computational restrictions but is difficult to judge due to the lack of adequate observational data with which to verify the performance of the models (Ren et al., 2008).

Traditionally, ecological models have been tested through comparison studies such as the Vegetation/Ecosystem Modeling and Analysis Project (VEMAP Members, 1995), the Carbon Land Model Project (Randerson et al., 2009), the Project for Intercomparison of Land-Surface Parameterization Schemes (Henderson-Sellers et al., 1996, 1995), and the Global Soil Wetness Projects (Dirmeyer et al., 2006; Dirmeyer, 1999) because evaluating the model performance, especially at larger scales, has been difficult due to the incompleteness of observation data sets. These models are not independent, however, because they have integrated the same theories and relied on similar data sets as they evolved (Reichstein et al., 2003). Therefore, while model comparison is an important task, extreme care must be exercised in deriving any conclusions.

Future research advances in this area will require the use of new observation data at suitable spatial and temporal scales (Seneviratne et al., 2010). Observation data from large-scale soil moisture monitoring in particular should be valuable to validate the simplification and scaling of ecological models. Wagner et al. (2003) found that modeled 0- to 50-cm monthly average soil moisture from the LPJ dynamic global vegetation model agreed "reasonably well" for tropical and temperate locations with values derived from a satellite microwave scatterometer, yielding Pearson correlation coefficients >0.6. The agreement was poorer for drier and colder climatic regions. Few studies, however, have used large-scale soil moisture data to improve the structure or parameterizations of ecological models or to improve model predictions through data assimilation.

Furthermore, the relationship between soil moisture and the terrestrial ecosystem is dynamic and interdependent: soil moisture constrains the properties of the ecosystem as described above, which, in turn, modifies the hydrology through evapotranspiration, leaf area index, and surface roughness (Breshears and Barnes, 1999). Newer generations of ecological models, especially dynamic global vegetation models, include these important feedback processes to simulate the effects of future climate change on natural vegetation and associated C and hydrologic cycles. Validation of these models may reveal an increased need for data from large-scale soil moisture observations across various ecosystems and for continuous expansion of observation networks.

Hydrologic Modeling and Forecasting

One motivation underlying many large-scale soil moisture monitoring efforts is the desire to more accurately model and forecast watershed dynamics, especially streamflow and flood events. Pauwels et al. (2001) demonstrated the possibility of improved stream discharge estimates through the assimilation of surface soil moisture estimates derived using data from the ESA satellites ERS1 and ERS2 into a land–atmosphere transfer scheme. The study was limited to bare soil conditions and small catchments (<20 km^2). The assimilation improved discharge estimates 20 to 50% in seven out of the 12 cases considered but degraded model accuracy by up to 10% in the remaining five cases. Francois et al. (2003) showed that the assimilation of ERS1 data into a simple two-layer land surface scheme through an extended Kalman filter approach improved the Nash–Sutcliffe efficiency (NSE) for streamflow from 70 to 85%. Their study involved a larger catchment (104 km^2) than that of Pauwels et al. (2001) and included vegetation cover. The sensitivity of simulated flow to soil moisture was highest when soil moisture itself was high.

The assimilation scheme was also able to correct for 5 to 10% errors in the input data, e.g., potential ET or precipitation.

More recent applications of large-scale soil moisture data for hydrologic modeling and forecasting have focused on newer satellite remote sensing data sets. Brocca et al. (2010) used a simple nudging scheme to assimilate the ASCAT surface soil wetness index into a rainfall–runoff model for five catchments (<700 km^2) in the Upper Tiber River basin in Italy. Assimilation increased the NSE for streamflow prediction during flood events in all five catchments, with increases ranging from 2 to 17%. In a subsequent study, RZSM was estimated from the ASCAT surface soil moisture data through application of an exponential filter, and both data types were then assimilated into a two-layer rainfall–runoff model using an ensemble Kalman filter approach (Brocca et al., 2012). Assimilation of the RZSM estimates produced a clear improvement in discharge prediction for a 137-km^2 catchment (NSE improved from 76 to 86%), while assimilation of surface soil moisture had only a small effect.

Thus far only a few studies have evaluated methods for using soil moisture data to improve hydrologic forecasting in catchments of >1000 km^2. One example is the work of Meier et al. (2011), in which the ERS1 and ERS2 soil water index was used, along with rainfall data, to drive a conceptual rainfall–runoff model in an ensemble Kalman filter framework assimilating observed discharge every 10 d. The method was applied to three catchments in the Zambezi River basin in southern Africa. The catchments ranged in size from 95,300 to 281,000 km^2. The catchment average soil water index correlated well with measured discharge when the data were shifted by a catchment-specific time lag. This time lag allowed 40-d lead time streamflow forecasts with a NSE value of 85% for the largest watershed, but in a catchment with steep slopes and little soil water storage, the lead time was as short as 10 d. Gains in streamflow forecast accuracy have even been demonstrated by assimilating point soil moisture observations from a single location within a catchment of 1120 km^2 together with streamflow data, suggesting that even sparse observation networks in large catchments can be quite useful (Fig. 22; Aubert et al., 2003). The effectiveness of the assimilation process was dominated by streamflow assimilation when considering the entire period, but the effectiveness of the assimilation process was dominated by soil moisture assimilation during flood events.

That large-scale soil moisture monitoring can benefit hydrologic modeling and forecasting is now well established, with gains in forecast efficiency of 10 to 20% being typical; however, significant challenges and uncertainties remain. Most of the research to date in this area has focused on the use of satellite-derived surface soil moisture products, with few studies using in situ soil moisture measurements within a data assimilation framework (Aubert et al., 2003; Chen et al., 2011). Thus, the world's growing in situ soil moisture monitoring infrastructure (Table 1) is a virtually unexplored resource in this context, and many opportunities exist to develop hydrologic forecasting tools that utilize that infrastructure.

A key challenge associated with assimilation of soil moisture data, regardless of the source, is to identify and overcome structural deficiencies in the hydrologic models themselves. For example, a data assimilation experiment using in situ soil moisture measurements in Oklahoma was generally unsuccessful in improving streamflow predictions from the widely used Soil and Water Assessment Tool (SWAT) model (Chen et al., 2011). The calibrated SWAT model significantly underestimated the vertical coupling of soil moisture between upper and lower soil layers, and the inadequate coupling was apparently a structural, rather than parametric, problem in the model. Thus, the ensemble Kalman filter assimilation approach was not effective in improving estimates of deep soil moisture or streamflow. This particular challenge of correctly representing linkages between soil moisture across two or more soil layers has been identified as a key concern in studies with other models as well (Brocca et al., 2012). Further research is needed to optimize the structure of SWAT and other hydrologic models to maximize the benefits from assimilating increasingly available large-scale soil moisture observations (Brocca et al., 2012).

Another challenge that has been encountered in this arena is uncertainty regarding proper characterization of model errors and observation errors within the assimilation procedure (Francois et al., 2003; Brocca et al., 2012). Statistical representations of model errors must often be made in a somewhat arbitrary or subjective fashion, and preexisting biases in either the observations or the model can be particularly problematic (Chen et al., 2011; Brocca et al., 2012). Nevertheless, research in this area appears to be gaining momentum, and opportunities abound to advance hydrologic modeling and forecasting with the help of existing and emerging large-scale soil moisture data sets.

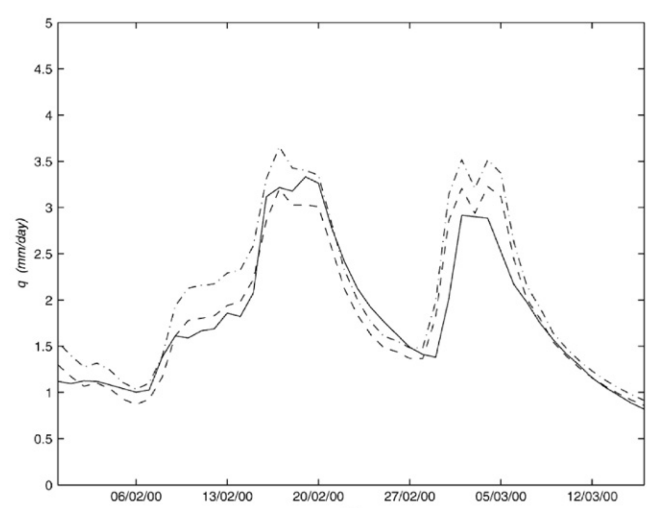

Fig. 22. Time series of streamflow (*q*) at the outlet of the Serein catchment in the Seine river basin in France for 1 Feb. to 15 Mar. 2000. The solid line indicates measured streamflow, the dash-dotted line indicates 1-d streamflow forecast without data assimilation, and the dashed line indicates 1-d streamflow forecast with assimilation of streamflow and in situ soil moisture data (Reprinted with permission from Elsevier from Aubert et al., 2003).

PRIMARY CHALLENGES AND OPPORTUNITIES

In this review, we have attempted to describe the state of the art in large-scale soil moisture monitoring and to identify some critical needs for research to optimize the use of increasingly available soil moisture data. We have considered: (i) emerging in situ and proximal sensing techniques, (ii) dedicated soil moisture remote sensing missions, (iii) soil moisture monitoring networks, and (iv) applications of large-scale soil moisture measurements. The primary challenges and opportunities in these topic areas can be summarized as follows. For emerging in situ and proximal sensing techniques (e.g., COSMOS and GPS), empirical confirmations of theoretical predictions regarding the variable measurement depths are needed. Calibration procedures for these methods, as well as the DTS methods, need to be further refined and standardized with due accounting for site-specific factors such as soil and vegetation characteristics that influence instrument performance. Spatial and temporal heterogeneity in these site-specific factors must also be considered in some instances, creating additional challenges. Also, the community of expertise for these methods, that is the number of researchers with the capability to advance these technologies, needs to be expanded.

Probably the largest share of scientific resources in this general topic area is currently devoted to the advancement of satellite remote sensing approaches for soil moisture monitoring. These investments are bearing fruit, but challenges and opportunities remain. One significant challenge is to further improve methods for estimating the RZSM, the information we often need, using surface soil moisture observations, the information satellites provide. Progress has been made toward this goal by using data assimilation into numerical models to retrieve the RZSM from near-surface observations. Improvements are also needed in downscaling relatively coarse-resolution remotely sensed soil moisture products to describe the subfootprint spatial variability, which plays an important role in many applications. Coarse-resolution, satellite-derived soil moisture products are challenging to validate (Reichle et al., 2004), so continuing efforts to effectively use these products for modeling and forecasting will probably play an important role in their evaluation. Although not primarily a scientific challenge, more work is needed to reduce problems associated with RFI. Similarly, continuity of missions is a necessity if remotely sensed soil moisture data are to be adopted for operational applications like NWP.

In contrast with remote sensing approaches, relatively few resources are currently devoted toward large-scale in situ soil moisture monitoring networks. Although the number of networks is growing steadily, the lack of standardization of procedures across networks is a significant challenge. There is a need for rigorous guidelines and standards to be developed and adopted worldwide for in situ soil moisture monitoring networks, similar to guidelines for the measurement of other meteorological variables. Best practice standards for sensor selection, calibration, installation, validation, and maintenance are needed, as well as standards for site selection, data quality assurance and quality control, data delivery, metadata delivery, and data archives. The recent recognition of soil moisture as an "essential climate variable" by the Global Climate Observing System and the development of the ISMN are positive steps in this direction, but much more is needed.

For both in situ networks and remote sensing approaches, sustainability is a significant challenge, perhaps underestimated. Societal and scientific needs for soil moisture data would seem to justify that our monitoring systems be designed to function without interruption for many decades. Current realities within science and society at large typically result in monitoring systems that are designed to function for only a few years. Researchers are rewarded for developing new systems and technologies, not for ensuring their long-term viability. Successful long-term operation of monitoring systems generally requires substantial state or federal support. Securing such long-term support for soil moisture monitoring systems is often difficult. Thus, determining effective pathways to transition monitoring systems from research mode to operational mode remains a key challenge.

In closing, we again note the growing need to develop the science necessary to make effective use of the rising number of large-scale soil moisture data sets. One area where significant progress seems possible in the near term is the use of large-scale soil moisture data for drought monitoring. Already some progress has been made using in situ data for this purpose, and approaches using remote sensing data seem sure to follow. Significant efforts have been devoted to the use of soil moisture observations within the area of NWP. In general, assimilation of soil moisture data has resulted in only modest improvements in forecast skill. The primary problem is that the current model structures are not well suited for assimilation of these data, and the model physics may not be properly parameterized to allow accurate soil moisture values. A smaller effort, but arguably greater progress, has been made in the assimilation of soil moisture data into models designed primarily for hydrologic prediction, especially rainfall–runoff models. Here gains in forecast efficiency of 10 to 20% are not uncommon. Nonetheless, as with NWP, a key challenge is to identify or create models that are structured in a way that is optimal for the assimilation of soil moisture data. To date, little or no progress has been made in using large-scale soil moisture observations to improve the structure, parameters, or forecasts of ecological models, and perhaps surprisingly, the same can be said for crop models. These topic areas are ripe with opportunities and challenges yet to be uncovered. Another frontier where the potential is great but the workers are few is the use of soil moisture observations in socioeconomic modeling and forecasting to address issues such as drought impacts and food security (Simelton et al., 2012).

We are optimistic that these challenges and opportunities can be addressed by improved communication and collaboration across the relevant disciplines. The international soil science community has much to contribute in this context. We hope that this review will be a small step toward further engaging that community in advancing the science and practice of large-scale soil moisture monitoring for the sake of improved Earth system monitoring, modeling, and forecasting.

ACKNOWLEDGMENTS

The contribution of Tyson Ochsner has been funded by the Oklahoma Agricultural Experiment Station. The contribution of Wouter Dorigo has been funded through the SMOS Soil Moisture Network Study– Operational Phase (ESA ESTEC Contract no.4000102722/10). The contributions of Eric Small and Kristine Larson were funded by grants from NASA (NNX10AU84G) and NSF (AGS 0935725). The contribution of Marek Zreda has been funded through the COSMOS project by the U.S. National Science Foundation (Grant no. ATM-0838491). The contribution of Eni Njoku was funded through the Jet Propulsion Laboratory, California Institute of Technology under contract with NASA.

REFERENCES

Alavi, N., A.A. Berg, J.S. Warland, G. Parkin, D. Verseghy, and P. Bartlett. 2010. Evaluating the impact of assimilating soil moisture variability data on latent heat flux estimation in a land surface model. Can. Water Resour. J. 35:157–172. doi:10.4296/cwrj3502157

Al Bitar, A., D. Leroux, Y.H. Kerr, O. Merlin, P. Richaume, A. Sahoo, and E.F. Wood. 2012. Evaluation of SMOS soil moisture products over continental U.S. using the SCAN/SNOTEL network. IEEE Trans. Geosci. Remote Sens. 50:1572–1586. doi:10.1109/TGRS.2012.2186581

Albergel, C., G. Balsamo, P. de Rosnay, J. Muñoz-Sabater, and S. Boussetta. 2012b. A bare ground evaporation revision in the ECMWF land-surface scheme: Evaluation of its impact using ground soil moisture and satellite microwave data. Hydrol. Earth Syst. Sci. 16:3607–3620. doi:10.5194/hess-16-3607-2012

Albergel, C., P. de Rosnay, C. Gruhier, J. Munoz-Sabater, S. Hasenauer, L. Isaksen, et al. 2012a. Evaluation of remotely sensed and modeled soil moisture products using global ground-based in situ observations. Remote Sens. Environ. 118:215–226. doi:10.1016/j.rse.2011.11.017

Albergel, C., E. Zakharova, J.-C. Calvet, M. Zribi, M. Pardé, J.-P. Wigneron, et al. 2011. A first assessment of the SMOS data in southwestern France using in situ and airborne soil moisture estimates: The CAROLS airborne campaign. Remote Sens. Environ. 115:2718–2728. doi:10.1016/j.rse.2011.06.012

Allen, R.G., L.S. Pereira, D. Raes, and M. Smith. 1998. Crop evapotranspiration: Guidelines for computing crop water requirements. Irrig. Drain. Pap. 56. FAO, Rome.

Anderson, W., B. Zaitchik, C. Hain, M. Anderson, M. Yilmaz, J. Mecikalski, and L. Schultz. 2012. Towards an integrated soil moisture drought monitor for East Africa. Hydrol. Earth Syst. Sci. Discuss. 9:4587–4631. doi:10.5194/hessd-9-4587-2012

André, J.-C., J.-P. Goutorbe, A. Perrier, F. Becker, P. Bessemoulin, P. Bougeault, et al. 1988. Evaporation over land surfaces: First results from HAPEX-MOBILHY special observing period. Ann. Geophys. 6:477–492.

André, J.-C., J.-P. Goutorbe, and A. Perrier. 1986. HAPEX-MOBILHY: A hydrologic atmospheric experiment for the study of water budget and evaporation flux at the climatic scale. Bull. Am. Meteorol. Soc. 67:138–144. doi:10.1175/1520-0477(1986)067<0138:HAHAEF>2.0.CO;2

Aubert, D., C. Loumagne, and L. Oudin. 2003. Sequential assimilation of soil moisture and streamflow data in a conceptual rainfall–runoff model. J. Hydrol. 280:145–161. doi:10.1016/S0022-1694(03)00229-4

Bachelet, D., J.M. Lenihan, C. Daly, R.P. Neilson, D.S. Ojima, and W.J. Parton. 2001. MC1: A dynamic vegetation model for estimating the distribution of vegetation and associated carbon, nutrients, and water: Technical documentation. Version 1.0. Gen. Tech. Rep. PNW-GTR-508. U.S. For. Serv. Pac. Northw. Res. Stn., Portland, OR.

Baker, J.M., and R.R. Allmaras. 1990. System for automating and multiplexing soil moisture measurement by time-domain reflectometry. Soil Sci. Soc. Am. J. 54:1–6. doi:10.2136/sssaj1990.03615995005400010001x

Baldocchi, D., E. Falge, L. Gu, R. Olson, D. Hollinger, S. Running, et al. 2001. FLUXNET: A new tool to study the temporal and spatial variability of ecosystem-scale carbon dioxide, water vapor, and energy flux densities. Bull. Am. Meteorol. Soc. 82:2415–2434. doi:10.1175/1520-0477(2001)082<2415:FANTTS>2.3.CO;2

Bartalis, Z., W. Wagner, V. Naeimi, S. Hasenauer, K. Scipal, H. Bonekamp, et al. 2007. Initial soil moisture retrievals from the METOP-A Advanced Scatterometer (ASCAT). Geophys. Res. Lett. 34:L20401. doi:10.1029/2007GL031088

Basara, J.B., and K.C. Crawford. 2002. Linear relationships between root-zone soil moisture and atmospheric processes in the planetary boundary layer. J. Geophys. Res. 107(D15). doi:10.1029/2001JD000633

Best, M., C. Jones, I. Dharssi, and R. Quaggin. 2007. A physically based soil moisture nudging scheme for the global model. Met Office Tech. Note. Met Office, Hadley Ctr., Exeter, UK.

Blonquist, J.M., S.B. Jones, and D.A. Robinson. 2005. Standardizing characterization of electromagnetic water content sensors: 2. Evaluation of seven sensing systems. Vadose Zone J. 4:1059–1069. doi:10.2136/vzj2004.0141

Blyth, E., D.B. Clark, R. Ellis, C. Huntingford, S. Los, M. Pryor, et al. 2010. A comprehensive set of benchmark tests for a land surface model of simultaneous fluxes of water and carbon at both the global and seasonal scale. Geosci. Model Dev. Discuss. 3:1829–1859. doi:10.5194/gmdd-3-1829-2010

Bolten, J.D., W.T. Crow, Z. Xiwu, T.J. Jackson, and C.A. Reynolds. 2010. Evaluating the utility of remotely sensed soil moisture retrievals for operational agricultural drought monitoring. IEEE J. Sel. Top. Appl. Earth Obs. Remote Sens. 3:57–66. doi:10.1109/JSTARS.2009.2037163

Bremond, L., A. Boom, and C. Favier. 2012. Neotropical C_3/C_4 grass distributions: Present, past and future. Global Change Biol. 18:2324–2334. doi:10.1111/j.1365-2486.2012.02690.x

Breshears, D.D., and F.J. Barnes. 1999. Interrelationships between plant functional types and soil moisture heterogeneity for semiarid landscapes within the grassland/forest continuum: A unified conceptual model. Landscape Ecol. 14:465–478. doi:10.1023/A:1008040327508

Bristow, K.L., G.S. Campbell, and K. Calissendorff. 1993. Test of a heat-pulse probe for measuring changes in soil water content. Soil Sci. Soc. Am. J. 57:930–934. doi:10.2136/sssaj1993.03615995005700040008x

Brocca, L., F. Melone, T. Moramarco, W. Wagner, V. Naeimi, Z. Bartalis, and S. Hasenauer. 2010. Improving runoff prediction through the assimilation of the ASCAT soil moisture product. Hydrol. Earth Syst. Sci. 14:1881–1893. doi:10.5194/hess-14-1881-2010

Brocca, L., T. Moramarco, F. Melone, W. Wagner, S. Hasenauer, and S. Hahn. 2012. Assimilation of surface- and root-zone ASCAT soil moisture products into rainfall–runoff modeling. IEEE Trans. Geosci. Remote Sens. 50:2542–2555. doi:10.1109/TGRS.2011.2177468

Brock, F.V., K.C. Crawford, R.L. Elliott, G.W. Cuperus, S.J. Stadler, H.L. Johnson, and M.D. Eilts. 1995. The Oklahoma Mesonet: A technical overview. J. Atmos. Ocean. Technol. 12:5–19. doi:10.1175/1520-0426(1995)012<0005:TOMATO>2.0.CO;2

Calvet, J.C., N. Fritz, F. Froissard, D. Suquia, A. Petitpa, and B. Piguet. 2007. In situ soil moisture observations for the CAL/VAL of SMOS: The SMOSMANIA network. In: Sensing and understanding our planet: International Geoscience and Remote Sensing Symposium, Barcelona, Spain. 23–28 July 2007. IEEE, Piscataway, NJ. p. 1196–1199.

Calvet, J.-C., J. Noilhan, and P. Bessemoulin. 1998. Retrieving the root-zone soil moisture from surface soil moisture or temperature estimates: A feasibility study based on field measurements. J. Appl. Meteorol. 37:371–386. doi:10.1175/1520-0450(1998)037<0371:rtrzsm>2.0.co;2

Campbell, G.S., C. Calissendorff, and J.H. Williams. 1991. Probe for measuring soil specific heat using a heat-pulse method. Soil Sci. Soc. Am. J. 55:291–293. doi:10.2136/sssaj1991.03615995005500010052x

Carroll, T.R. 1981. Airborne soil moisture measurement using natural terrestrial gamma radiation. Soil Sci. 132:358–366. doi:10.1097/00010694-198111000-00006

Carslaw, H.S., and J.C. Jaeger. 1959. Conduction of heat in solids. 2nd ed. Oxford Univ. Press, Oxford, UK.

Chang, A.T.C., S.G. Atwater, V.V. Salomonson, J.E. Estes, D.S. Simonett, and M.L. Bryan. 1980. L-band radar sensing of soil moisture. IEEE Trans. Geosci. Remote Sens. GE-18:303–310. doi:10.1109/TGRS.1980.350306

Chen, F., W.T. Crow, P.J. Starks, and D.N. Moriasi. 2011. Improving hydrologic predictions of a catchment model via assimilation of surface soil moisture. Adv. Water Resour. 34:526–536. doi:10.1016/j.advwatres.2011.01.011

Chen, F., and J. Dudhia. 2001. Coupling an advanced land surface hydrology model with the Penn State–NCAR MM5 modeling system: I. Model implementation and sensitivity. Mon. Weather Rev. 129:569–585. doi:10.1175/1520-0493(2001)129<0569:CAALSH>2.0.CO;2

Chew, C., E. Small, K. Larson, and V. Zavorotny. 2013. Effects of near-surface soil moisture on GPS SNR data: Development of a retrieval algorithm for volumetric soil moisture. IEEE Trans. Geosci. Remote Sens. (in press). doi:10.1109/TGRS.2013.2242332

Collow, T.W., A. Robock, J.B. Basara, and B.G. Illston. 2012. Evaluation of SMOS retrievals of soil moisture over the central United States with currently available in situ observations. J. Geophys. Res. 117:D09113. doi:10.1029/2011JD017095

Curran, P.J. 1978. A photographic method for the recording of polarised visible light for soil surface moisture indications. Remote Sens. Environ. 7:305–322. doi:10.1016/0034-4257(78)90022-6

Crow, W.T., A.A. Berg, M.H. Cosh, A. Loew, B.P. Mohanty, R. Panciera, et al. 2012. Upscaling sparse ground-based soil moisture observations for the validation of coarse-resolution satellite soil moisture products. Rev. Geophys. 50:RG2002. doi:10.1029/2011RG000372

Cuenca, R.H., J. Brouwer, A. Chanzy, P. Droogers, S. Galle, S.R. Gaze, et al. 1997. Soil measurements during HAPEX-Sahel intensive observation period. J. Hydrol. 188–189:224–266. doi:10.1016/S0022-1694(96)03161-7

Das, N.N., D. Entekhabi, and E.G. Njoku. 2011. An algorithm for merging SMAP radiometer and radar data for high-resolution soil-moisture retrieval. IEEE Trans. Geosci. Remote Sens. 49:1504–1512. doi:10.1109/TGRS.2010.2089526

de Rosnay, P., M. Drusch, D. Vasiljevic, G. Balsamo, C. Albergel, and L. Isaksen. 2013. A simplified Extended Kalman Filter for the global operational soil moisture analysis at ECMWF. Q. J. R. Meteorol. Soc. 139:1199–1213. doi:10.1002/qj.2023

de Rosnay, P., C. Gruhier, F. Timouk, F. Baup, E. Mougin, P. Hiernaux, et al. 2009. Multi-scale soil moisture measurements at the Gourma meso-scale site in Mali. J. Hydrol. 375:241–252. doi:10.1016/j.jhydrol.2009.01.015

Denning, A.S., editor. 2005. Science implementation strategy for the North American Carbon Program. U.S. Carbon Cycle Sci. Progr., Washington, DC.

Desilets, D., and M. Zreda. 2001. On scaling cosmogenic nuclide production rates for altitude and latitude using cosmic-ray measurements. Earth Planet. Sci. Lett. 193:213–225. doi:10.1016/S0012-821X(01)00477-0

Desilets, D., and M. Zreda. 2003. Spatial and temporal distribution of secondary cosmic-ray nucleon intensities and applications to in situ cosmogenic dating. Earth Planet. Sci. Lett. 206:21–42. doi:10.1016/S0012-821X(02)01088-9

Desilets, D., M. Zreda, and T. Ferré. 2010. Nature's neutron probe: Land-surface hydrology at an elusive scale with cosmic rays. Water Resour. Res. 46:W11505. doi:10.1029/2009WR008726

Desilets, D., M. Zreda, and T. Prabu. 2006. Extended scaling factors for in situ cosmogenic nuclides: New measurements at low latitude. Earth Planet. Sci. Lett. 246:265–276. doi:10.1016/j.epsl.2006.03.051

Dharssi, I., K. Bovis, B. Macpherson, and C. Jones. 2011. Operational assimilation of ASCAT surface soil wetness at the Met Office. Hydrol. Earth Syst. Sci. 15:2729–2746. doi:10.5194/hess-15-2729-2011

Dickey, F.M., C. King, J.C. Holtzman, and R.K. Moore. 1974. Moisture dependency of radar backscatter from irrigated and non-irrigated fields at 400 MHz and 13.3 GHz. IEEE Trans. Geosci. Electron. 12:19–22. doi:10.1109/TGE.1974.294326

Dickinson, R.E., A. Henderson-Sellers, P.J. Kennedy, and M.F. Wilson. 1986. Biosphere–Atmosphere Transfer Scheme (BATS) for the NCAR CCM. Natl. Ctr. for Atmos. Res., Boulder, CO.

Dirmeyer, P. 1999. Assessing GCM sensitivity to soil wetness using GSWP data. J. Meteorol. Soc. Jpn. 77(1B):367–385.

Dirmeyer, P.A., X. Gao, M. Zhao, Z. Guo, T. Oki, and N. Hanasaki. 2006. GSWP-2 : Multimodel analysis and implications for our perception of the land surface. Bull. Am. Meteorol. Soc. 87:1381–1397. doi:10.1175/BAMS-87-10-1381

Dobriyal, P., A. Qureshi, R. Badola, and S.A. Hussain. 2012. A review of the methods available for estimating soil moisture and its implications for water resource management. J. Hydrol. 458–459:110–117. doi:10.1016/j.jhydrol.2012.06.021

Dorigo, W.A., W. Wagner, R. Hohensinn, S. Hahn, C. Paulik, A. Xaver, et al. 2011b. The International Soil Moisture Network: A data hosting facility for global in situ soil moisture measurements. Hydrol. Earth Syst. Sci. 15:1675–1698. doi:10.5194/hess-15-1675-2011

Dorigo, W.A., A. Xaver, M. Vreugdenhil, A. Gruber, A. Hegyiová, A.D. Sanchis-Dufau, et al. 2013. Global automated quality control of in situ soil moisture data from the International Soil Moisture Network. Vadose Zone J. 12(3). doi:10.2136/vzj2012.0097

Dorigo, W., P. van Oevelen, W. Wagner, M. Drusch, S. Mecklenburg, A. Robock, and T. Jackson. 2011a. A new international network for in situ soil moisture data. Eos Trans. Am. Geophys. Union 92:141–142. doi:10.1029/2011EO170001

Douville, H., P. Viterbo, J.-F. Mahfouf, and A. Beljaars. 2000. Evaluation of the optimum interpolation and nudging techniques for soil moisture analysis using FIFE data. Mon. Weather Rev. 128:1733–1756. doi:10.1175/1520-0493(2000)128<1733:EOTOIA>2.0.CO;2

Draper, C., J.-F. Mahfouf, and J. Walker. 2011. Root-zone soil moisture from the assimilation of screen-level variables and remotely sensed soil moisture. J. Geophys. Res. 116:D02127. doi:10.1029/2010JD013829

Drusch, M., and P. Viterbo. 2007. Assimilation of screen-level variables in ECMWF's Integrated Forecast System: A study on the impact on the forecast quality and analyzed soil moisture. Mon. Weather Rev. 135:300–314. doi:10.1175/MWR3309.1

Drusch, M., K. Scipal, P. de Rosnay, G. Balsamo, E. Andersson, P. Bougeault, and P. Viterbo. 2009. Towards a Kalman Filter based soil moisture analysis system for the operational ECMWF Integrated Forecast System. Geophys. Res. Lett. 36:L10401. doi:10.1029/2009GL037716

Ek, M.B., and R.H. Cuenca. 1994. Variation in soil parameters: Implications for modeling surface fluxes and atmospheric boundary-layer development. Boundary-Layer Meteorol. 70:369–383. doi:10.1007/BF00713776

Ek, M.B., and A.A.M. Holtslag. 2004. Influence of soil moisture on boundary layer cloud development. J. Hydrometeorol. 5:86–99. doi:10.1175/1525-7541(2004)005<0086:IOSMOB>2.0.CO;2

Ek, M.B., and L. Mahrt. 1994. Daytime evolution of relative humidity at the boundary-layer top. Mon. Weather Rev. 122:2709–2721. doi:10.1175/1520-0493(1994)122<2709:DEORHA>2.0.CO;2

Ek, M.B., K.E. Mitchell, Y. Lin, E. Rogers, P. Grummann, V. Koren, et al. 2003. Implementation of Noah land surface model advances in the National Centers for Environmental Prediction operational mesoscale Eta model. J. Geophys. Res. 108:8851. doi:10.1029/2002JD003296

Entekhabi, D., E.G. Njoku, P.E. O'Neill, K.H. Kellogg, W.T. Crow, W.N. Edelstein, et al. 2010. The soil moisture active passive (SMAP) mission. Proc. IEEE 98:704–716. doi:10.1109/JPROC.2010.2043918

Escorihuela, M.J., A. Chanzy, J.P. Wigneron, and Y.H. Kerr. 2010. Effective soil moisture sampling depth of L-band radiometry: A case study. Remote Sens. Environ. 114:995–1001. doi:10.1016/j.rse.2009.12.011

Evett, S.R. 2001. Exploits and endeavors in soil water management and conservation using nuclear techniques. In: Nuclear techniques in integrated plant nutrient, water, and soil management: Proceedings of an International Symposium, Vienna, Austria. 16–20 Oct. 2000. C&S Pap. Ser. 11. Int. Atomic Energy Agency, Vienna. p. 151–177.

Field, C.B., R.B. Jackson, and H.A. Mooney. 1995. Stomatal responses to increased CO_2: Implications from the plant to the global scale. Plant Cell Environ. 18:1214–1225. doi:10.1111/j.1365-3040.1995.tb00630.x

Foley, J.A., I.C. Prentice, N. Ramankutty, S. Levis, D. Pollard, S. Sitch, and A. Haxeltine. 1996. An integrated biosphere model of land surface processes, terrestrial carbon balance, and vegetation dynamics. Global Biogeochem. Cycles 10:603–628. doi:10.1029/96GB02692

Francois, C., A. Quesney, and C. Ottlé. 2003. Sequential assimilation of *ERS-1* SAR data into a coupled land surface–hydrological model using an extended Kalman filter. J. Hydrometeorol. 4:473–487. doi:10.1175/1525-7541(2003)4<473:SAOESD>2.0.CO;2

Franz, T.E., M. Zreda, R. Rosolem, and T.P.A. Ferré. 2012. Field validation of a cosmic-ray neutron sensor using a distributed sensor network. Vadose Zone J. 11(4). doi:10.2136/vzj2012.0046

Franz, T.E., M. Zreda, R. Rosolem, and T.P.A. Ferré. 2013. A universal calibration function for determination of soil moisture with cosmic-ray neutrons. Hydrol. Earth Syst. Sci. 17:453–460. doi:10.5194/hess-17-453-2013

Fredlund, D.G., and D.K.H. Wong. 1989. Calibration of thermal conductivity sensors for measuring soil suction. Geotech. Test. J. 12:188–194. doi:10.1520/GTJ10967J

Friedlingstein, P., P. Cox, R. Betts, L. Bopp, W. von Bloh, V. Brovkin, et al. 2006. Climate–carbon cycle feedback analysis: Results from the C^4MIP model intercomparison. J. Clim. 19:3337–3353. doi:10.1175/JCLI3800.1

Gardner, W., and D. Kirkham. 1952. Determination of soil moisture by neutron scattering. Soil Sci. 73:391–402. doi:10.1097/00010694-195205000-00007

Global Climate Observing System. 2010. Implementation plan for the Global Observing System for Climate in support of the UNFCCC. IP-10. World Meteorol. Org., Geneva, Switzerland.

Georgiadou, Y., and A. Kleusberg. 1988. On carrier signal multipath effects in relative GPS positioning. Manuscr. Geod. 13:172–179.

Gerten, D., S. Schaphoff, U. Haberlandt, W. Lucht, and S. Sitch. 2004. Terrestrial vegetation and water balance: Hydrological evaluation of a dynamic global vegetation model. J. Hydrol. 286:249–270. doi:10.1016/j.jhydrol.2003.09.029

Gil-Rodríguez, M., L. Rodríguez-Sinobas, J. Benítez-Buelga, and R. Sánchez-Calvo. 2013. Application of active heat pulse method with fiber optic temperature sensing for estimation of wetting bulbs and water distribution in drip emitters. Agric. Water Manage. 120:72–78. doi:10.1016/j.agwat.2012.10.012

Gordon, W.S., J.S. Famiglietti, N.L. Fowler, T.G.F. Kittel, and K.A. Hibbard. 2004. Validation of simulated runoff from six terrestrial ecosystem models: Results from VEMAP. Ecol. Appl. 14:527–545. doi:10.1890/02-5287

Gruber, A., W. Dorigo, S. Zwieback, A. Xaver, and W. Wagner. 2013. Characterizing coarse-scale representativeness of in situ soil moisture measurements from the International Soil Moisture Network. Vadose Zone J. 12(2). doi:10.2136/vzj2012.0170

Guttman, N.B. 1999. Accepting the standardized precipitation index: A calculation algorithm. J. Am. Water Resour. Assoc. 35:311–322. doi:10.1111/j.1752-1688.1999.tb03592.x

Haxeltine, A., and I.C. Prentice. 1996. BIOME3: An equilibrium terrestrial biosphere model based on ecophysiological constraints, resource availability, and competition among plant functional types. Global Biogeochem. Cycles 10(4):693–709. doi:10.1029/96GB02344

Hallikainen, M., F. Ulaby, M. Dobson, M. El-Rayes, and L. Wu. 1985. Microwave dielectric behavior of wet soil: I. Empirical models and experimental observations. IEEE Trans. Geosci. Remote Sens. GE-23:25–34. doi:10.1109/TGRS.1985.289497

Heitman, J.L., J.M. Basinger, G.J. Kluitenberg, J.M. Ham, J.M. Frank, and P.L. Barnes. 2003. Field evaluation of the dual-probe heat-pulse method for measuring soil water content. Vadose Zone J. 2:552–560.

Henderson-Sellers, A., A.J. Pitman, P.K. Love, P. Irannejad, and T.H. Chen. 1995. The Project for Intercomparison of Land Surface Parameterization Schemes (PILPS): Phases 2 and 3. Bull. Am. Meteorol. Soc. 76:489–503. doi:10.1175/1520-0477(1995)076<0489:TPFIOL>2.0.CO;2

Henderson-Sellers, A., K. McGuffie, and A.J. Pitman. 1996. The Project for Intercomparison of Land-Surface Parameterization Schemes (PILPS): 1992 to 1995. Clim. Dyn. 12:849–859. doi:10.1007/s003820050147

Hess, H. 2001. Assimilation of screen-level observations by variational soil moisture analysis. Meteorol. Atmos. Phys. 77:145–154. doi:10.1007/s007030170023

Hoeben, R., and P.A. Troch. 2000. Assimilation of active microwave observation data for soil moisture profile estimation. Water Resour. Res. 36:2805–2819. doi:10.1029/2000WR900100

Hollinger, S.E., and S.A. Isard. 1994. A soil moisture climatology of Illinois. J. Clim. 7:822–833. doi:10.1175/1520-0442(1994)007<0822:ASMCOI>2.0.CO;2

Hoogenboom, G. 1993. The Georgia automated environmental monitoring network. Southeast. Clim. Rev. 4:12–18.

Hubbard, K.G., J. You, V. Sridhar, E. Hunt, S. Korner, and G. Roebke. 2009. Near-surface soil-water monitoring for water resources management on a wide-area basis in the Great Plains. Great Plains Res. 19:45–54.

Hunt, E.D., K.G. Hubbard, D.A. Wilhite, T.J. Arkebauer, and A.L. Dutcher. 2009. The development and evaluation of a soil moisture index. Int. J. Climatol. 29:747–759. doi:10.1002/joc.1749

Illston, B.G., J. Basara, D.K. Fischer, R.L. Elliott, C. Fiebrich, K.C. Crawford, et al. 2008. Mesoscale monitoring of soil moisture across a statewide network. J. Atmos. Ocean. Technol. 25:167–182. doi:10.1175/2007JTECHA993.1

Ise, T., and P.R. Moorcroft. 2006. The global-scale temperature and moisture dependencies of soil organic carbon decomposition: An analysis using a mechanistic decomposition model. Biogeochemistry 80:217–231. doi:10.1007/s10533-006-9019-5

Jackson, T.J., M.H. Cosh, R. Bindlish, P.J. Starks, D.D. Bosch, M.S. Seyfried, et al. 2010. Validation of Advanced Microwave Scanning Radiometer soil moisture products. IEEE Trans. Geosci. Remote Sens. 48:4256–4272. doi:10.1109/TGRS.2010.2051035

Jackson, T.J., and T.J. Schmugge. 1989. Passive microwave remote-sensing system for soil-moisture: Some supporting research. IEEE Trans. Geosci. Remote Sens. 27:225–235. doi:10.1109/36.20301

Jackson, T.J., and T.J. Schmugge. 1991. Vegetation effects on the microwave emission of soils. Remote Sens. Environ. 36:203–212. doi:10.1016/0034-4257(91)90057-D

Jackson, T.J., R. Bindlish, M.H. Cosh, T.J. Zhao, P.J. Starks, D.D. Bosch, et al. 2012. Validation of Soil Moisture and Ocean Salinity (SMOS) soil moisture over watershed networks in the U.S. IEEE Trans. Geosci. Remote Sens. 50:1530–1543. doi:10.1109/TGRS.2011.2168533

Jacquette, E., A. Al Bitar, A. Mialon, Y. Kerr, A. Quesney, F. Cabot, and P. Richaume. 2010. SMOS CATDS Level 3 global products over land. SPIE Proc. 7824:12. doi:10.1117/12.865093

Jenkinson, D.S., and K. Coleman. 1994. Calculating the annual input of organic matter to soil from measurements of total organic carbon and radiocarbon. Eur. J. Soil Sci. 45:167–174. doi:10.1111/j.1365-2389.1994.tb00498.x

Katzberg, S., O. Torres, M. Grant, and D. Masters. 2005. Utilizing calibrated GPS reflected signals to estimate soil reflectivity and dielectric constant: Results from SMEX02. Remote Sens. Environ. 100:17–28. doi:10.1016/j.rse.2005.09.015

Keller, M., D.S. Schimel, W.W. Hargrove, and F.M. Hoffman. 2008. A continental strategy for the National Ecological Observatory Network. Front. Ecol. Environ. 6:282–287. doi:10.1890/1540-9295(2008)6[282:ACSFTN]2.0.CO;2

Kerr, Y.H., P. Waldteufel, P. Richaume, J.P. Wigneron, P. Ferrazzoli, A. Mahmoodi, et al. 2012. The SMOS soil moisture retrieval algorithm. IEEE Trans. Geosci. Remote Sens. 50:1384–1403. doi:10.1109/TGRS.2012.2184548

Kerr, Y.H., P. Waldteufel, J.P. Wigneron, S. Delwart, F. Cabot, J. Boutin, et al. 2010. The SMOS mission: New tool for monitoring key elements of the global water cycle. Proc. IEEE 98:666–687. doi:10.1109/JPROC.2010.2043032

Kerr, Y.H., P. Waldteufel, J.-P. Wigneron, J.-M. Martinuzzi, J. Font, and M. Berger. 2001. Soil moisture retrieval from space: The Soil Moisture and Ocean Salinity (SMOS) mission. IEEE Trans. Geosci. Remote Sens. 39:1729–1735. doi:10.1109/36.942551

Knoll, G.F. 2000. Radiation detection and measurement. John Wiley & Sons, New York.

Kumar, M., G. Bhatt, and C. Duffy. 2010. The role of physical, numerical and data coupling in a mesoscale watershed model (PIHM). http://www.pihm.psu.edu/pub/PIHM_2010.pdf

Lagerloef, G.S.E. 2001. Satellite measurements of salinity. In: S.T.J. Steele and K. Turekian, editors, Encyclopedia of ocean sciences. Academic Press, London. p. 2511–2516.

Larson, K.M., J.J. Braun, E.E. Small, V.U. Zavorotny, E.D. Gutmann, and A.L. Bilich. 2010. GPS multipath and its relation to near-surface soil moisture content. IEEE J. Sel. Top. Appl. Earth Obs. Remote Sens. 3:91–99. doi:10.1109/JSTARS.2009.2033612

Larson, K.M., E.E. Small, E. Gutmann, A. Bilich, P. Axelrad, and J. Braun. 2008a. Using GPS multipath to measure soil moisture fluctuations: Initial results. GPS Solut. 12:173–177. doi:10.1007/s10291-007-0076-6

Larson, K.M., E.E. Small, E.D. Gutmann, A.L. Bilich, J.J. Braun, and V.U. Zavorotny. 2008b. Use of GPS receivers as a soil moisture network for water cycle studies. Geophys. Res. Lett. 35:L24405. doi:10.1029/2008GL036013

Law, B.E., E. Falge, L. Gu, D.D. Baldocchi, P. Bakwin, P. Berbigier, et al. 2002. Environmental controls over carbon dioxide and water vapor exchange of terrestrial vegetation. Agric. For. Meteorol. 113:97–120. doi:10.1016/S0168-1923(02)00104-1

Le Houérou, H.N. 1996. Climate change, drought and desertification. J. Arid Environ. 34:133–185. doi:10.1006/jare.1996.0099

Le Vine, D. 1988. Synthetic aperture microwave radiometer. Lab. Oceans 1:237–238.

Le Vine, D.M., A.J. Griffis, C.T. Swift, and T.J. Jackson. 1994. ESTAR: A synthetic aperture microwave radiometer for remote sensing applications. Proc. IEEE 82:1787–1801. doi:10.1109/5.338071.

Le Vine, D.M., M. Kao, A.B. Tanner, C.T. Swift, and A. Griffis. 1990. Initial results in the development of a synthetic aperture microwave radiometer. IEEE Trans. Geosci. Remote Sens. 28:614–619. doi:10.1109/TGRS.1990.572965

Li, B., and R. Avissar. 1994. The impact of spatial variability of land-surface characteristics on land-surface heat fluxes. J. Clim. 7:527–537. doi:10.1175/1520-0442(1994)007<0527:TIOSVO>2.0.CO;2

Li, C., S. Frolking, and T.A. Frolking. 1992. A model of nitrous oxide evolution from soil driven by rainfall events: 1. Model structure and sensitivity. J. Geophys. Res. 97(D9):9759–9776. doi:10.1029/92JD00509

Lowe, S.T., J.L. LaBrecque, C. Zuffada, L.J. Romans, L.E. Young, and G. A. Hajj. 2002. First spaceborne observation of an Earth-reflected GPS signal. Radio Sci. 37(1). doi:10.1029/2000RS002539

Mahfouf, J.-F. 1991. Analysis of soil moisture from near-surface parameters: A feasibility study. J. Appl. Meteorol. 30:1534–1547. doi:10.1175/1520-0450(1991)030<1534:AOSMFN>2.0.CO;2

Mahfouf, J.-F., K. Bergaoui, C. Draper, C. Bouyssel, F. Taillefer, and L. Taseva. 2009. A comparison of two off-line soil analysis schemes for assimilation of screen-level observations. J. Geophys. Res. 114:D08105. doi:10.1029/2008JD011077

Mahrt, L., and H.-L. Pan. 1984. A two-layer model of soil hydrology. Boundary-Layer Meteorol. 29:1–20. doi:10.1007/BF00119116

Manabe, S. 1969. Climate and the ocean circulation. Mon. Weather Rev. 97:739–774. doi:10.1175/1520-0493(1969)097<0739:CATOC>2.3.CO;2

McPherson, R.A., C.A. Fiebrich, K.C. Crawford, J.R. Kilby, D.L. Grimsley, J.E. Martinez, et al. 2007. Statewide monitoring of the mesoscale environment: A technical update on the Oklahoma Mesonet. J. Atmos. Ocean. Technol. 24:301–321. doi:10.1175/JTECH1976.1

Meier, P., A. Frömelt, and W. Kinzelbach. 2011. Hydrological real-time modelling in the Zambezi river basin using satellite-based soil moisture and rainfall data. Hydrol. Earth Syst. Sci. 15:999–1008. doi:10.5194/hess-15-999-2011

Merlin, O., A. Al Bitar, J.P. Walker, and Y. Kerr. 2010. An improved algorithm for disaggregating microwave-derived soil moisture based on red, near-infrared and thermal-infrared data. Remote Sens. Environ. 114:2305–2316. doi:10.1016/j.rse.2010.05.007

Merlin, O., C. Rudiger, A. Al Bitar, P. Richaume, J.P. Walker, and Y.H. Kerr. 2012. Disaggregation of SMOS soil moisture in southeastern Australia. IEEE Trans. Geosci. Remote Sens. 50:1556–1571. doi:10.1109/TGRS.2011.2175000

Mishra, A.K., and V.P. Singh. 2010. A review of drought concepts. J. Hydrol. 391:202–216. doi:10.1016/j.jhydrol.2010.07.012

Moghaddam, M. 2009. Polarimetric SAR phenomenology and inversion techniques for vegetated terrain. In: T. Warner, editor, SAGE remote sensing handbook. Sage Publ., London. p. 79–93. doi:10.4135/9780857021052.n6

Moghaddam, M., S. Saatchi, and R. Cuenca. 2000. Estimating subcanopy soil moisture with radar. J. Geophys. Res. 105(D11):14899–14911. doi:10.1029/2000JD900058

Monna, W.A.A., and J.G. van der Vliet. 1987. Facilities for research and weather observations on the 213-m tower at Cabauw and at remote locations. KNMI Sci. Rep. WP-87-5. R. Neth. Meteorol. Inst., De Bilt, the Netherlands.

Montaldo, N., J.D. Albertson, M. Mancini, and G. Kiely. 2001. Robust simulation of root zone soil moisture with assimilation of surface soil moisture data. Water Resour. Res. 37:2889–2900. doi:10.1029/2000WR000209

Moorcroft, P.R., G.C. Hurtt, and S.W. Pacala. 2001. A method for scaling vegetation dynamics: The ecosystem demography model (ED). Ecol. Monogr. 71:557–585. doi:10.1890/0012-9615(2001)071[0557:AMFSVD]2.0.CO;2

Mozny, M., M. Trnka, Z. Zalud, P. Hlavinka, J. Nekovar, V. Potop, and M. Virag. 2012. Use of a soil moisture network for drought monitoring in the Czech Republic. Theor. Appl. Climatol. 107:99–111. doi:10.1007/s00704-011-0460-6

Narasimhan, B., and R. Srinivasan. 2005. Development and evaluation of Soil Moisture Deficit Index (SMDI) and Evapotranspiration Deficit Index (ETDI) for agricultural drought monitoring. Agric. For. Meteorol. 133:69–88. doi:10.1016/j.agrformet.2005.07.012

Neilson, R.P. 1995. A model for predicting continental-scale vegetation distribution and water balance. Ecol. Appl. 5:362–385. doi:10.2307/1942028

Njoku, E.G., T.J. Jackson, V. Lakshmi, T.K. Chan, and S.V. Nghiem. 2003. Soil moisture retrieval from AMSR-E. IEEE Trans. Geosci. Remote Sens. 41:215–229. doi:10.1109/TGRS.2002.808243

Ochsner, T.E., R. Horton, and T. Ren. 2003. Use of the dual-probe heat-pulse technique to monitor soil water content in the vadose zone. Vadose Zone J. 2:572–579.

Oliva, R., E. Daganzo, Y. Kerr, S. Mecklenburg, S. Nieto, P. Richaume, and C. Gruhier. 2012. SMOS RF interference scenario: Status and actions taken to improve the RFI environment in the 1400–1427 MHz passive band. IEEE Trans. Geosci. Remote Sens. 50:1427–1439. doi:10.1109/TGRS.2012.2182775

Orchard, V.A., and F.J. Cook. 1983. Relationship between soil respiration and soil moisture. Soil Biol. Biochem. 15:447–453. doi:10.1016/0038-0717(83)90010-X

Owe, M., R.A.M. de Jeu, and J.P. Walker. 2001. A methodology for surface soil moisture and vegetation optical depth retrieval using the Microwave Polarization Difference Index. IEEE Trans. Geosci. Remote Sens. 39:1643–1654. doi:10.1109/36.942542

Palecki, M.A., and P.Ya. Groisman. 2011. Observing climate at high elevations using United States Climate Reference Network approaches. J. Hydrometeorol. 12:1137–1143. doi:10.1175/2011JHM1335.1

Palmer, W.C. 1965. Meteorological drought. Res. Pap. 45. U.S. Weather Bureau, Washington, DC.

Pan, H.-L., and L. Mahrt. 1987. Interaction between soil hydrology and boundary-layer development. Boundary-Layer Meteorol. 38:185–202. doi:10.1007/BF00121563

Pan, Y., J.M. Melillo, A.D. McGuire, D.W. Kicklighter, L.F. Pitelka, K. Hibbard, et al. 1998. Modeled responses of terrestrial ecosystems to elevated atmospheric CO_2: A comparison of simulations by the biogeochemistry models of the Vegetation/Ecosystem Modeling and Analysis Project (VEMAP). Oecologia 114:389–404. doi:10.1007/s004420050462

Parton, W.J., M. Hartman, D. Ojima, and D. Schimel. 1998. DAYCENT and its land surface submodel: Description and testing. Global Planet. Change 19:35–48. doi:10.1016/S0921-8181(98)00040-X

Parton, W.J., D.S. Schimel, C.V. Cole, and D.S. Ojima. 1987. Analysis of factors controlling soil organic matter levels in Great Plains grasslands. Soil Sci. Soc. Am. J. 51:1173. doi:10.2136/sssaj1987.03615995005100050015x

Parrens, M., E. Zakharova, S. Lafont, J.-C. Calvet, Y. Kerr, W. Wagner, and J.-P. Wigneron. 2012. Comparing soil moisture retrievals from SMOS and ASCAT over France. Hydrol. Earth Syst. Sci. 16:423–440. doi:10.5194/hess-16-423-2012

Pauwels, V.R.N., R. Hoeben, N.E.C. Verhoest, and F.P. De Troch. 2001. The importance of the spatial patterns of remotely sensed soil moisture in the improvement of discharge predictions for small-scale basins through data assimilation. J. Hydrol. 251:88–102. doi:10.1016/S0022-1694(01)00440-1

Peel, M.C., B.L. Finlayson, and T.A. McMahon. 2007. Updated world map of the Köppen-Geiger climate classification. Hydrol. Earth Syst. Sci. 11:1633–1644. doi:10.5194/hess-11-1633-2007

Peled, E., E. Dutra, P. Viterbo, and A. Angert. 2009. Technical note: Comparing and ranking soil-moisture indices performance over Europe, through remote-sensing of vegetation. Hydrol. Earth Syst. Sci. Discuss. 6:6247–6264. doi:10.5194/hessd-6-6247-2009

Phene, C.J., G.J. Hoffman, and S.L. Rawlins. 1971. Measuring soil matric potential in situ by sensing heat dissipation within a porous body: I. Theory and sensor construction. Soil Sci. Soc. Am. J. 35:27–33. doi:10.2136/sssaj1971.03615995003500010015x

Piles, M., A. Camps, M. Vall-Llossera, I. Corbella, R. Panciera, C. Rudiger, et al. 2011. Downscaling SMOS-derived soil moisture using MODIS visible/infrared data. IEEE Trans. Geosci. Remote Sens. 49:3156–3166. doi:10.1109/TGRS.2011.2120615

Pratt, D.A., and C.D. Ellyett. 1979. The thermal inertia approach to mapping of soil moisture and geology. Remote Sens. Environ. 8:151–168. doi:10.1016/0034-4257(79)90014-2

Prentice, I., W. Cramer, S. Harrison, R. Leemans, R. Monserud, and A. Solomon. 1992. A global biome model based on plant physiology and dominance, soil properties and climate. J. Biogeogr. 19:117–134. doi:10.2307/2845499

Purcell, L.C., T.R. Sinclair, and R.W. McNew. 2003. Drought avoidance assessment for summer annual crops using long-term weather data. Agron. J. 95:1566–1576. doi:10.2134/agronj2003.1566

Qu, Y., and C.J. Duffy. 2007. A semidiscrete finite volume formulation for multiprocess watershed simulation. Water Resour. Res. 43:W08419. doi:10.1029/2006WR005752

Randerson, J.T., F.M. Hoffman, P.E. Thornton, N.M. Mahowald, K. Lindsay, Y.-H. Lee, et al. 2009. Systematic assessment of terrestrial biogeochemistry in coupled climate–carbon models. Global Change Biol. 15:2462–2484. doi:10.1111/j.1365-2486.2009.01912.x

Reece, C.F. 1996. Evaluation of a line heat dissipation sensor for measuring soil matric potential. Soil Sci. Soc. Am. J. 60:1022–1028. doi:10.2136/sssaj1996.03615995006000040009x

Reichle, R.H., W.T. Crow, R.D. Koster, J.S. Kimball, and G.J.M. De Lannoy. 2012. SMAP Level 4 Surface and Root Zone Soil Moisture (L4_SM) data product algorithm theoretical basis document. Global Modeling and Assimilation Office, NASA Goddard Space Flight Ctr., Greenbelt, MD. http://smap.jpl.nasa.gov/files/smap2/L4_SM_InitRel_v1.pdf (accessed 11 June 2013).

Reichle, R.H., R.D. Koster, J. Dong, and A.A. Berg. 2004. Global soil moisture from satellite observations, land surface models, and ground data: Implications for data assimilation. J. Hydrometeorol. 5:430–442. doi:10.1175/1525-7541(2004)005<0430:GSMFSO>2.0.CO;2

Reichstein, M., A. Rey, A. Freibauer, J. Tenhunen, R. Valentini, J. Banza, et al. 2003. Modeling temporal and large-scale spatial variability of soil respira-

tion from soil water availability, temperature and vegetation productivity indices. Global Biogeochem. Cycles 17:1104. doi:10.1029/2003GB002035
Ren, D., L.M. Leslie, and D.J. Karoly. 2008. Sensitivity of an ecological model to soil moisture simulations from two different hydrological models. Meteorol. Atmos. Phys. 100:87–99. doi:10.1007/s00703-008-0297-4
Richards, L.A. 1931. Capillary conduction of liquids through porous mediums. Physics 1:318–333. doi:10.1063/1.1745010
Rivera Villarreyes, C.A., G. Baroni, and S.E. Oswald. 2011. Integral quantification of seasonal soil moisture changes in farmland by cosmic-ray neutrons. Hydrol. Earth Syst. Sci. 15:3843–3859. doi:10.5194/hess-15-3843-2011
Robinson, D.A., C.S. Campbell, J.W. Hopmans, B.K. Hornbuckle, S.B. Jones, R. Knight, et al. 2008. Soil moisture measurement for ecological and hydrological watershed-scale observatories: A review. Vadose Zone J. 7:358–389. doi:10.2136/vzj2007.0143
Robock, A., K. Ya Vinnikov, C.A. Schlosser, N.A. Speranskaya, and Y. Xue. 1995. Use of midlatitude soil moisture and meteorological observations to validate soil moisture simulations with biosphere and bucket models. J. Clim. 8:15–35. doi:10.1175/1520-0442(1995)008<0015:UOMSMA>2.0.CO;2
Robock, A., K.Y. Vinnikov, G. Srinivasan, J.K. Entin, S.E. Hollinger, N.A. Speranskaya, et al. 2000. The global soil moisture data bank. Bull. Am. Meteorol. Soc. 81:1281–1299. doi:10.1175/1520-0477(2000)081<1281:TGSMDB >2.3.CO;2
Robock, A., M. Mu, K. Vinnikov, I.V. Trofimova, and T.I. Adamenko. 2005. Forty-five years of observed soil moisture in the Ukraine: No summer desiccation (yet). Geophys. Res. Lett. 32:L03401. doi:10.1029/2004GL021914
Rodriguez-Alvarez, N., X. Bosch-Lluis, A. Camps, M. Vall-Ilossera, E. Valencia, J.F. Marchan-Hernandez, and I. Ramos-Perez. 2009. Soil moisture retrieval using GNSS-R techniques: Experimental results over a bare soil field. IEEE Trans. Geosci. Remote Sens. 47:3616–3624. doi:10.1109/TGRS.2009.2030672
Rodriguez-Alvarez, N., X. Bosch-Lluis, A. Camps, A. Aguasca, M. Vall-llossera, E. Valencia, et al. 2011a. Review of crop growth and soil moisture monitoring from a ground-based instrument implementing the interference pattern GNSS-R technique. Radio Sci. 46:RS0C03. doi:10.1029/2011RS004680
Rodriguez-Alvarez, N., A. Camps, M. Vall-Ilossera, X. Bosch-Lluis, A. Monerris, I. Ramos-Perez, et al. 2011b. Land geophysical parameters retrieval using the interference pattern GNSS-R technique. IEEE Trans. Geosci. Remote Sens. 49:71–84. doi:10.1109/TGRS.2010.2049023
Rosolem, R., W.J. Shuttleworth, M. Zreda, T.E. Franz, X. Zeng, and S.A. Kurc. 2013. The effect of atmospheric water vapor on the cosmic-ray soil moisture signal. J. Hydrometeorol. (in press). doi:10.1175/JHM-D-12-0120.1
Sayde, C., C. Gregory, M. Gil-Rodriguez, N. Tufillaro, S. Tyler, N. van de Giesen, et al. 2010. Feasibility of soil moisture monitoring with heated fiber optics. Water Resour. Res. 46:W06201. doi:10.1029/2009WR007846
Schaap, M.G., F.J. Leij, and M.Th. van Genuchten. 2001. ROSETTA: A computer program for estimating soil hydraulic parameters with hierarchical pedotransfer functions. J. Hydrol. 251:163–176. doi:10.1016/S0022-1694(01)00466-8
Schaefer, G.L., M.H. Cosh, and T.J. Jackson. 2007. The USDA Natural Resources Conservation Service Soil Climate Analysis Network (SCAN). J. Atmos. Ocean. Technol. 24:2073–2077. doi:10.1175/2007JTECHA930.1
Scheffer, M., M. Holmgren, V. Brovkin, and M. Claussen. 2005. Synergy between small- and large-scale feedbacks of vegetation on the water cycle. Global Change Biol. 11:1003–1012. doi:10.1111/j.1365-2486.2005.00962.x
Schmugge, T., P. Gloersen, T. Wilheit, and F. Geiger. 1974. Remote sensing of soil moisture with microwave radiometers. J. Geophys. Res. 79:317–323. doi:10.1029/JB079i002p00317
Schmugge, T., and T. Jackson. 1994. Mapping surface soil moisture with microwave radiometers. Meteorol. Atmos. Phys. 54:213–223. doi:10.1007/BF01030061
Schneider, J.M., D.K. Fisher, R.L. Elliott, G.O. Brown, and C.P. Bahrmann. 2003. Spatiotemporal variations in soil water: First results from the ARM SGP CART Network. J. Hydrometeorol. 4:106–120. doi:10.1175/1525-7541(2003)004<0106:SVISWF>2.0.CO;2
Schroeder, J.L., W.S. Burgett, K.B. Haynie, I. Sonmez, G.D. Skwira, A.L. Doggett, and J.W. Lipe. 2005. The West Texas Mesonet: A technical overview. J. Atmos. Ocean. Technol. 22:211–222. doi:10.1175/JTECH-1690.1
Scott, B.L., T.E. Ochsner, B.G. Illston, C.A. Fiebrich, J.B. Basara, and A.J. Sutherland. 2013. New soil property database improves Oklahoma Mesonet soil moisture estimates. J. Atmos. Ocean. Tech. (in press). doi:10.1175/JTECH-D-13-00084.1
Scott, R.W., E.C. Krug, S.L. Burch, C.R. Mitdarfer, and P.F. Nelson. 2010. Investigations of soil moisture under sod in east-central Illinois. Rep. Invest. 119. Illinois State Water Surv., Champaign.
Selker, J.S., L. Thevenaz, H. Huwald, A. Mallet, W. Luxemburg, N. van de Giesen, et al. 2006. Distributed fiber-optic temperature sensing for hydrologic systems. Water Resour. Res. 42:W12202. doi:10.1029/2006WR005326
Sellers, P., R. Dickinson, D. Randall, A. Betts, F. Hall, J. Berry, et al. 1997. Modeling the exchanges of energy, water, and carbon between continents and the atmosphere. Science 275:502–509. doi:10.1126/science.275.5299.502
Sellers, P.J., Y. Mintz, Y.C. Sud, and A. Dalcher. 1986. A simple biosphere model (SIB) for use within general circulation models. J. Atmos. Sci. 43:505–531. doi:10.1175/1520-0469(1986)043<0505:ASBMFU>2.0.CO;2
Seneviratne, S.I., T. Corti, E.L. Davin, M. Hirschi, E.B. Jaeger, I. Lehner, et al. 2010. Investigating soil moisture–climate interactions in a changing climate: A review. Earth Sci. Rev. 99:125–161. doi:10.1016/j.earscirev.2010.02.004
Seuffert, G., H. Wilker, P. Viterbo, M. Drusch, and J.-F. Mahfouf. 2004. The usage of screen-level parameters and microwave brightness temperature for soil moisture analysis. J. Hydrometeorol. 5:516–531. doi:10.1175/1525-7541(2004)005<0516:TUOSPA>2.0.CO;2
Shao, Y., and A. Henderson-Sellers. 1996. Modeling soil moisture: A Project for Intercomparison of Land Surface Parameterization Schemes Phase 2(b): GEWEX Continental-Scale International Project (GCIP). J. Geophys. Res. 101(D3):7227–7250. doi:10.1029/95JD03275
Simelton, E., E.G. Fraser, M. Termansen, T. Benton, S. Gosling, A. South, et al. 2012. The socioeconomics of food crop production and climate change vulnerability: A global scale quantitative analysis of how grain crops are sensitive to drought. Food Secur. 4:163–179. doi:10.1007/s12571-012-0173-4
Simpson, J.A. 2000. The cosmic ray nucleonic component: The invention and scientific uses of the neutron monitor. Space Sci. Rev. 93:11–32. doi:10.1023/A:1026567706183
Sitch, S., B. Smith, I.C. Prentice, A. Arneth, A. Bondeau, W. Cramer, et al. 2003. Evaluation of ecosystem dynamics, plant geography and terrestrial carbon cycling in the LPJ dynamic global vegetation model. Global Change Biol. 9:161–185. doi:10.1046/j.1365-2486.2003.00569.x
Small, E.E., K.M. Larson, and J.J. Braun. 2010. Sensing vegetation growth with reflected GPS signals. Geophys. Res. Lett. 37:L12401. doi:10.1029/2010GL042951
Smith, A.B., J.P. Walker, A.W. Western, R.I. Young, K.M. Ellett, R.C. Pipunic, et al. 2012. The Murrumbidgee Soil Moisture Monitoring Network data set. Water Resour. Res. 48:W07701. doi:10.1029/2012wr011976
Song, Y., M.B. Kirkham, J.M. Ham, and G.J. Kluitenberg. 1999. Dual probe heat pulse technique for measuring soil water content and sunflower water uptake. Soil Tillage Res. 50:345–348. doi:10.1016/S0167-1987(99)00014-8
Sridhar, V., K.G. Hubbard, J. You, and E.D. Hunt. 2008. Development of the soil moisture index to quantify agricultural drought and its user friendliness in severity–area–duration assessment. J. Hydrometeorol. 9:660–676. doi:10.1175/2007JHM892.1
Steele-Dunne, S.C., M.M. Rutten, D.M. Krzeminska, M. Hausner, S.W. Tyler, J. Selker, et al. 2010. Feasibility of soil moisture estimation using passive distributed temperature sensing. Water Resour. Res. 46:W03534. doi:10.1029/2009WR008272
Striegl, A.M., and S.P. Loheide II. 2012. Heated distributed temperature sensing for field scale soil moisture monitoring. Ground Water 50:340–347. doi:10.1111/j.1745-6584.2012.00928.x
Su, Z., J. Wen, L. Dente, R. van der Velde, L. Wang, Y. Ma, et al. 2011. The Tibetan Plateau observatory of plateau scale soil moisture and soil temperature (Tibet-Obs) for quantifying uncertainties in coarse resolution satellite and model products. Hydrol. Earth Syst. Sci. 15:2303–2316. doi:10.5194/hess-15-2303-2011
Sutinen, R., P. Hänninen, and A. Venäläinen. 2008. Effect of mild winter events on soil water content beneath snowpack. Cold Reg. Sci. Technol. 51: 56–67. doi:10.1016/j.coldregions.2007.05.014
Suyker, A.E., S.B. Verma, and G.G. Burba. 2003. Interannual variability in net CO_2 exchange of a native tallgrass prairie. Global Change Biol. 9:255–265. doi:10.1046/j.1365-2486.2003.00567.x
Svoboda, M., D. LeComte, M. Hayes, R. Heim, K. Gleason, J. Angel, et al. 2002. The drought monitor. Bull. Am. Meteorol. Soc. 83:1181–1190.
Tarara, J.M., and J.M. Ham. 1997. Measuring soil water content in the laboratory and field with dual-probe heat-capacity sensors. Agron. J. 89:535–542. doi:10.2134/agronj1997.00021962008900040001x

Topp, G.C. 2006. TDR reflections: My thoughts and experiences on TDR. In: TDR 2006: 3rd International Symposium and Workshop on Time Domain Reflectometry for Innovative Soils Applications, West Lafayette, IN. 17–20 Sept. 2006. Geotech. Eng., Purdue Univ., West Lafayette, IN. Paper B1. https://engineering.purdue.edu/TDR/Papers/B1_Topp.pdf.

Topp, G.C., J.L. Davis, and A.P. Annan. 1980. Electromagnetic determination of soil water content: Measurements in coaxial transmission lines. Water Resour. Res. 16:574–582. doi:10.1029/WR016i003p00574

Torres, G.M., R.P. Lollato, and T.E. Ochsner. 2013. Comparison of drought probability assessments based on atmospheric water deficit and soil water deficit. Agron. J. 105:428–436. doi:10.2134/agronj2012.0295

Tyler, S.W., J.S. Selker, M.B. Hausner, C.E. Hatch, T. Torgersen, C.E. Thodal, and S.G. Schladow. 2009. Environmental temperature sensing using Raman spectra DTS fiber-optic methods. Water Resour. Res. 45:W00D23. doi:10.1029/2008WR007052

Ulaby, F.T., M.C. Dobson, and D.R. Brunfeldt. 1983. Improvement of moisture estimation accuracy of vegetation-covered soil by combined active/passive microwave remote sensing. IEEE Trans. Geosci. Remote Sens. GE-21:300–307. doi:10.1109/TGRS.1983.350557

VEMAP Members. 1995. Vegetation/Ecosystem Modeling and Analysis Project: Comparing biogeography and biogeochemistry models in a continental-scale study of terrestrial ecosystem responses to climate change and CO_2 doubling. Global Biogeochem. Cycles 9:407–437. doi:10.1029/95GB02746

Verhoef, A. 1995. Surface energy balance of shrub vegetation in the Sahel. Ph.D. diss. Wageningen Agric. Univ., Wageningen, the Netherlands.

Verhoef, A., and S.J. Allen. 2000. A SVAT scheme describing energy and CO_2 fluxes for multi-component vegetation: Calibration and test for a Sahelian savannah. Ecol. Modell. 127:245–267. doi:10.1016/S0304-3800(99)00213-6

Verhoef, A., S.J. Allen, and C.R. Lloyd. 1999. Seasonal variation of surface energy balance over two Sahelian surfaces. Int. J. Climatol. 19:1267–1277. doi:10.1002/(SICI)1097-0088(199909)19:11<1267::AID-JOC418>3.0.CO;2-S

Vinnikov, K.Y., A. Robock, S. Qiu, and J.K. Entin. 1999. Optimal design of surface networks for observation of soil moisture. J. Geophys. Res. 104:19743–19749. doi:10.1029/1999JD900060

Wagner, W., G. Bloschl, P. Pampaloni, J.C. Calvet, B. Bizzarri, J.P. Wigneron, and Y. Kerr. 2007. Operational readiness of microwave remote sensing of soil moisture for hydrologic applications. Nord. Hydrol. 38:1–20. doi:10.2166/nh.2007.029

Wagner, W., S. Hahn, R. Kidd, T. Melzer, Z. Bartalis, S. Hasenauer, et al. 2013. The ASCAT soil moisture product: A review of its specifications, validation results, and emerging applications. Meteorol. Z. 22:5–33. doi:10.1127/0941-2948/2013/0399

Wagner, W., G. Lemoine, and H. Rott. 1999. A method for estimating soil moisture from ERS scatterometer and soil data. Remote Sens. Environ. 70:191–207. doi:10.1016/S0034-4257(99)00036-X

Wagner, W., K. Scipal, C. Pathe, D. Gerten, W. Lucht, and B. Rudolf. 2003. Evaluation of the agreement between the first global remotely sensed soil moisture data with model and precipitation data. J. Geophys. Res. 108:4611. doi:10.1029/2003JD003663

Pan, W., R.P. Boyles, J.G. White, and J.L. Heitman. 2012. Characterizing soil physical properties for soil moisture monitoring with the North Carolina Environment and Climate Observing Network. J. Atmos. Ocean. Technol. 29:933–943. doi:10.1175/JTECH-D-11-00104.1

Weiss, J.D. 2003. Using fiber optics to detect moisture intrusion into a landfill cap consisting of a vegetative soil barrier. J. Air Waste Manage. Assoc. 53:1130–1148. doi:10.1080/10473289.2003.10466268

Western, A.W., and G. Blöschl. 1999. On the spatial scaling of soil moisture. J. Hydrol. 217:203–224. doi:10.1016/S0022-1694(98)00232-7

Xu, L., D.D. Baldocchi, and J. Tang. 2004. How soil moisture, rain pulses, and growth alter the response of ecosystem respiration to temperature. Global Biogeochem. Cycles 18:GB4002. doi:10.1029/2004GB002281

Yang, H., K. Auerswald, Y. Bai, and X. Han. 2011. Complementarity in water sources among dominant species in typical steppe ecosystems of Inner Mongolia, China. Plant Soil 340:303–313. doi:10.1007/s11104-010-0307-4

Yang, K., T. Koike, I. Kaihotsu, and J. Qin. 2009. Validation of a dual-pass microwave land data assimilation system for estimating surface soil moisture in semiarid regions. J. Hydrometeorol. 10:780–793. doi:10.1175/2008JHM1065.1

Zavorotny, V., K. Larson, J. Braun, E. Small, E. Gutmann, and A. Bilich. 2010. A physical model for GPS multipath caused by land reflections: Toward bare soil moisture retrievals. IEEE J. Sel. Top. Appl. Earth Obs. Remote Sens. 3:100–110. doi:10.1109/JSTARS.2009.2033608

Zehe, E., R. Becker, A. Bárdossy, and E. Plate. 2005. Uncertainty of simulated catchment runoff response in the presence of threshold processes: Role of initial soil moisture and precipitation. J. Hydrol. 315:183–202. doi:10.1016/j.jhydrol.2005.03.038

Zhao, L., K. Yang, J. Qin, Y. Chen, W. Tang, C. Montzka, et al. 2013. Spatiotemporal analysis of soil moisture observations within a Tibetan mesoscale area and its implication to regional soil moisture measurements. J. Hydrol. 482:92–104. doi:10.1016/j.jhydrol.2012.12.033

Zreda, M., D. Desilets, T.P.A. Ferré, and R.L. Scott. 2008. Measuring soil moisture content non-invasively at intermediate spatial scale using cosmic-ray neutrons. Geophys. Res. Lett. 35:L21402. doi:10.1029/2008GL035655

Zreda, M., W.J. Shuttleworth, X. Zeng, C. Zweck, D. Desilets, T. Franz, and R. Rosolem. 2012. COSMOS: The COsmic-ray Soil Moisture Observing System. Hydrol. Earth Syst. Sci. 16:4079–4099. doi:10.5194/hess-16-4079-2012

Zreda, M., X. Zeng, J. Shuttleworth, C. Zweck, T. Ferré, T. Franz, et al. 2011. Cosmic-ray neutrons, an innovative method for measuring area-average soil moisture. GEWEX News 21(3):6–10.

Zweck, C., M. Zreda, and D. Desilets. 2011. Empirical confirmation of the subkilometer footprint of cosmic-ray soil moisture probes. In: Abstracts, 8th EGU General Assembly 2011, Vienna, Austria. 3–8 Apr. 2011. Copernicus Gesellschaft, Göttingen, Germany.